RESPONSE OF THE FEMUR TO EXERCISE DURING RECOVERY BETWEEN TWO BOUTS OF HINDLIMB UNLOADING IN ADULT MALE RATS

A Thesis

by

ESTELA GONZALEZ

Submitted to the Office of Graduate Studies of
Texas A&M University
in partial fulfillment of the requirements for the degree of

MASTER OF SCIENCE

August 2012

Major Subject: Mechanical Engineering

Response of the Femur to Exercise During Recovery Between Two Bouts of Hindlimb Unloading in Adult Male Rats

RESPONSE OF THE FEMUR TO EXERCISE DURING RECOVERY BETWEEN TWO BOUTS OF HINDLIMB UNLOADING IN ADULT MALE RATS

A Thesis

by

ESTELA GONZALEZ

Submitted to the Office of Graduate Studies of
Texas A&M University
in partial fulfillment of the requirements for the degree of

MASTER OF SCIENCE

Approved by:

Chair of Committee,	Harry A. Hogan
Committee Members,	Susan A. Bloomfield
	Julie S. Linsey
Head of Department,	Jerald Caton

August 2012

Major Subject: Mechanical Engineering

ABSTRACT

Response of the Femur to Exercise During Recovery Between Two Bouts of Hindlimb Unloading in Adult Male Rats. (August 2012)

Estela Gonzalez, B.S., Columbia University

Chair of Advisory Committee: Dr. Harry A. Hogan

Mechanical unloading with microgravity exposure during spaceflight induces bone loss in weight bearing bones. Combined with loss of bone due to aging, this disuse bone loss puts astronauts at increased risk of fracture upon returning to 1G conditions. It is important to study countermeasures, such as exercise, to mitigate or prevent this bone loss. This study utilized the hindlimb unloaded (HU) rat model to characterize the effects of resistance exercise on recovery dynamics in-between two bouts of HU. In the larger project adult male Sprague-Dawley rats, six months of age, were divided into the following groups: baseline (sacrificed at 6 months of age); aging cage controls (did not undergo any treatment, sacrificed at 7, 8, 9, 10, and 12 months of age); 1HU7 (one month of HU at 6 months of age followed by three months of ambulatory recovery); 2HU10 (one month of HU at 6 months of age, ambulatory recovery for two months, one month HU at 9 months of age, and final two month ambulatory recovery); 1HU10 (one month HU at 9 months of age and two month ambulatory recovery); and 2HU+Ex (One month HU at 6 months of age, two month resistance exercise recovery, and a 2nd bout of

HU at 9 months of age). This thesis focused on the 2HU+Ex data, while utilizing data from other groups for comparisons. The data in this thesis includes *ex vivo* densitometric and biomechanical properties at the femoral neck (FN), femur midshaft diaphysis (FD), and distal femur metaphysis (DFM).

All compartments of BMC increased following exercise recovery above AC at the FN and DFM. Ambulatory recovery values revealed incomplete recovery in total and cortical BMC at the DFM and full recovery in other parameters. DFM and FD vBMD data indicated there were further benefits of exercise during recovery. Geometric data revealed periosteal apposition at the DFM and FN following exercise recovery. FD mechanical properties did not produce benefits of exercise. However, FN maximum force increased above all other groups after exercise recovery. Elastic modulus of the DFM showed benefits of exercise recovery in the response to the 2^{nd} HU.

TABLE OF CONTENTS

Page

Page

LIST OF FIGURES

Page

Page

Page

Page

LIST OF TABLES

Page

INTRODUCTION

Long duration spaceflight induces numerous negative physiological effects for astronauts. Spaceflight specifically affects the musculoskeletal system, as normally weight-bearing lower limbs are unloaded in microgravity. It is imperative to understand the changes that occur in a microgravity environment in order to make space travel as safe as possible, as well as to prevent any long-term physiological deficiencies posing a threat to individuals in spaceflight.

Prior research has shown that bone mass is lost during space travel, raising concerns that crewmembers may be susceptible to early onset osteoporosis. Lang et al. [1] performed a longitudinal pre- and post-flight study of bone mineral density (BMD) in astronauts who underwent International Space Station (ISS) missions of four to six months in duration. In this study, hip region dual X-ray absorptiometry (DXA) measurements revealed losses of 1.2-1.5% per month in BMD, despite crewmembers undertaking an intense exercise program [1]. This rate of loss is about 10-fold faster than that observed in older women predisposed to osteoporosis [2]. A more recent study by Lang et al. [3] used Quantitative Computed Tomography (QCT) to characterize the femoral neck, trochanteric region, and both combined. The data indicated that subjects who were exposed to gravitational unloading during a 4-6 month period experienced a loss of bone mass, cortical thinning, as well as a decline in estimated bone strength indices at the proximal femur. At the femoral neck they found a cancellous vBMD loss

---

This thesis follows the style of *Acta Astonautica.*

of 16.5% due to spaceflight, while during recovery there was only a 6.8% recovery of vBMD. After one year of recovery time, volumetric BMD did not fully recover to pre-flight values for the individuals [3]. These data reveal significant information about the potential increased risk of injury for astronauts upon returning to Earth.

The changes in bone after spaceflight and even after recovery are also of concern to NASA. A study by Carpenter et al. [4] measured BMD and bone geometry of eight astronauts at four different time points: before launch, immediately after returning to Earth, one year after return, and 2-4.5 years after return. QCT data of the proximal femur revealed that changes in trabecular bone density and structure remained even after several years of returning to Earth [4]. The average cancellous BMD lost at the femoral neck (14%) of astronauts corresponded to approximately one third of lifetime of loss (46%) in men, as measured by QCT [5]. The impact microgravity has on bone, combined with loss of bone with increasing age, poses increased risk of fracture for astronauts once they return to Earth. It is imperative that countermeasures are developed to prevent bone loss and enhance recovery to help reduce the potential for fractures for those individuals exposed to microgravity.

Although exercise is one important countermeasure currently used by astronauts, it has not proven successful enough to prevent significant bone mineral loss [6]. The exercise regimen will have to be assessed in order to determine what changes must be made to better minimize bone loss and enhance recovery [6]. Bed rest studies provide a ground-based human model for spaceflight. A study by Rittweger et al. [7] divided male participants into two groups, one performing progressive resistive and vibration exercise

and another that served as the control group. Both groups underwent 8 weeks of horizontal bed rest. An exercise program combining vibration and resistance training prevented bone losses from the tibia, measured by pQCT. The control group tibial bone loss was significant, most prominently in the distal epiphysis due to endocortical resorption, which is in agreement with the astronaut study conducted by Lang et al. [1]. The combined resistive and vibration exercise regimen provided an effective countermeasure for bone loss in the tibia, while Lang et al.'s [1] astronaut data revealed significant bone loss at the proximal femur despite regular exercise while in space. Rittweger et al. [7] suggest that in order to prevent bone loss, muscle strength must also be maintained.

There are other differences between the two studies. While the bed rest study shows prevention of loss at the tibia, the model does not indicate any losses for total hip BMC or significant losses in the cancellous compartment in contrast with the ISS study by Lang et al. [1]. Despite success in preventing bone loss at the tibia, the bed rest model does not offer a conclusive treatment plan. Further investigation is merited to determine what exercise mode can be incorporated during spaceflight or during recovery on Earth.

Animal models offer an insightful method of understanding potential treatments for microgravity induced bone deficits. Utilizing one such rodent model, Fluckey et al. [8] observed that BMD in rats exposed to flywheel resistance training during simulated microgravity was not different from control rats that were not subjected to simulated microgravity, supporting efficacy of resistance exercise training conducted *during* the period of unloading to protect against bone loss [8]. These studies show promising

results, but further investigations should be conducted until the current astronaut exercise regimen effectively prevents bone loss.

Research in this field has clinical significance which extends beyond astronaut bone health. As medical advances are made and populations age, osteoporosis has become a major public health concern. Osteoporosis is a skeletal disorder which affects bone strength and leads to increased risk of fracture; in particular, femoral neck osteoporosis results in several hundred thousand hip fractures each year [9]. Clinically, bone density is used to determine the integrity of bone and as a predictor of strength. However, bone density does not provide all of the information. Bone quality is one other essential facet to consider when assessing bone strength. Bone quality consists of the material composition of bone, architectural factors, and mechanical characteristics [10]. All of these factors considered together offer a more effective way of predicting bone strength and preventing osteoporotic fractures. Research in this field is critical to protect the aging population and astronauts in future missions.

The hindlimb unloading (HU) rat model is a ground based method of simulating effects of weightlessness in microgravity. The hindlimbs of rats are unloaded so that they are no longer weight bearing, thereby producing a cephalic fluid shift. The model mimics weightlessness, suppressing osteoblast numbers and bone formation rates resulting in bone loss [11]. Utilizing this model has clear advantages: firstly, a larger number of subjects which are more homogenous than human subjects can be utilized; secondly, it allows for tight control of subjects being exposed to multiple simulated

microgravity bouts; and, finally, it allows for investigating the response associated with recovery during reloading [12].

This study utilized the adult male rat model to characterize the effects of resistance exercise during recovery between two unloading bouts. Densitometric and biomechanical properties are characterized *ex vivo* at the femur at three different anatomical sites: the femoral neck (FN), femur midshaft diaphysis (FD), and distal femur metaphysis (DFM). These data reveal information about the impact of resistance exercise on bone health during recovery and the effects of exercise on the response to a 2^{nd} HU exposure.

OBJECTIVES

It is clear that further investigations need to be conducted to provide insight into countermeasures for maintaining preflight integrity of bone. This experiment is the final component of a three-part study that focused on loss and recovery from simulated microgravity exposures. This project utilizes six month-old adult male Sprague-Dawley rats that were assigned to baseline (BL), aging cage control (AC), and hindlimb unloaded (HU) groups by body weight and total (integral) volumetric bone mineral density (vBMD) at the proximal tibia metaphysis. The HU animals were suspended for 28 days, allowed to recover for 56 days, and suspended a second time for 28 days. The two previous components of this study, composed of ambulatory cage activity during recovery, revealed that, in general, at the distal and proximal femur vBMD, BMC, and ultimate strength decline after the 1st HU and these parameters recover to AC values after a 56 day ambulatory recovery period. However, a 2nd HU exposure tends to result in significant pre- to post- HU reductions of many parameters with post HU values also falling below age-matched AC [13-15]. The purpose of this study is to introduce a resistance exercise protocol, consisting of a squat jumping model [16], during the recovery period in-between two HU bouts.

The objectives of this experiment are to:

1. Characterize the effects of resistance exercise following a bout of hindlimb unloading (HU) on recovery of biomechanical and densitometric properties of the rat femur.
2. Characterize the effects of resistance exercise during recovery following an initial HU bout on the response of a 2nd HU exposure for densitometric and biomechanical properties of the rat femur.
3. Compare mechanical properties with densitometric properties of the femur after exercise recovery.
4. Compare alterations in bone with exercise during recovery and HU at three anatomic sites of interest: the femoral neck, femur diaphysis, and the distal femur metaphysis.

I hypothesize that at the femur, the femoral neck, femur diaphysis, and distal femur metaphysis, densitometric (BMC and vBMD) and mechanical properties (ultimate force or stress) will not only recover but significantly exceed aging control values after exercise recovery. During previous experiments [13, 14] many of these parameters recovered to AC values within two months of weight bearing ambulatory recovery. I hypothesize that exercise during recovery will improve bone structural and mechanical properties further than weight bearing during recovery.

I hypothesize that exercise during recovery will have no effect on the 2nd HU exposure. Specifically, I think pre- to post–HU changes will be similar for the 2nd HU of the exercise recovery animals and ambulatory weight bearing recovery animals.

I also hypothesize that the percent changes will be similar for mechanical and densitometric properties in response to exercise during recovery and for the second HU.

Finally, I hypothesize the densitometric and mechanical properties at FN and DFM will follow similar patterns. Further, I believe the FD will be less affected by exercise recovery and 2nd HU since it is composed of mainly cortical bone, while the DFM and FN are mixed bone sites made up of cortical and cancellous bone.

BACKGROUND

The experiment conducted for this thesis is part of a larger study funded by the National Aeronautics and Space Administration (NASA) through grant number NNX08AQ35G. The purpose of the overall project was to utilize a rat model to study the effects of multiple simulated microgravity exposures and recovery dynamics on bone health. This research also aims to characterize the effects of weight-bearing recovery, between two unloading bouts, with and without exercise. Through this research we are able to obtain information about bone including bone density, size, geometry, and strength at different sites. This thesis will focus on changes in these measures of bone integrity in the femur, at the femoral neck (FN), distal femur metaphysis (DFM), and femur midshaft diaphysis (FD). The first two sites are "mixed" bone sites, consisting of both cancellous and cortical bone, whereas the FD is purely cortical bone. The information presented will better predict the impact of multiple missions on astronaut bone health and will also give insight as to potential exercise countermeasures that could be employed during recovery in-between missions to protect bone.

Bone Biology

The skeleton is a unique structure which allows for locomotion while protecting vital internal organs and providing a support system for the body [17]. Bone, a calcified tissue, makes up most of the human skeleton [18]. In addition, bone adapts to resist mechanical forces and is self-repairing [19, 20].

Long bones typically consist of a cylindrical midshaft, also called diaphysis, and at the ends two wider portions called, epiphyses [19]. The diaphysis is made up of almost exclusively of compact bone called cortical bone. The epiphyses region is made up of a thin shell of cortical bone; however, this region of the long bone is strengthened by cancellous bone [17]. This composite structure takes advantage of the strength and components of both materials, making it more resistant to stresses and absorbing more energy before fracture [17]. The metaphysis, also a mixed site, connects the diaphysis to the epiphysis of the long bone (Figure 1).

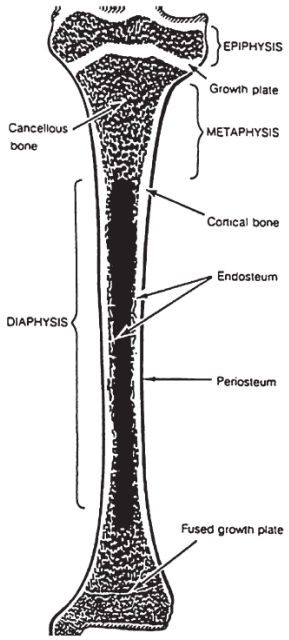

Figure 1: Schematic view of long bone (tibia). The midshaft is a cylindrical structure, called the diaphysis, composed of mainly cortical bone. The metaphyses are at the ends of the long bone and are composed of both cortical and cancellous bone [21].

Cortical bone, a dense calcified bone, makes up the outer shell of bone. This type of bone has only microscopic porosities. This compact bone is made of lamellar bone with Haversian and Volkmann canal systems. It is surrounded by an osteogenic tissue called the periosteum. The periosteum contains cells with the ability to form new bone, by mature osteoblasts. The interior of bone is covered by a thin layer of bone cells called the endosteum containing osteoclasts, osteoblasts, and bone lining cells [9, 18]. Cancellous bone, also called cancellous or spongy bone, is made up of a network of plates and rods individually known as trabeculae. This bone type is found inside the long bone and fills the metaphysis and epiphysis regions of bone. The femoral neck is also a mixed site with both cortical and cancellous bone (Figure 2).

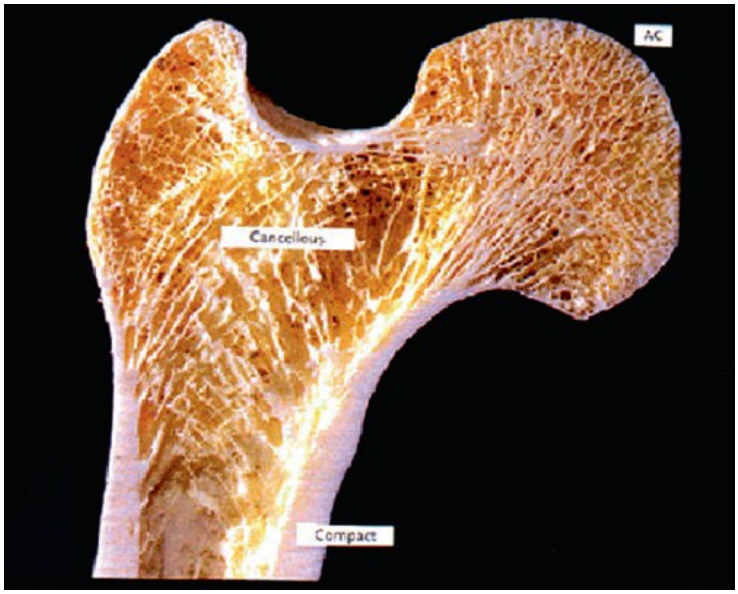

Figure 2: Proximal femur of adult long bone. In the femoral neck region, the interior portion of the bone is made up of interconnected struts or cancellous bone. The exterior portion of the bone is made up of dense cortical bone [17].

Bone is continuously remodeled in order to repair micro damage and replace aging tissue to maintain bone architecture and mass to support mechanical loading. The cells which are responsible for bone remodeling are osteoblasts and osteoclasts (Figure 3). Osteoblasts are bone forming cells. They produce unmineralized bone matrix, osteoid, which is then mineralized. Osteoclasts are bone resorbing cells. They tunnel through bone and create cavities later to be filled with new bone by osteoblasts [18]. A third type of bone cell not pictured in Figure 3 are osteocytes, formed when osteoblasts are left behind and trapped after bone formation has occurred. They are mechanosensory cells and respond to mechanical strains by communicating with other cells when remodeling is needed. During disuse the osteoblast and osteoclast relationship uncouples, resorption increases in the endocortical surfaces while there are decreases in bone formation in the periosteum.

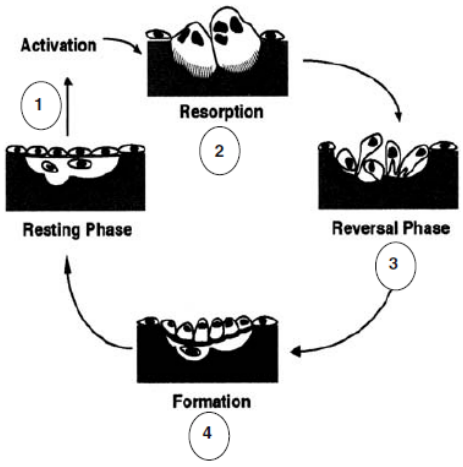

Figure 3: Cancellous bone remodeling cycle. First activation occurs and osteoclasts are recruited to resorb bone. During the reversal phase osteoclast activity subsides and osteoblasts are recruited to form new bone. The new bone is then mineralized and returns to a resting phase [20].

The Hindlimb Unloading Rodent Model

This study utilized a ground based model to simulate spaceflight. The following criteria make the hindlimb unloaded (HU) model an accurate representation of microgravity on rat bones: (1) The rat should not be overly stressed. A sign that a mature rat is stressed is that it begins to lose weight. (2) Model should allow for reloading and recovery after the disuse period. (3) The effect on muscle should be consistent with microgravity effects. The load bearing muscle mass decreases while non-load bearing muscle mass remains constant. (4) A cephalic fluid shift should be produced [11].

The HU rat model has been accepted as a reliable method of simulating spaceflight[11, 12]. Over short term experiments it has been shown to induce minimal changes in cortical bone structure while producing adverse effects in sites with high cancellous bone, such as the distal femur metaphysis [22]. Since it has demonstrated to be an effective model for mimicking spaceflight and also proven to be useful in providing reliable physiological effects during reloading and recovery, the HU rat model was chosen for this study [11, 12].

Computed Tomography

Peripheral Quantitative Computed Tomography (pQCT) offers a means of producing 3-dimensional imaging of bone. A typical resolution is 70 μm. Utilizing this imagining technique allows one to track information of changing properties throughout a

study. Properties obtained from the pQCT include true volumetric bone mineral density (vBMD), bone mineral content (BMC), area, and moments of inertia.

A pQCT scanner can differentiate between cancellous and cortical bone. This is important because cortical and cancellous bone respond differently during unloading and reloading [22]. Imaging allows for prediction of strength and potential fracture and is reported to correlate with mechanical strength [23]. Data obtained from pQCT analysis combined with destructive mechanical testing allows for creating a more complete analysis of the integrity of bone.

Mechanical Adaptation

Bone self-repairs and adapts to a changing environment [24]. Wolff's law states that bone adapts to demands placed on it by mechanical loads. When stresses act on bone, it modifies its structure to optimize strength [9]. For example, when there is an increase in load, over time the bone gains mineral content and/or adds bone on existing surfaces to increase strength. At the femoral neck, a highly cancellous region, it is also common for trabeculae to line up in the direction of principle stresses [25]. This adaptability protects bone from fracture. Bone also adapts to reduced loads. In a study utilizing an unloading rat model for young rats, growth in bone mass in the hindlimbs decreased after only one week of unloading [26]. This adaptability makes unloading during spaceflight an issue for astronaut safety when they return to load bearing on Earth.

Bone Mechanical Testing

Biomechanical properties of bone vary depending on the site. There are several techniques that can be utilized to determine the integrity of bone including tensile, compressive, bending, or torsional tests. Loads can be applied to bone and analyses can be conducted on the resulting load-displacement curve. This curve has two regions: elastic and plastic. Within the elastic region, the deformation of the bone increases proportionally to the load applied. If the bone is unloaded within this region, it returns to its original shape. The slope of this elastic region is the stiffness, or rigidity, of the bone [27]. This is a structural property which is dependent on the size or geometry of the bone [17]. If the deformation continues into the plastic region, bone will be permanently deformed or damaged.

Material properties are independent of geometry. Stress is the applied force per unit area and strain is defined as the change in length divided by original length. A prototypical stress-strain curve (Figure 4) demonstrates the relationship between the two material properties. The slope of the curve is the elastic or Young's modulus which measures the ability of a material to resist deformation. Toughness can also be calculated by utilizing the stress-strain curve. Toughness is defined as the area under the curve and determines how much energy can be absorbed before the material fails or fractures [17]. The yield point represents the transition from elastic to plastic region. Any loads above this point will cause irreversible damage. To identify the yield point, a line parallel to the linear region is found and offset by 0.03 to 0.2 strain [17].

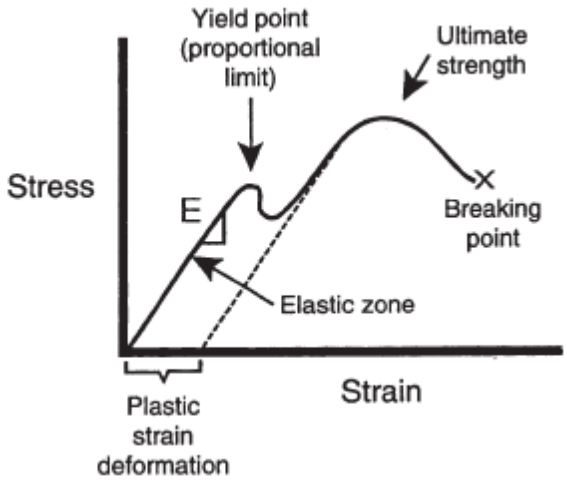

Figure 4: The stress-strain curve can be divided into two regions the elastic and plastic region. The yield point is the point at which elastic deformation will become plastic deformation. The breaking point is the point at which bone will fracture. [17]

Testing Configurations

Destructive testing is useful for measuring biomechanical properties of long bone in rodents. To determine properties of the femur diaphysis, a three-point bending test is conducted to failure. The bone is supported near its two ends and loaded by an advancing head at the midpoint of the shaft.

Femoral neck mechanical testing is often conducted in the axial direction. The femoral head is loaded in a vertical direction parallel to the long axis of the femoral shaft similar to human "stance" [28, 29]. However, this does not accurately reflect the most common form of hip fracture, which results from a side fall [30]. For this reason we also test rodent femoral necks to failure in a lateral configuration. While this test does not take into account the large impact force from a fall, it does offer some insight into the differences in maximum force that can be sustained by the femoral neck in the lateral

direction with continuous loading [25]. Both of these testing configurations result in a combination of bending, shear, and compression [22].

Compressive tests are performed to determine mechanical properties of the cancellous bone in the distal femur metaphysis. This testing method is not as accurate as other methods because of end and structural effects. This could include large stress concentrations from misalignment with the compressing platen, friction at the platen and specimen interface, or the nonhomogeneous structure of cancellous bone [27, 31]. Compressive testing is done primarily for simplicity and is beneficial because the natural mode of loading of cancellous bone is compressive [31]. Compressive tests measure Elastic or Young's modulus, compressive strength or stress, and energy absorption. A cancellous core specimen can be cut out from surrounding cortical bone before it is crushed [31].There are also methods of testing metaphysis specimens in which a 4 mm slice of the distal femur is cut. A cylindrical indenter smaller than the diameter of the marrow cavity is used to compress the cancellous bone until a depth of 2 mm is reached [28, 29, 32, 33]. This study will utilize a similar method.

Resistance Exercise

Exercise has been used as a countermeasure for disuse associated with spaceflight; however, it has not been effective in preventing bone loss in human crew members aboard ISS. Exercise, in general, has the advantage of benefiting not only the musculoskeletal system but also the cardiovascular and immunological systems. Developing an exercise regimen which allows bone to recover to pre-flight condition is

critical to protect astronauts from fracture after return to weight-bearing on Earth. Resistive exercise has been shown to provide a greater osteogenic stimulus than aerobic exercise [34]. Resistive exercise (combined with whole body vibration) during a human subject bed rest study prevented losses in weight bearing bones [7]. Another 17-week bed rest study with an exercise regimen similar to that of a weight lifter produced a protective effect in DXA BMD measurements in the lumbar spine, total hip, heel, total body and pelvis. Control bed rest subjects without exercise had an increase in resorption markers with no change in bone formation markers, while the exercised bed rest subjects had an increase in both resorption and formation markers. This resulted in less uncoupling of formation and resorption during disuse [34].

Rat models have also been used to assess the effects of exercise. The rat model allows for destructive testing for determination of mechanical strength of bone along with densitometric properties. A previously published study using adult rats that underwent 4 weeks of HU with flywheel resistance exercise training showed positive exercise results on muscle and bone outcomes. Distal femur BMD in exercise-trained rats remained at control levels, while HU rats without exercise had significant BMD reductions. Soleus muscle was also maintained to pre-HU values in the exercised group [8]. These studies all suggest the importance of mechanical loading in the form of exercise to protect bone. To make exercise an effective bone loss countermeasure, the existing astronaut exercise regimen will have to be assessed and modified.

METHODS

Animals

Adult male Sprague-Dawley rats, purchased from Harlan in Houston, TX, were used for this study. The rats were allowed to acclimate to the animal facility environment for two weeks, at the end of which they were six months old. The animal facility is located at Texas A&M University and is accredited by the American Association for Accreditation of Laboratory Animal Care. The animals were singly housed in a temperature controlled room (23 ± 2°C) with 12 hour light (10PM-10AM) and 12 hour dark cycles (10AM-10PM). They were given Harlan Teklad 8604 standard rat chow and water *ad-libitum*. All animal procedures were approved and conducted in accordance with the Texas A&M University Institutional Animal Care and Use Committee regulations which meet federal requirements of the Animal Welfare Act, the Public Health Service Policy, and the Humane Care and Use of Laboratory Animals.

Experimental Design

Adult male Sprague-Dawley rats, six months of age, were separated into groups by body weight and total vBMD from *in vivo* pQCT so there would be no differences among groups at the start of the experiment. Refer to Figure 5 for animal groupings and sacrifice points. A total of 325 rats were used to populate 16 different groups to provide excised bone samples for end point data. Number of animals per group can be found in

the Appendix. Listed below are the three main groupings and description of animal subgroup treatment.

1. Baseline (BL) – Sacrificed at the beginning of the experiment (Day 0) at six months of age.
2. Aging Cage Control (AC) – Animals that did not undergo any treatment, sacrificed at 7, 8, 9, 10, and 12 months of age.
3. Hindlimb unloaded (HU) – Animals that underwent at least one period of HU treatment.
    a. Double HU (2HU): One month HU at six months of age, followed by two month recovery consisting of normal (weight bearing) cage activity, followed by a 2nd bout of HU, and a final two-month ambulatory recovery after the 2nd HU (previous experiment).
        - 1HU7 – One month HU beginning at 6 months of age
        - 1HU7+R1 – One month HU at 6 months of age and ambulatory recovery for one month
        - 1HU7+R2 - One month HU at 6 months of age and ambulatory recovery for two months
        - 1HU7+R3 - One month HU at 6 months of age and ambulatory recovery for three months
        - 2HU10 - One month HU at 6 months of age, ambulatory recovery for two months, another bout of one month HU starting at 9 months of age and ending at 10 months of age

- 2HU10+R2 - One month HU at 6 months of age, ambulatory recovery for two months, another bout of one month HU starting at 9 months of age and ending at 10 months of age, a final ambulatory recovery for 2 months

b. Single Aging HU (1HU): One month HU at nine months of age, followed by two month ambulating recovery (previous experiment).
    - 1HU10 – Single one month HU bout starting at 9 months of age and ending at 10 months
    - 1HU10+R2 - Single one month HU bout starting at 9 months of age and ending at 10 months and two month ambulatory recovery for 2 months
c. Exercise Double HU (2HU+Ex): One month HU at six months of age, followed by two month resistance exercise recovery, followed by a 2nd bout of HU.
    - 1HU7 - One month HU at 6 months of age
    - 1HU7+EX - One month HU at 6 months of age, followed by two month resistance exercise recovery
    - 2HU10+EX - One month HU at 6 months of age, followed by two month resistance exercise recovery, and a final 2nd bout of HU starting at age 9 month and ending at age 10 month

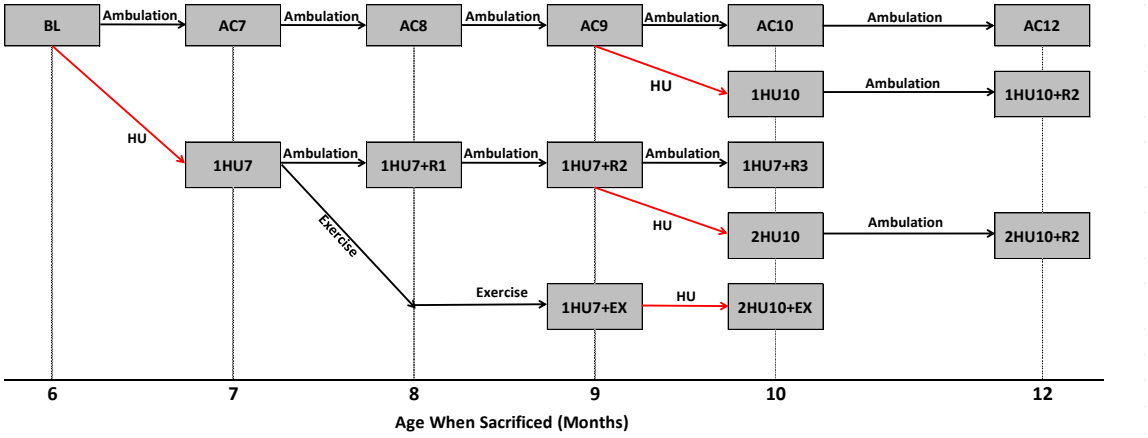

Figure 5: Experimental design.Rat subgroups are identified in boxes and age of sacrifice is indicated.Red arrows indicate periods of HU.

The data obtained during this study is from the exercise Double HU (2HU+Ex) group described by a bout of unloading, two months of resistance exercise recovery, followed by a 2nd bout of unloading. Other data are included for comparison, but were first generated in previous studies reported by Scott Morgan [14], Josh Davis [13], and Josh Kupke [15].

Hindlimb Unloading Model

The hindlimb unloading (HU) rat model offers a ground based analog and was used in this study to simulate microgravity exposure. The animals were suspended by their tails with custom-made harnesses that remove gravitational load from the hindquarters as previously described [12], (Figure 6). The animals were observed and cared for daily by veterinary technicians and graduate students to assure their overall health condition. For the first week of suspension, the AC and HU animals were pair-fed

to balance food intake. Summarized below are the steps taken to apply the tail harness on the first day of HU.

The rat was first injected with 0.3 mL of Atropine/Saline mixture subcutaneously. This prevents the rat from developing lung problems associated with suppressed blood flow, blood pressure, and heart rate when administered anesthesia. Next the rat was injected with 0.3 mL of Ketamine: DexaDomitor mixture (3:2) of anesthesia. This dose paralyzes and anesthetizes the animal for 30 to 45 minutes. The tail of the animal was then cleaned using a toothbrush and soapy water. This removes any dead or dirty skin. The tail was then dried with a towel and acetone spray and an adhesive spray sprayed on the left and right sides of the tail. Custom harnesses constructed from medical tape, bobby pins, and paper clips were glued to the left and right sides of the tail. To keep animals hydrated, 1.5 mL of saline was administered subcutaneously. Once the glue dried, the animal was given a 0.1 mL injection of Antiseden via intramuscular injection to wake it from anesthesia. The rats were then placed in custom made HU cages with a heating pad under cage floor without suspending the hindlimbs, allowing full weight bearing for 24 hours to recover and adjust to new cages and harnesses. After this acclimation period the animal was suspended. Harnesses are attached to a swivel that allows the rat to rotate and move about the cage freely using their forelimbs[12]. The height of the rat's hindquarters was adjusted so the hind limbs could not contact the ground, resulting in an approximate 30° head down tilt.

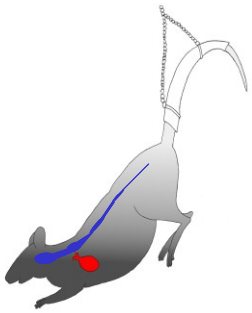

Figure 6: Hindlimb unloading rodent model. This rat model mimics the effects of spaceflight by unloading the hindquarters of a rat. Our tail harness is a modified version of the illustration but animal posture is the same. The body is at a thirty degree head-down tilt producing a cephalic fluid shift.

Exercise Protocol

A squat/jumping resistance exercise protocol was performed by rats assigned to 1HU7+Ex and 2HU10+Ex for the two month recovery period in-between HU bouts. This exercise protocol is beneficial because it is voluntary and the animal remains conscious, rather than anesthetized. This reduces the stress of the animal.

Operant conditioning began one week after the completion of the 1st HU. The exercise training sessions began one hour after the dark cycle started. The animals were conditioned to depress an illuminated bar located on the wall of a Plexiglas box (height 35 cm) fitted with an electric grid floor (21 x 21 cm). The height of the illuminated bar (22 cm) exceeded the height of the animal's full extension. This required them to jump to reach the illuminated bar. The rats were trained with negative reinforcement, receiving an electrical foot shock (1 mA, 60 Hz) from the electrical grid they stand on for the first conditioning trials. This was used to train rats to perform vertical jumping

movement. They learned to depress the illuminated bar, after which the light on the bar and the electric grid are turned off [16].

One week conditioning consisted of 3 sessions (Monday, Wednesday, and Friday) with 50 jumps during each session. Following conditioning were 18 training sessions over a six week period. A Velcro and leather vest was worn over the scapula to which an increasing amount of weight was added over the next six weeks. The animals began the exercise routine with 80 grams of added weight, 50 jumps, in session 1 and ended with 270 grams, 11 jumps, in session 18 (20-60% of body weight). Total exercise volume decreased (increased resistance and decreased repetitions) by 5%/week for a total of 30% over 6 week training period, (Table 1). Exercise volume decreased to accommodate increasing intensity from increasing weight. The goal of this exercise protocol was to overload skeletal muscle of the hindlimbs during each successive training session in hope of providing an anabolic stimulus to musculoskeletal tissue.

Table 1: Resistance exercise jump/squat training routine during 7-week period. Exercise volume defined as the product of repetitions and weight. Exercise volume decreases 5% per week.

Week	Repetitions	Weight (grams)
0 (Operant Conditioning)	50	0
1	50	80
2	35	110
3	24	150
4	18	190
5	14	230
6	11	270

Ex Vivo pQCT

A Stratec XCT-Research M peripheral quantitative computed tomography (pQCT) scanner (Norland Corporation, Fort Atkinson, WI) was used to scan *ex vivo* at the left and right femoral neck (FN) regions, left femur midshaft diaphysis (FD), and left femur distal metaphysis (DFM). Scans had a slice thickness of 0.5 mm with voxel resolution of 70 μm. The machine was calibrated every day with a hydroxyapatite cone phantom to ensure accurate bone parameter measurements.

After bones were excised they were wrapped in gauze, soaked in phosphate buffered saline (PBS) and frozen at -35˚F for storage. In preparation for scanning, the bones were taken out of the freezer and thawed. Left femurs were placed with the posterior side up in a vial filled with PBS to keep them from drying out during scanning. A scout scan was performed and a reference line placed midway between the medial/lateral condyles and the intercondylar fossa. Four slices of 0.5 mm thickness were taken of the metaphysis region at distances of 3.5, 4.0, 4.5, and 5.0 mm proximal to the reference line. The total scan area was 2 mm in height (Figure 7). The FD was scanned at the midshaft with total scan height of 0.5 mm.

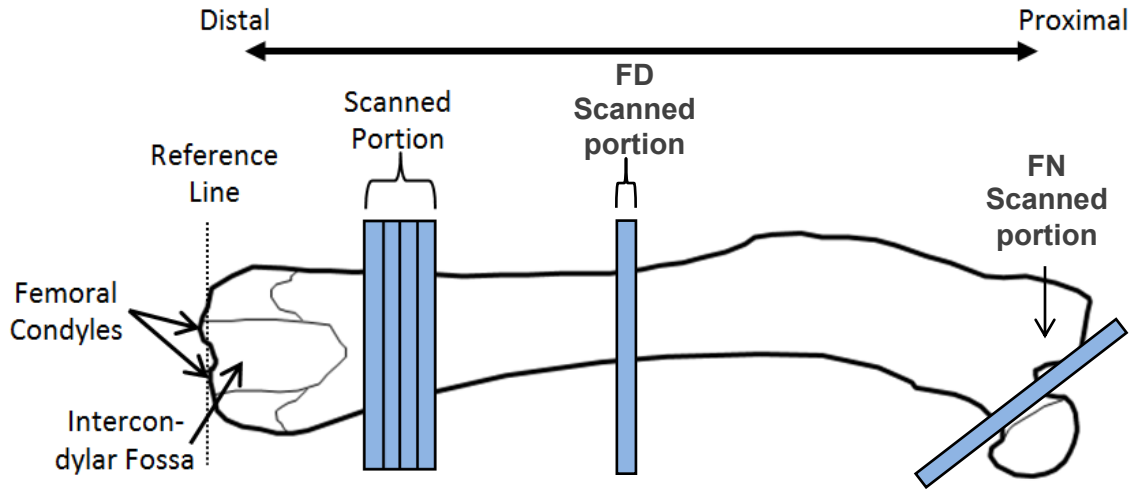

Figure 7: Femur pQCT scan locations. The femur was scanned during a single process at the distal femur metaphysic and the femur midshaft diaphysis. The scan lines were placed in regions of interest and mineral data was obtained for each half millimeter increment. Four scan lines were chosen for the metaphysis region and one scan line was used for the midshaft. In a separate scanning session the FN was scanned with the FN axis perpendicular to the scanning axis of pQCT scanner.

The FN scanning procedure was similar. The proximal half of each femur (generated after three-point bending to failure or from bones cut during tissue harvest) was thawed to room temperature and placed in a custom FN mold that holds the femoral neck axis perpendicular to the scanning axis of the CT scanner (Figure 7). A scout scan was performed in order to place the scan lines in the neck region, below the femoral head. There were three slices of 0.5 mm each which accumulate to a total scan length of 1.5 mm.

Densitometric Analysis

In order to differentiate between cortical and cancellous bone regions, in the DFM and FN, contour and peel algorithms were used. These algorithms were provided

by Stratec XCT software (v6.00, Norland Corp., Fort Atkinson, WI). The contour algorithm differentiates between density of cortical bone and surrounding PBS solution or air. The peel algorithm determines the endocortical border between cortical and cancellous bone. This allows for differentiation between cancellous and cortical bone (Table 2).

Table 2: Contour and peel algorithm thresholds. These thresholds are used by pQCT scanning software to differentiate between air and cortical bone and cortical and cancellous bone in order to obtain mineral data.

Site	Contour Threshold (mg/mm^3)	Peel Threshold (mg/mm^3)
DFM	450	800
FD	650	650
FN	710	1200

Strength indices are derived from densitometric data. Structural Strength Index (SSI) is a parameter taken directly from pQCT. SSI is a moment of resistance and is weighted by bone density. Compressive Strength Index (CSI) is calculated from the product of the square of the density and the area. The Bending Strength Index (BSI) is calculated from the quotient of polar moment of inertia (I_P) and bone width.

RPC Specimen Preparation

The distal part of the femur was utilized for reduced platen compression testing. A Well Diamond Wire Saw (Model 3242, Norcross, Georgia) was utilized to cut a DFM specimen. The shaft of the femur was clamped and tightened and remained horizontal

during the procedure. A diamond wire with a diameter of 0.3 mm was used to cut horizontally across the bone; the first cut was made just proximal to the intercondylar fossa and the second cut 2.3 mm proximal to the first (Figure 8).

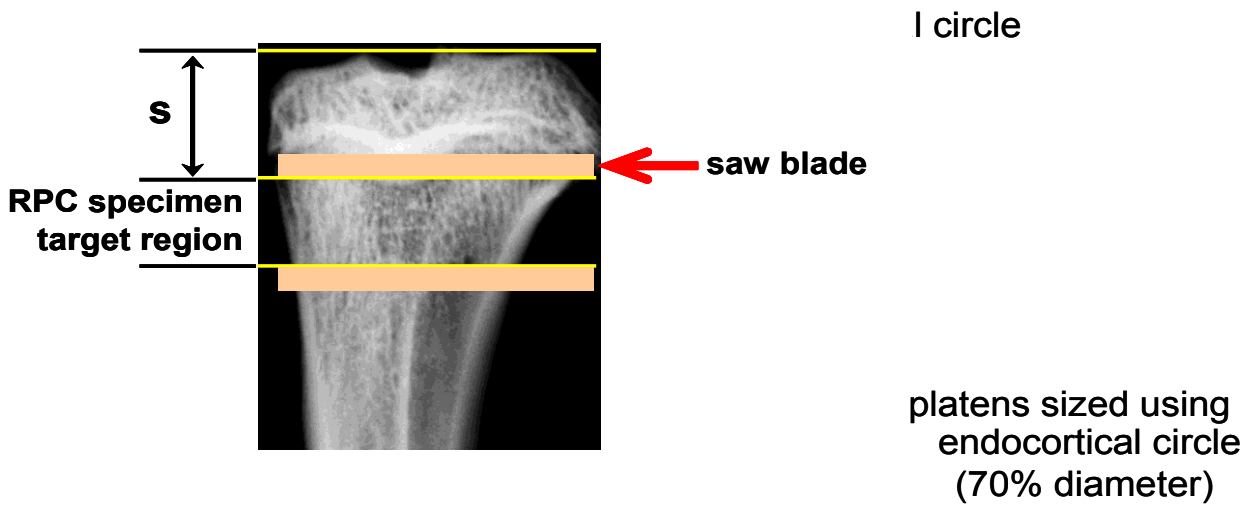

Figure 8: Reduced platen compression testing saw blade location. The image presented is a proximal tibia but the cutting procedure is the same for distal femur. RCP specimens must be cut 2 mm in thickness in order to compress cancellous bone in the distal femur metaphysis. The first cut is made just proximal to the growth plate and the second cut is made 2.3 mm proximal to the first cut. The diamond wire used is 0.3 mm in diameter so the final specimen will be 2 mm thick.

After machining these test specimens, pictures were taken of both sides of the specimen. Of the two images, the smaller was chosen, and imported into Adobe Photoshop for platen sizing. Pixels were converted to dimensions in mm. The endocortical diameter of the specimen was found utilizing Photoshop tools. This diameter was then scaled by 0.7 (Figure 9). The final diameter was utilized for choosing a platen size when compressing the cancellous core during mechanical testing.

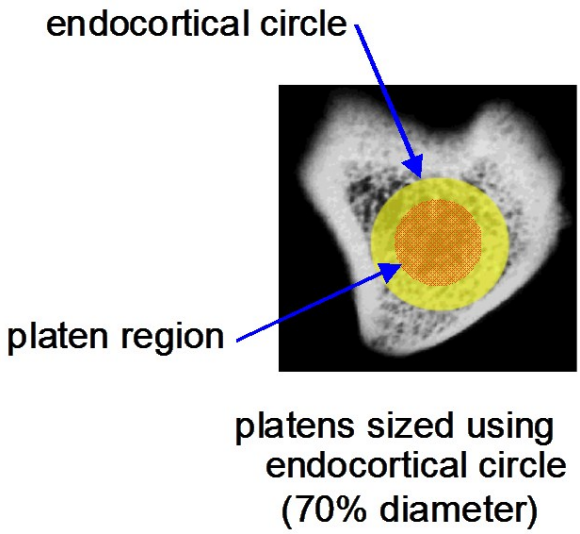

Figure 9: Sample sizing of platen for reduced platen compression testing of cancellous bone. The image presented is a proximal tibia but the cutting procedure is the same for distal femur. The inner circle diameter is found by uploading an image into Adobe Photoshop and sizing the largest endocortical circle. The endocortical circle diameter is then sized by 70% and this diameter is then used for the platen size chosen for each specimen.

Specimens were stored in a -35˚F freezer until ready for mechanical testing. They were individually wrapped in PBS soaked gauze, plastic wrap, and foil.

Mechanical Testing

All mechanical testing was performed using an Instron 3345 Mechanical Testing System (Norwood, MA). Force and displacement data for all testing methods were collected by Bluehill software (version 2.14.582, Instron Bluehill). Mechanical testing data from Instron were written to Excel files. These data were then run through a custom Matlab program called Datmet. This program was created in the Bone Biomechanics Laboratory at Texas A&M University by Scott Bouse [35]. The program is used to

calculate mechanical properties such as stiffness, max force, yield force, energy to yield, and various displacements at each site.

Femur Diaphysis

For three-point bending tests the femurs were removed from freezer and allowed to thaw overnight in a refrigerator. Once brought to room temperature the bones were placed with the anterior side down on two supports at 15 mm apart. They were loaded with a 1000 N load cell at the midshaft by a hammer until fracture, see Figure 10. The rate of quasi-static load is 2.54 mm/min or 0.1 in/min. Data were recorded at 10Hz.

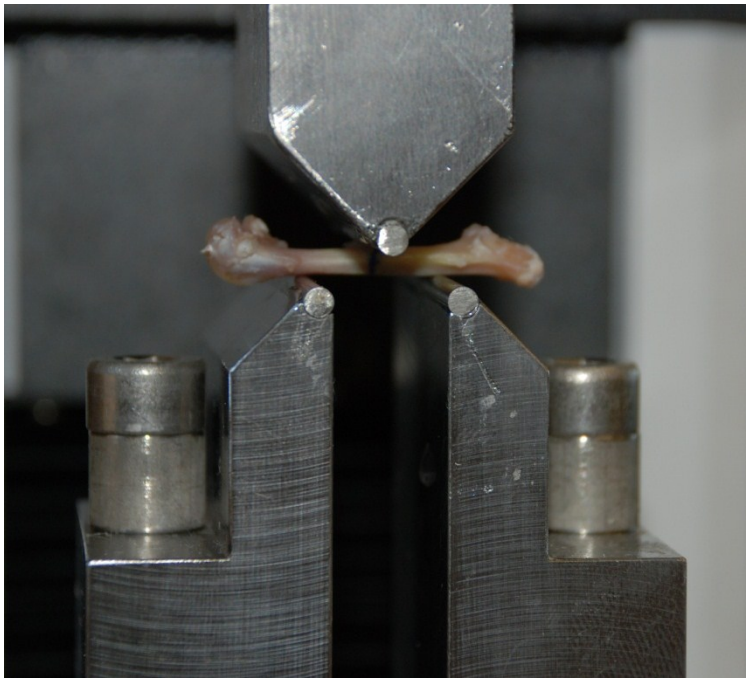

Figure 10: Three point bending bone placement. The femur is placed with the posterior side up on two supports separated by 15 mm. A hammer descends quasistatically until the bone fractures.

From this test mechanical properties can be calculated including maximum load and stiffness [28]. Material properties can also be obtained using the formulas below.

$$\text{Ultimate stress} = \frac{Ultimate\ load * span * APdia}{8 * CSMI} \quad (1)$$

$$\text{Elastic modulus} = \frac{Stiffness * span^3}{48 * CSMI} \quad (2)$$

$$\text{Pre-yield toughness} = \frac{0.75 * energy\ to\ yield * APdia^2}{L * CSMI} \quad (3)$$

The ultimate load is obtained from mechanical testing data and the span is the distance between supports. For the rat femur in this study the span was 15 mm [27, 29]. AP diameter is the anteroposterior diameter which can be measured using calipers at the midshaft. CSMI is the cross sectional moment of inertia which is a variable which is obtained from pQCT data. Energy to yield is the area under the load-deformation curve up to the yield point. L is the length of the femur which can also be measured using calipers.

Femoral Neck

The strength of the femoral neck has been shown to depend upon the direction or loading in humans. Therefore, femoral necks were loaded in either the axial and lateral configuration. For both cases a quasi-static load to failure was applied at a rate of 2.54 mm/min with a 1000 N load cell.

The right femoral neck was tested in the axial loading configuration. The diaphysis portion, or shaft, of the broken femur is positioned in a testing fixture with

various size holes. The hole which provided a secure fit to the shaft was chosen in order to maintain vertical alignment of the shaft. The femoral head was preloaded 5 N in order to allow the shaft to settle into the hole. Load to fracture is applied at the femoral head by a 10 mm cylindrical platen. The load is parallel to the long axis of the femur in a manner similar to stance loading (Figure 11).

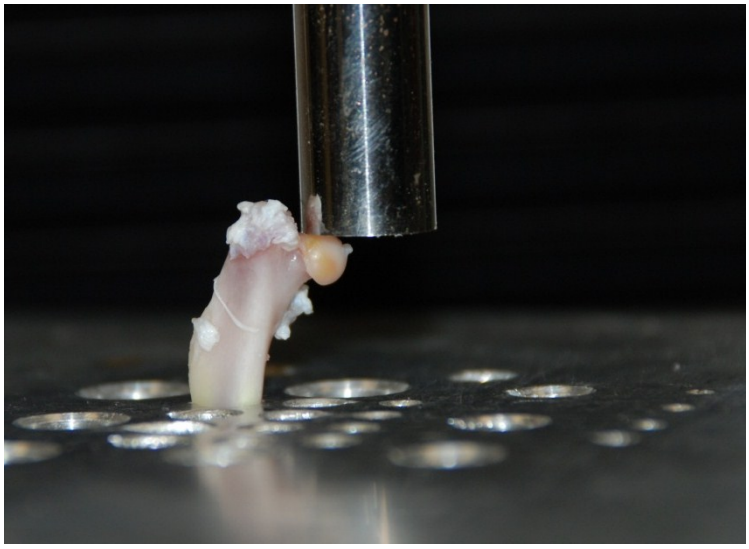

Figure 11: Axial femoral neck testing configuration. Femoral neck strength depends on loading configuration. The axial loading configuration is similar to stance loading and is conducted so that a load is applied parallel to the axis of the cylindrical shaft of the femur.

The left femoral neck was tested in a lateral loading configuration. Load to fracture is applied in a manner similar to a lateral "fall." An adjustable testing clamp made of two plates with rubber supports was used to hold the femoral shaft. The shaft is inserted between the two rubber supports and secured from rotating or falling out. The proximal femur shaft was at approximately a 10 degree angle with the horizontal (Figure 12). The surface on which the trochanter rested was covered with rubber to keep it from crushing during testing. The femoral head was preloaded 5N in order to ensure that the

trochanter was in contact with the rubber. Load to fracture was applied at the femoral head by a 10 mm cylindrical platen.

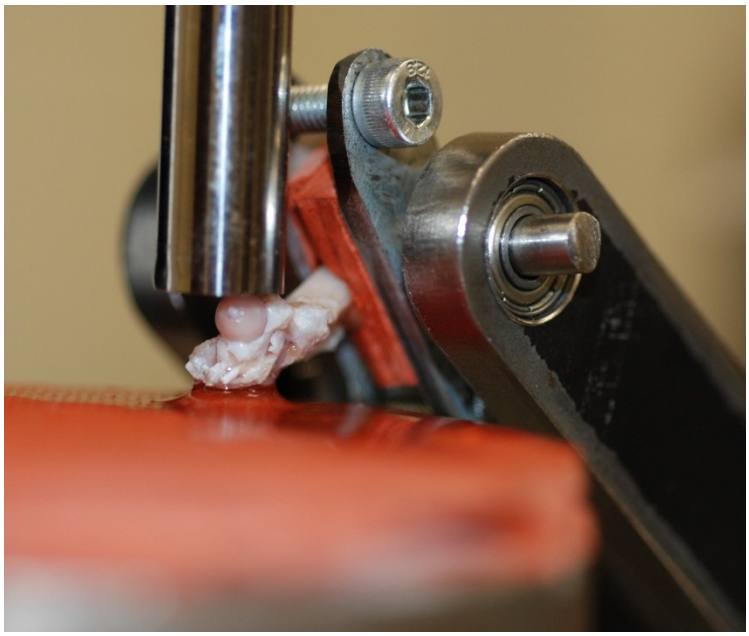

Figure 12: Lateral FN testing configuration. Femoral neck strength depends on loading configuration. The lateral loading configuration is similar to a side fall. However, this loading configuration does not take into account the impact of a side fall.

Distal Femur Metaphysis

Reduced platen compression testing was used to test the cancellous properties of the machined specimen from the DFM. The cancellous bone was compressed between two platens using a 100 N load cell. The platens' sizes were chosen based to correspond with 70% of the endocortical diameter of the smaller side. The bottom platen did not move but held the distal part of the specimen slice. The top platen was fitted into a jig which was adjusted downward until it was positioned at the center of the cancellous region. Once the specimen was positioned properly between the two platens (Figure 13),

the compression test began. The cross-head moved quasi-statically at a rate of 0.25 mm/min. Force-displacement data were recorded at 10 Hz.

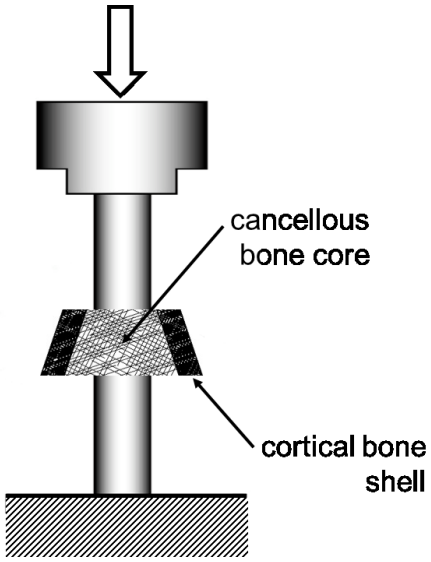

Figure 13: Cancellous compressive testing of distal femur metaphysis (DFM). The DFM specimen is cut with a diamond wire saw and is two millimeters in thickness. The cancellous bone core is then compressed with individually sized platens. The smaller or proximal side of the specimen is placed on top while the distal part is placed on the bottom platen. The bottom platen does not move while the top platen moves downward to compress cancellous bone and obtain mechanical data of cancellous core.

Material properties of cancellous bone were calculated utilizing geometry of the specimen and the size of the compressive platen chosen to compress cancellous bone. Stress, strain, and elastic modulus can be found using engineering formulas.

$$\text{Stress} = \frac{F}{Area} \tag{4}$$

$$\text{Strain} = \frac{x_f - x_i}{x_i} = \frac{\Delta x}{x_i} \tag{5}$$

$$\text{Elastic modulus} = \frac{Stress}{strain} = \frac{x_i * F}{\Delta x * Area} = \frac{x_i * k}{Area} \tag{6}$$

Stress was calculated as the quotient of the force (collected from Instron) and the cross sectional area of the platen used. Strain was calculated according to formula (5) where Δx is the compressive displacement and x_i is the initial thickness of the specimen. Elastic modulus was found according to formula (6) where k is the stiffness of the cancellous bone.

Data Analysis

Statistical analysis included comparisons between groups and was performed using SigmaStat 3.5 software. Unpaired Student's *t*-tests were utilized to compare group mean values at each endpoint with $p<0.05$ for significance. When comparing multiple groups at a single time point, *t*-tests were chosen over Analysis of Variance (ANOVA) to simplify the analysis of data. Experiment error rate could be corrected for by adjusting the significance level, alpha, by the number of comparisons being performed with a Bonferroni correction or a similar correction method.

Matlab scripts were also used to verify and generate the p-values in a readable format (p-values are reported in the Appendix). Since we are performing t-tests, we test for normality of the input datasets and equal variance between them instead of assuming this to be the case. The scripts first test normality using Matlab's version of Lilliefor's test, "lillietest." If both input datasets are determined to be normal, then Matlab's version of the Bartlett test, "vartestn," will be used to test for equal variance between the two datasets. If the data are distributed normally and have equal variance, then an unpaired student t-test is run. If either the normality or equal variance tests fail, then Matlab's

version of a Mann-Whitney U-test is run. This “ranksum” test does not assume normality or equal variance of the data. All tests were run at a 5% significance level.

RESULTS

Throughout the experiment animal body weights were recorded weekly. Body weight is an important indicator of stress level during HU. Only in the first week after HU were there decreases but body weights recovered soon after. Some animals developed tail tip necrosis and were not included in the study. The number of animals per group for each site can be found in the Appendix section.

The absolute value and standard error results will be presented in tables at the beginning of each section. Graphs of bone densitometric and mechanical properties will follow as percent baseline and standard error. Group means represent a mean percent change from the baseline value. Yellow highlighting indicates periods of HU exposure. The blue line with the square data points are the aging control (AC) group. This group of animals did not undergo any treatment and was sacrificed at 7, 8, 9, 10, and 12 months of age. The red solid line with square data points indicates the animals who underwent a bout of unloading at age 6 months and then had ambulatory recovery for three months, namely (1HU7, 1HU7+R1, 1HU7+R2, 1HU6+R3). The red dashed line with solid triangular points indicates a second unloading bout for the animals with a two month ambulatory recovery (2HU10). Following a second HU these animals were allowed another ambulatory recovery of two months (2HU10+R2). The single aging HU starting at 9 months of age is indicated by the dotted red line with the circular data points (1HU). Following the HU these animals were allowed an ambulatory recovery of two months (1HU10+R2). Finally, the solid green line with the square data points indicates the group

that experienced one month HU ending at 7 months of age (1HU7), followed by two months of resistance exercise recovery (1HU7+Ex), and ending with a 2nd bout of HU (2HU10+Ex).

Femoral Neck Densitometric Properties

Absolute values for densitometric properties of the FN are provided in Table 3. BMC presents decreases after the first HU ending at month 7 (1HU7). Both total (Figure 14) and cortical (Figure 15) BMC decrease significantly from BL and are significantly lower than AC7. Cancellous BMC (Figure 16) decreases from baseline as well; however, the change is not significant. For 1HU7+Ex (1HU7 plus two month resistance exercise period) total, cortical, and cancellous BMC recovers to well above AC9 and the 1HU7+R2 group means (1HU7 plus two month ambulatory period). A second bout of HU illustrates decreases across all compartments for the 2HU10 groups; however, total and cortical BMC show a slight (non-significant) increase for the 2HU10+Ex group mean. 2HU10+Ex is the post 2nd HU point in the 2HU+Ex data. After the second unloading, 2HU10+Ex remained above AC10 while 2HU10 remained below AC10. These data help to confirm the benefits of resistance exercise for enhancing recovery of BMC at the femoral neck which is maintained even during a 2nd HU.

Total (Figure 17) and especially cancellous (Figure 19) volumetric bone mineral density reveal significant losses (-15%) after the first hindlimb unloading period. The loss recovers to baseline and aging control level for the 1HU7+Ex group while 1HU7+R2 recovers only to aging control in the cancellous compartment. The second hindlimb unloading bout shows a non-significant increase for 2HU10+Ex group in total volumetric bone mineral density and a non-significant decrease for the 2HU10 and 1HU10 groups. The cancellous compartment follows a similar trend. Post-hindlimb unloading, 2HU10+Ex and 2HU10 both remain at aging control level in total volumetric bone mineral density The cancellous compartment demonstrates volumetric bone mineral denisty for 2HU10+Ex to be above AC10 while 2HU10 and 1HU10 fall below aging control. Cortical volumetric bone mineral density (Figure 18) reveals increases in all groups as the animals age, with no pre- to post-hindlimb unloading changes for any groups.

Table 3: Mineral properties for total, cancellous, and cortical BMC and vBMD of the right femoral neck

	Total BMC (mg/mm)	Total vBMD (mg/cm^3)	Cancellous BMC (mg/mm)	Cancellous vBMD (mg/cm^3)	Cortical BMC (mg/mm)	Cortical vBMD (mg/cm^3)
6 Months Old						
BL6	4.94 (0.09)	1120.9 (10.4)	1.60 (0.08)	758.9 (8.2)	3.33 (0.07)	1434.60 (3.85)
7 Months Old						
AC7	5.01 (0.12)	1149.9 (13.1)	1.53 (0.10)	778.1 (14.4)	3.49 (0.08)	1442.8 (5.88)
1HU7	4.60 (0.10)*†	1043.6 (16.1)*†	1.45 (0.07)	645.0 (12.3)*†	3.15 (0.06)*†	1441.3 (6.00)
8 Months Old						
AC8	5.18 (0.12)*	1130.1 (16.3)	1.67 (0.10)	766.5 (15.2)	3.52 (0.06)*	1447.5 (6.61)
1HU7+R1	4.71 (0.12)†	1074.5 (15.7)*†	1.52 (0.10)	692.3 (14.2)*†	3.19 (0.07)†	1437.4 (6.00)
9 Months Old						
AC9	5.01 (0.14)	1148.7 (16.9)	1.47 (0.12)	742.0 (15.7)	3.54 (0.06)*	1461.3 (8.86)*
1HU7+R2	4.90 (0.11)	1177.6 (14.7)*	1.24 (0.10)*	726.8 (16.3)*	3.66 (0.05)*	1469.0 (6.63)*
1HU7+Ex	5.88 (0.19)*Ψ†	1148.9 (17.7)	1.85 (0.17)Ψ†	774.9 (19.6)	4.03 (0.09)*Ψ†	1448.54 (6.03)Ψ
10 Months Old						
AC10	5.28 (0.11)*	1151.3 (11.9)	1.46 (0.08)	728.4 (13.9)	3.82 (0.06)*	1464.11 (5.86)*
1HU7+R3	5.34 (0.17)*	1157.6 (16.4)	1.41 (0.11)	720.5 (21.0)	3.93 (0.10)*	1463.4 (8.92)*
1HU10	4.81 (0.08)†	1105.0 (17.6)†	1.28 (0.07)*	650.3 (16.8)*†#	3.53 (0.06)*†	1458.7 (5.20)*
2HU10	4.62 (0.12)*†	1157.0 (14.1)	1.13 (0.08)*†	682.8 (13.2)*†	3.49 (0.06)*†#	1474.6 (5.11)*
2HU10+Ex	5.89 (0.11)*†	1178.1 (18.4)*	1.65 (0.14)	771.2 (14.6)†	4.24 (0.10)*†	1460.86 (5.43)*
12 Months Old						
AC12	5.09 (0.12)	1210.2 (14.0)*	1.15 (0.10)*	720.4 (18.4)*	3.93 (0.07)*	1495.0 (5.92)*
1HU10+R2	4.93 (0.09)	1169.1 (14.7)*	1.18 (0.07)*	691.6 (13.0)*	3.75 (0.05)*†	1480.7 (4.59)*
2HU10+R2	4.90 (0.12)	1232.5 (13.8)*	1.02 (0.08)*	723.0 (23.6)	3.88 (0.08)*	1497.6 (3.82)*

Values are presented as mean ± SE

*** Indicates significant difference from baseline value, $p < 0.05$**

† Indicates significant difference from age-matched control value at same time point, $p<0.05$

 # Indicates significant difference from pre- to post-HU value within same group, $p<0.05$

Ψ Indicates significant difference from 1HU7+Ex to 1HU7+R2, $p<0.05$

Symbols c

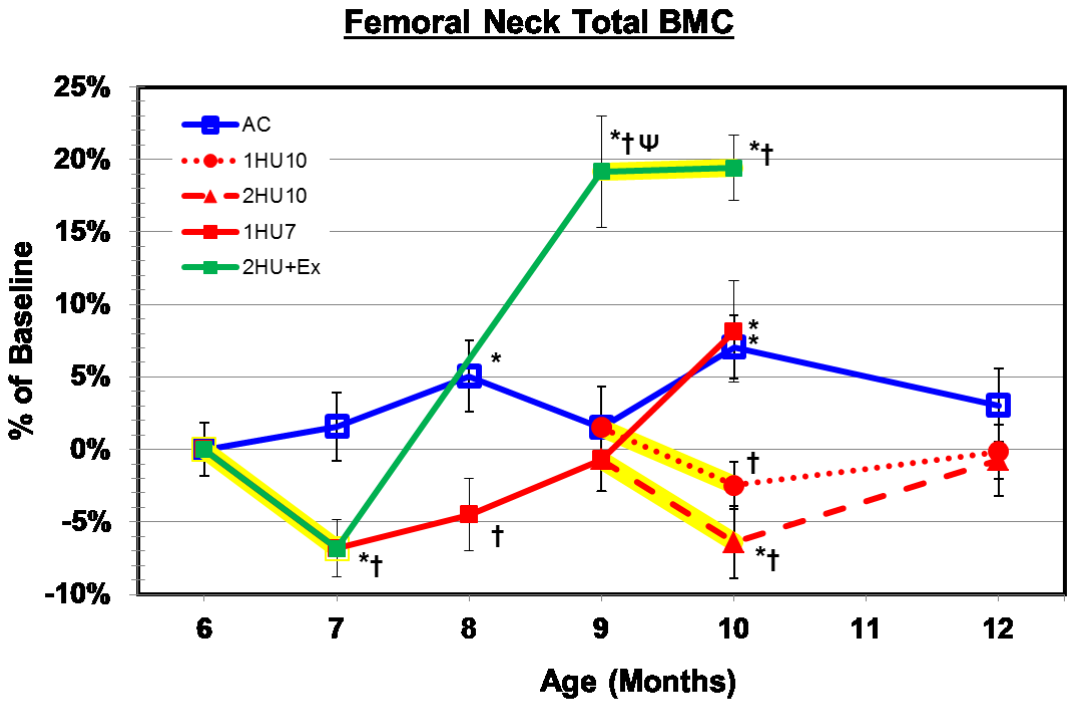

Figure 14: Changes in total (integral) BMC of the right femoral neck. Numerical data are presented in Table 3. Yellow highlighting indicates HU treatment. 1HU7 decreases (-6.82%) from baseline (BL) with a significant difference from AC. The exercised group recovers above baseline, AC (+17.37%), and the 1HU7+R2 (+19.99%) group. After the second unloading period the 1HU10 and 2HU10 are both significantly lower than AC while 2HU10+Ex is higher than AC (+11.53%). Pre- to post-HU values for the 9- 10 month period show decreases (n.s.) for 1HU10 and 2HU10, however 2HU10+Ex shows a slight increase (0.21%, n.s.).
Values are presented as mean ± SE
*** Indicates significant difference from baseline value; p<0.05**
† Indicates significant difference from age-matched cage control value at same time point; p<0.05
 # Indicates significant difference from pre- to post-HU value within same group; p<0.05
Ψ Indicates significant difference between 1HU7+Ex and 1HU7+R2; p<0.05

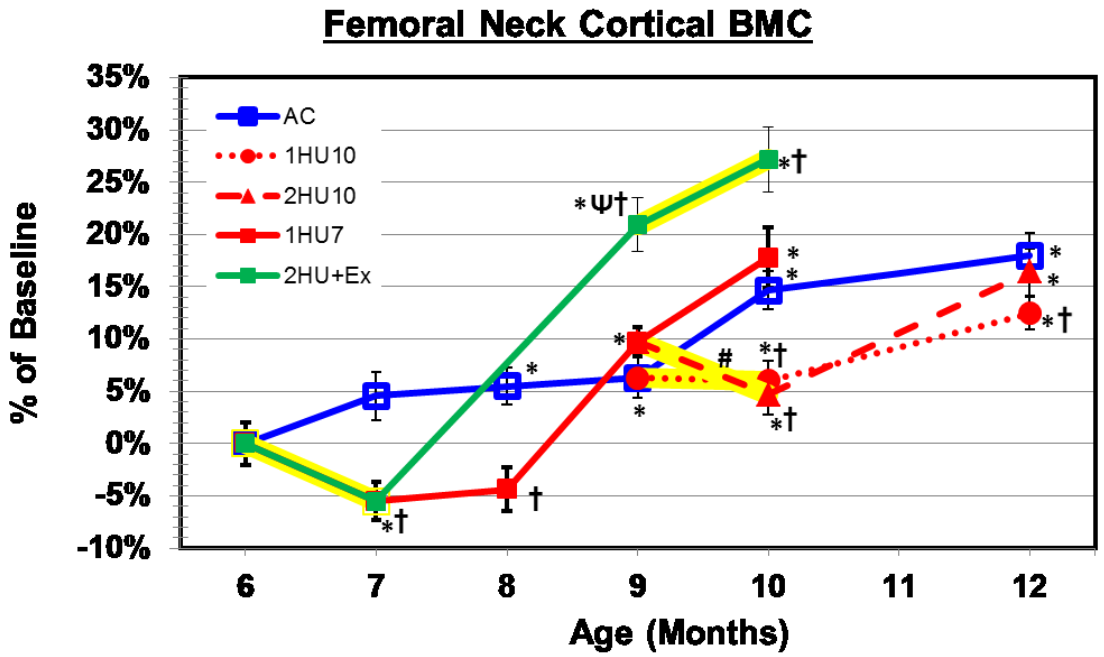

Figure 15: Changes in cortical BMC of the right femoral neck. Numerical data are presented in Table 3. Yellow highlighting indicates HU treatment. 1HU7 decreases (-5.51%) from baseline (BL) with a significant difference from AC. The exercised group recovers above baseline, AC (+13.74%), and the 1HU7+R2 (+10.18%) group. After the second unloading period the 1HU10 and 2HU10 are both significantly lower than AC while 2HU10+Ex is higher than AC (+10.90%). Pre- to post-HU values for the 9- 10 month period show significant decreases for the 2HU10 group; however, 2HU10+Ex shows an increase after HU (5.18%, n.s.).

Values are presented as mean ± SE

*** Indicates significant difference from baseline value; p<0.05**

† Indicates significant difference from age-matched cage control value at same time point; p<0.05

 # Indicates significant difference from pre- to post-HU value within same group; p<0.05

Ψ Indicates significant difference between 1HU7+Ex and 1HU7+R2; p<0.05

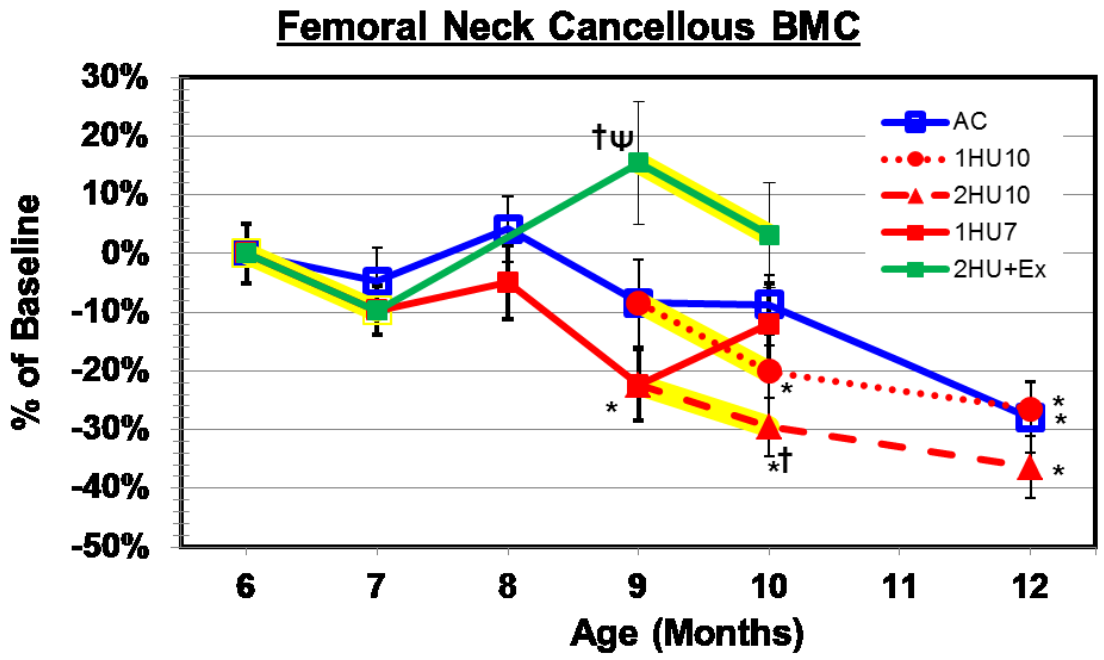

Figure 16: Changes in cancellous BMC of the right femoral neck. Numerical data are presented in Table 3. Yellow highlighting indicates HU treatment. 1HU7 decreases (-9.66%, n.s.) from baseline (BL). The exercised group recovers above AC (+26.11%), and the 1HU7+R2 (+48.89%) group. After the second unloading period the 2HU10 is significantly lower than AC while 2HU10+Ex not significantly different from AC (+13.09%, n.s.). Pre- to post-HU values for the 9- 10 month period show non-significant decreases for the 1HU10, 2HU10, and 2HU10+Ex groups.
Values are presented as mean ± SE
*** Indicates significant difference from baseline value; $p<0.05$**
† Indicates significant difference from age-matched cage control value at same time point; $p<0.05$
 # Indicates significant difference from pre- to post-HU value within same group; $p<0.05$
Ψ Indicates significant difference between 1HU7+Ex and 1HU7+R2; $p<0.05$

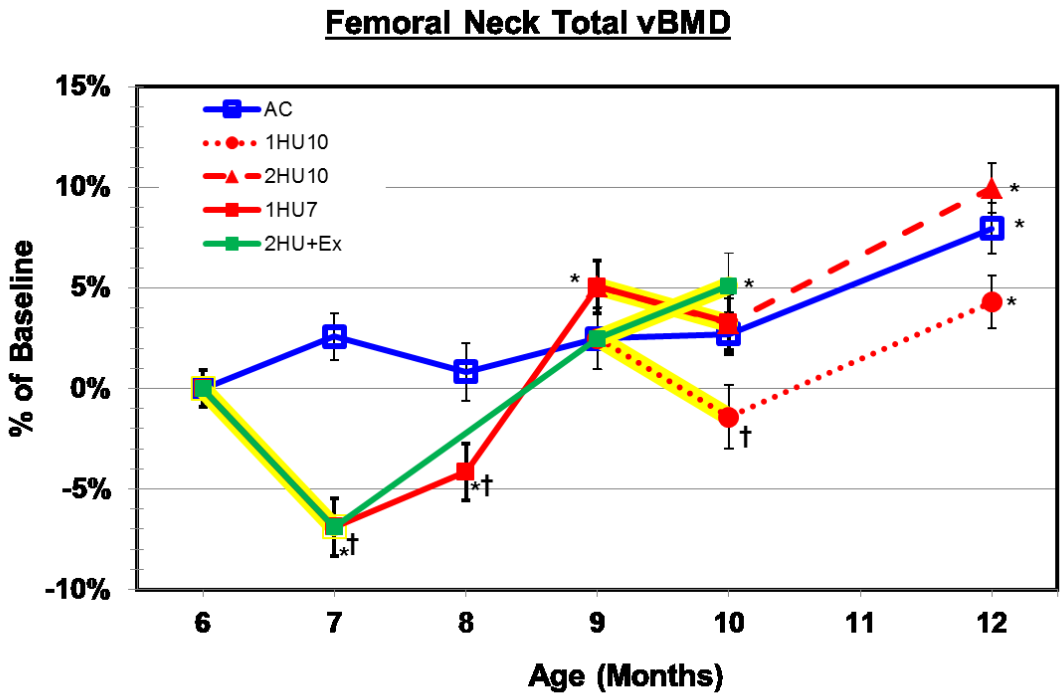

Figure 17: Changes in total vBMD of the right femoral neck. Numerical data are presented in Table 3. Yellow highlighting indicates HU treatment. 1HU7 decreases (-6.90%) from baseline (BL) with a significant difference from AC. At month 9, the exercised group recovers to BL, AC, and 1HU7+R2 level. After the second unloading period the 1HU10 group falls below AC while 2HU10 and 2HU10+Ex are at AC level. Pre- to post-HU values for the 9- 10 month period show decreases for the 2HU10 and 1HU10 groups (n.s), however 2HU10+Ex shows an increase after HU (2.54%, n.s.). Values are presented as mean ± SE
*** Indicates significant difference from baseline value; $p<0.05$**
† Indicates significant difference from age-matched cage control value at same time point; $p<0.05$
 # Indicates significant difference from pre- to post-HU value within same group; $p<0.05$
Ψ Indicates significant difference between 1HU7+Ex and 1HU7+R2; $p<0.05$

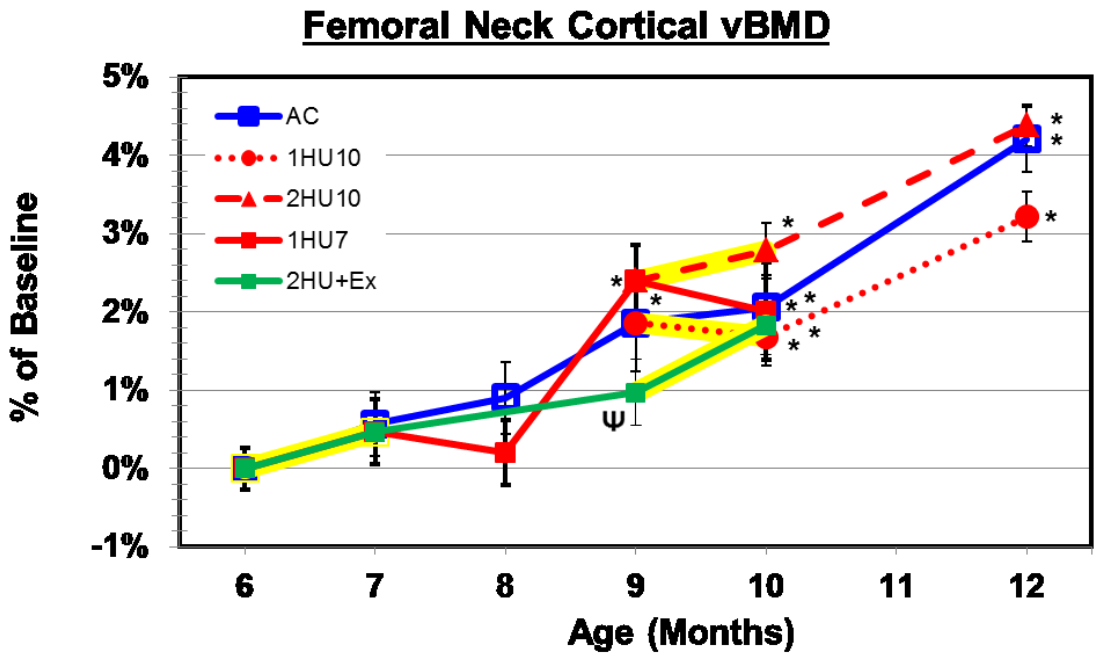

Figure 18: Changes in cortical vBMD of the right femoral neck. Numerical data are presented in Table 3. Yellow highlighting indicates HU treatment. Cortical vBMD shows increases for all groups with variations due to treatments. At month 9, the exercised group falls below 1HU7+R2 level (-1.4%). After the second unloading period all groups are above BL and within AC level. Pre- to post-HU values for the 9- 10 month period show no significant changes.
Values are presented as mean ± SE
*** Indicates significant difference from baseline value; $p<0.05$**
† Indicates significant difference from age-matched cage control value at same time point; $p<0.05$
 # Indicates significant difference from pre- to post-HU value within same group; $p<0.05$
Ψ Indicates significant difference between 1HU7+Ex and 1HU7+R2; $p<0.05$

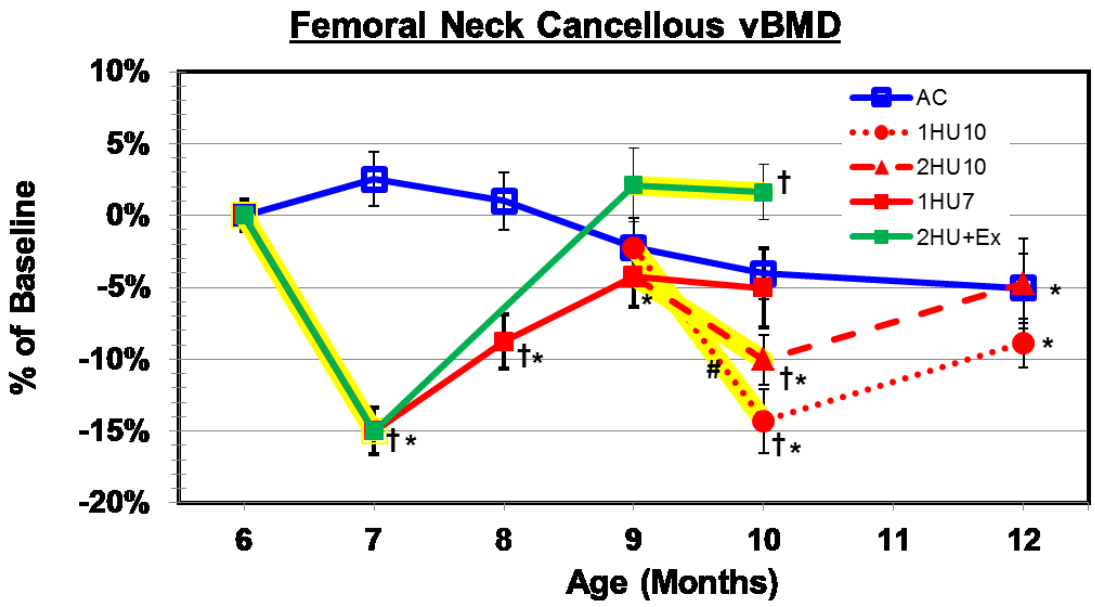

Figure 19: Changes in cancellous vBMD of the right femoral neck. Numerical data are presented in Table 3. Yellow highlighting indicates HU treatment. 1HU7 decreases (-15.01%) from baseline (BL) with a significant difference from AC. At month 9, the exercised group recovers to BL, AC, and 1HU7+R2 level. After the second unloading period the 1HU10 and 2HU10 groups fall below AC while 2HU10+Ex group is significantly higher (+5.88%) than AC. Pre- to post-HU values for the 9-10 month period show significant decreases for the 1HU10 group, however, 2HU10+Ex and 2HU10 groups show slight non-significant decreases after HU.
Values are presented as mean ± SE
*** Indicates significant difference from baseline value; $p<0.05$**
† Indicates significant difference from age-matched cage control value at same time point; $p<0.05$
 # Indicates significant difference from pre- to post-HU value within same group; $p<0.05$
Ψ Indicates significant difference between 1HU7+Ex and 1HU7+R2; $p<0.05$

Femoral Neck Geometric Properties

Table 4 lists absolute values of geometric properties for the right femoral neck. In addition, percent change versus baseline group values are illustrated in total area (Figure 20), cortical area (Figure 21), endocortical area (Figure 22), cortical thickness (Figure 23), maximum moment of inertia (Figure 24), minimum moment of inertia (Figure 25), and polar moment of inertia (Figure 26).

Total femoral neck area reveals no differences pre- to post-HU. The only differences occur at month nine and ten. 2HU+Ex total area at nine months of age (1HU7+Ex, data point after two months of exercise recovery but before 2nd hindlimb unloading bout) and 10 months of age (2HU10+Ex, data point after two months of exercise recovery and after 2nd hindlimb unloading bout) is significantly greater than AC and BL while 2HU10 is significantly lower than AC10. Cortical area is more affected by HU. There is a significant pre- to post-HU decrease for 1HU7 and 2HU10 (1st and 2nd hindlimb unloading periods of ambulatory recovery group).

Similar to the total area,1HU7+Ex and 2HU10+Ex cortical area is significantly greater than aging control and baseline while 2HU10 and 1HU10 is significantly lower than aging control at month 10. Endocortical area shows no change due to HU treatment. Cortical thickness follows a similar pattern as cortical area for the exercise during recovery rats. There is a significant pre- to post-HU decrease for 1HU7. At month 9 cortical thickness is only higher than AC9 for the 2HU+R2 group and at month 10 1HU10 falls below AC10.

Maximum moment of inertia shows few changes for non–exercised groups. With exercise during recovery, 1HU7+Ex recovers above baseline (+33%) and AC9 (+34%). After the second HU, 2HU10+Ex remains above baseline while 2HU10 falls below AC10. Minimum moment of inertia of the cortical bone area also demonstrates the same patterns are maximum moment of inertia. Polar moment of inertia also follows the same trends; however, 2HU10+Ex remains above baseline and AC10 after the 2nd HU.

Table 4: Geometric properties for the right femoral neck

	Total Area (mm^2)	Endocortical Area (mm^2)	Cortical Area (mm^2)	Cortical Thickness (μm)	I_{max} (mm^4)	I_{min} (mm^4)	I_p (mm^4)
6 Months Old							
BL6	4.43 (0.11)	2.11 (0.10)	2.32 (0.05)	0.37 (0.01)	2.54 (0.10)	1.39 (0.05)	3.93 (0.14)
7 Months Old							
AC7	4.38 (0.14)	1.96 (0.11)	2.42 (0.05)	0.39 (0.01)*	2.59 (0.15)	1.38 (0.06)	4.00 (0.20)
1HU7	4.42 (0.12)	2.24 (0.11)	2.19 (0.04)*†	0.34 (0.01)*†	2.32 (0.07)	1.37 (0.05)	3.69 (0.11)
8 Months Old							
AC8	4.62 (0.15)	2.18 (0.13)	2.43 (0.05)*	0.38 (0.01)	2.69 (0.13)	1.53 (0.07)*	4.22 (0.19)
1HU7+R1	4.41 (0.16)	2.19 (0.14)	2.22 (0.05)†	0.35 (0.01)†	2.41 (0.13)	1.32 (0.06)†	3.73 (0.17)
9 Months Old							
AC9	4.39 (0.17)	1.96 (0.15)	2.43 (0.04)*	0.40 (0.01)*	2.52 (0.17)	1.49 (0.07)	4.01 (0.24)
1HU7+R2	4.19 (0.13)	1.69 (0.12)*	2.49 (0.04)*	0.42 (0.01)*	2.45 (0.10)	1.40 (0.08)	3.85 (0.15)
1HU7+Ex	5.16 (0.23)*Ψ†	2.37 (0.21)Ψ	2.78 (0.06)*Ψ†	0.42 (0.01)*†	3.39 (0.17)*Ψ†	1.78 (0.11)*Ψ†	5.16 (0.26)*Ψ†
10 Months Old							
AC10	4.62 (0.13)	2.01 (0.11)	2.61 (0.04)*	0.42 (0.01)*	2.98 (0.15)*	1.56 (0.06)*	4.54 (0.20)*
1HU7+R3	4.64 (0.19)	1.95 (0.14)	2.69 (0.07)*	0.43 (0.01)*	2.98 (0.17)*	1.62 (0.12)*	4.60 (0.26)*
1HU10	4.39 (0.13)	1.97 (0.12)	2.42 (0.04)*†	0.39 (0.01)*†	2.56 (0.15)	1.45 (0.05)	4.02 (0.19)
2HU10	4.02 (0.14)*†	1.65 (0.11)*†	2.37 (0.04)†#	0.41 (0.01)*	2.28 (0.13)†	1.31 (0.07)†	3.59 (0.19)†
2HU10+Ex	5.04 (0.14)*†	2.14 (0.17)	2.90 (0.07)*†	0.45 (0.02)*	3.42 (0.15)*	1.74 (0.05)*	5.15 (0.19)*†
12 Months Old							
AC12	4.22 (0.13)	1.59 (0.11)*	2.63 (0.05)*	0.45 (0.01)*	2.62 (0.13)	1.47 (0.06)	4.09 (0.19)
1HU10+R2	4.25 (0.13)	1.71 (0.11)*	2.53 (0.04)*†	0.43 (0.01)*	2.54 (0.15)	1.45 (0.05)	3.99 (0.19)
2HU10+R2	4.00 (0.12)*	1.40 (0.10)*	2.60 (0.05)*	0.46 (0.01)*	2.38 (0.11)	1.36 (0.06)	3.73 (0.18)

Values are presented as mean ± SE

*** Indicates significant difference from baseline value, $p < 0.05$**

† Indicates significant difference from age-matched control value at same time point, $p<0.05$

 # Indicates significant difference from pre- to post-HU value within same group, $p<0.05$

Ψ Indicates significant difference from 1HU7+Ex to 1HU7+R2, $p<0.05$

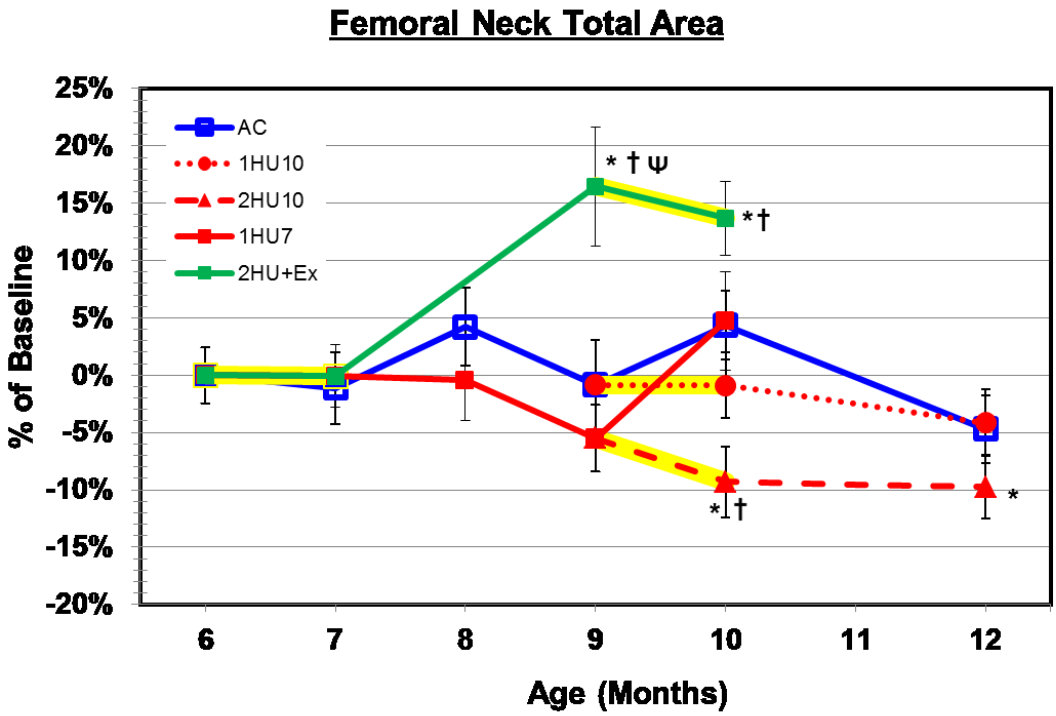

Figure 20: Changes in total area of the right femoral neck. Numerical data are presented in Table 4. Yellow highlighting indicates HU treatment. 1HU7 shows no significant differences from baseline (BL) or AC. At month 9, the exercised group recovers above BL, AC (+17.45%), and 1HU7+R2 (23.24%). After the second unloading period the 1HU10 (n.s.) and 2HU10 groups fall below AC while 2HU10+Ex group is significantly higher (+8.95%) than AC. Pre- to post-HU values for the 9-10 month period show non-significant decreases for all groups.
Values are presented as mean ± SE
*** Indicates significant difference from baseline value; $p<0.05$**
† Indicates significant difference from age-matched cage control value at same time point; $p<0.05$
 # Indicates significant difference from pre- to post-HU value within same group; $p<0.05$
Ψ Indicates significant difference between 1HU7+Ex and 1HU7+R2; $p<0.05$

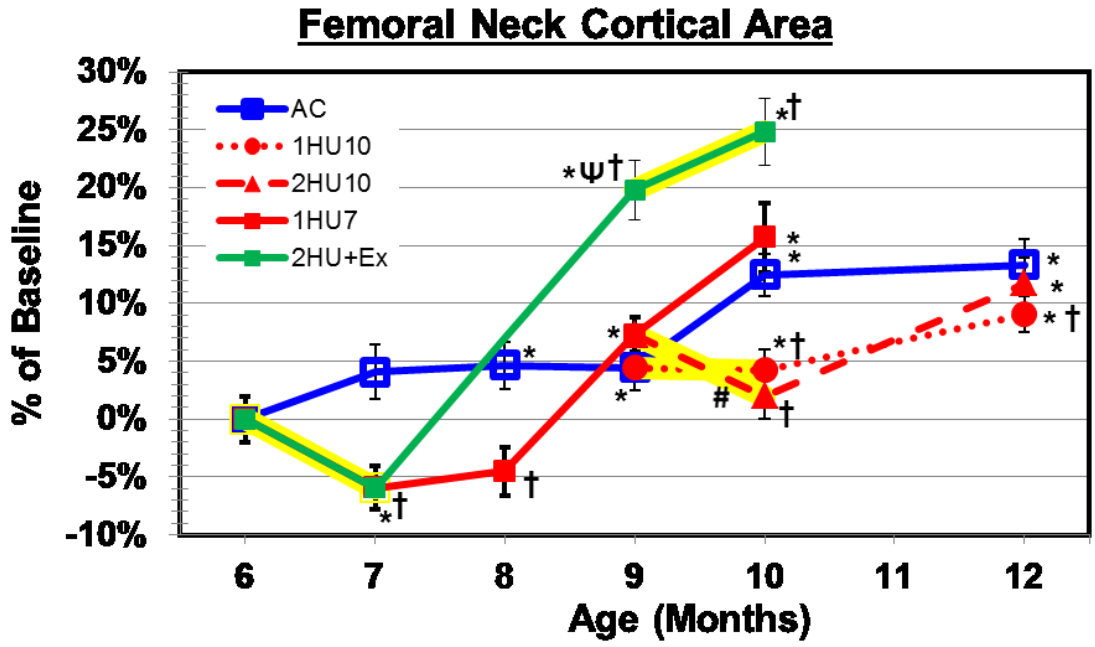

Figure 21: Changes in total area of the right femoral neck. Numerical data are presented in Table 4. Yellow highlighting indicates HU treatment. 1HU7 decreases (-5.92%) from baseline (BL) with a significant difference from AC. The exercised group recovers above baseline, AC (+14.70%), and the 1HU7+R2 (+11.65%) group. After the second unloading period the 1HU10 and 2HU10 are both significantly lower than AC while 2HU10+Ex is higher than AC (+10.98%). Pre- to post-HU values for the 9- 10 month period shows significant decreases for the 2HU10 group, however 2HU10+Ex shows an increase after HU (4.21%, n.s.).
Values are presented as mean ± SE
*** Indicates significant difference from baseline value; p<0.05**
† Indicates significant difference from age-matched cage control value at same time point; p<0.05
 # Indicates significant difference from pre- to post-HU value within same group; p<0.05
Ψ Indicates significant difference between 1HU7+Ex and 1HU7+R2; p<0.05

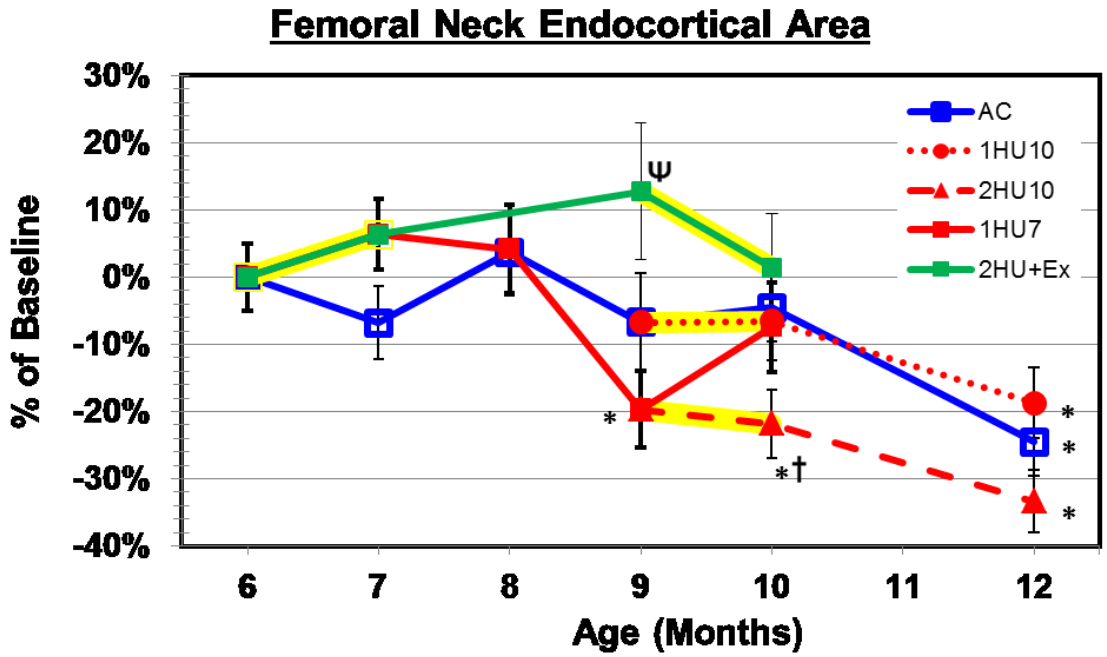

Figure 22: Changes in endocortical area of the right femoral neck. Numerical data are presented in Table 4. Yellow highlighting indicates HU treatment. Endocortical area fluctuates as the animal age. At month 9 the exercised group recovers above (+48.89%) the 1HU7+R2 group. After the second unloading period the 2HU10 is significantly lower than AC while 2HU10+Ex not significantly different from AC (+6.24%, n.s.). Pre- to post-HU values for the 9- 10 month period show non-significant changes for the 1HU10, 2HU10, and 2HU10+Ex groups.
Values are presented as mean ± SE
*** Indicates significant difference from baseline value; $p<0.05$**
† Indicates significant difference from age-matched cage control value at same time point; $p<0.05$
 # Indicates significant difference from pre- to post-HU value within same group; $p<0.05$
Ψ Indicates significant difference between 1HU7+Ex and 1HU7+R2; $p<0.05$

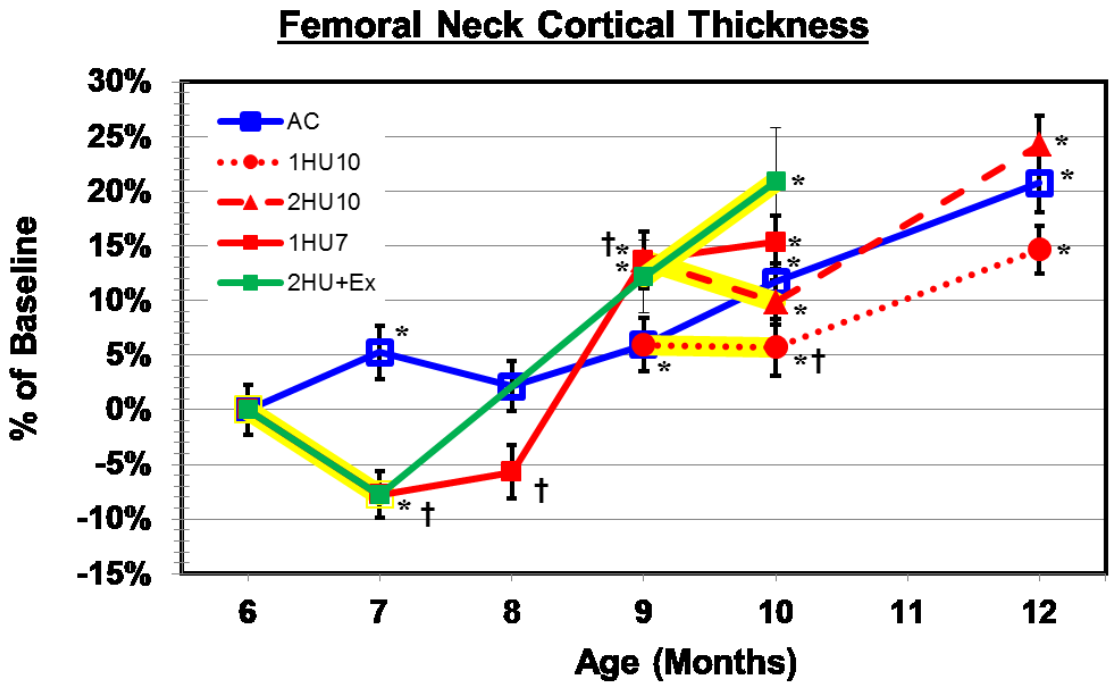

Figure 23: Changes in cortical thickness of the right femoral neck. Numerical data are presented in Table 4. Yellow highlighting indicates HU treatment. 1HU7 decreases (-7.75%) from baseline (BL) with a significant difference from AC. After recovery the exercised group recovers to 1HU7+R2 and AC level. After the second unloading period the 1HU10 group is significantly lower than AC while 2HU10+Ex and 2HU10 groups are at AC level. Pre- to post-HU values for the 9- 10 month period shows non-significant decreases for the 2HU10 and 1HU10 groups, however 2HU10+Ex shows an increase after HU (+7.77%, n.s.).
Values are presented as mean ± SE
*** Indicates significant difference from baseline value; $p<0.05$**
† Indicates significant difference from age-matched cage control value at same time point; $p<0.05$
 # Indicates significant difference from pre- to post-HU value within same group; $p<0.05$
Ψ Indicates significant difference between 1HU7+Ex and 1HU7+R2; $p<0.05$

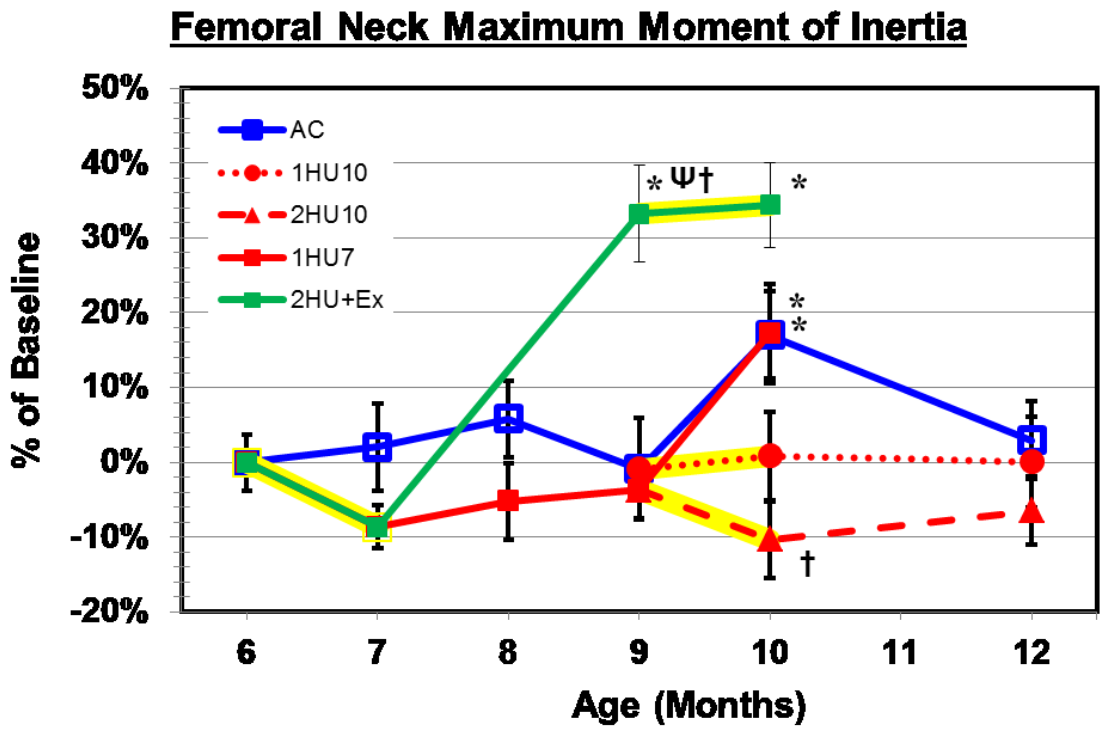

Figure 24: Changes in maximum moment of inertia of the right femoral neck. Numerical data are presented in Table 4. Yellow highlighting indicates HU treatment. 1HU7 has no significant effects. After recovery the exercised group recovers above 1HU7+R2 (+38.33%) and AC level (34.26%). After the second unloading period the 2HU10 group is significantly lower than AC while 2HU10+Ex is above (+14.84%) AC. Pre- to post-HU values for the 9- 10 month period show non-significant changes for all groups.
Values are presented as mean ± SE
*** Indicates significant difference from baseline value; $p<0.05$**
† Indicates significant difference from age-matched cage control value at same time point; $p<0.05$
 # Indicates significant difference from pre- to post-HU value within same group; $p<0.05$
Ψ Indicates significant difference between 1HU7+Ex and 1HU7+2; $p<0.05$

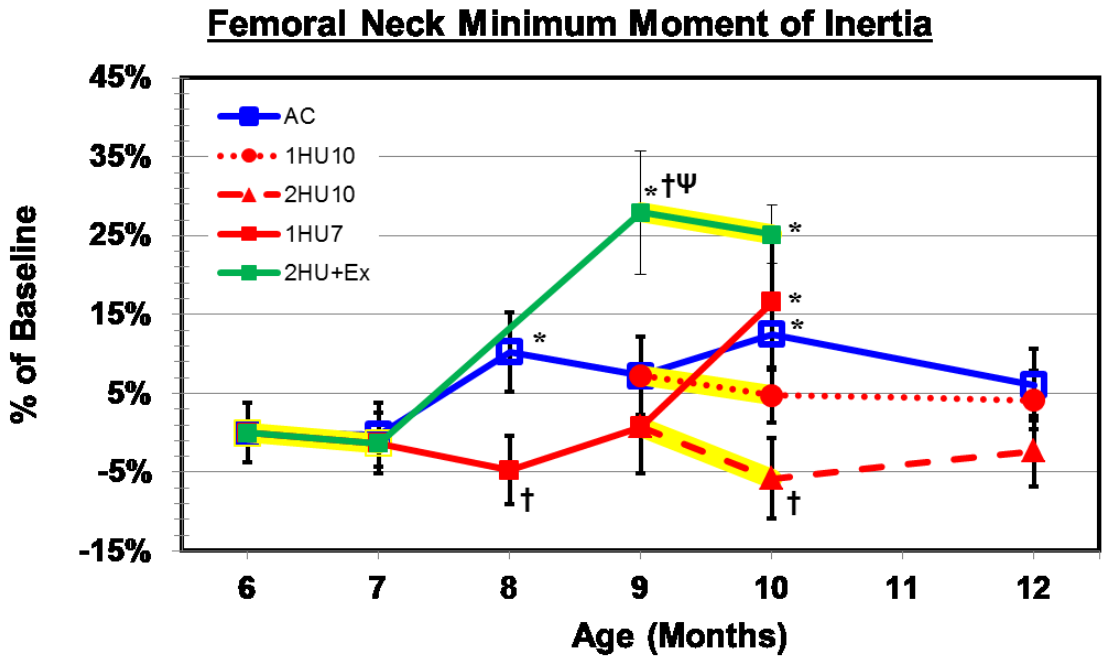

Figure 25: Changes in minimum moment of inertia of the right femoral neck. Numerical data are presented in Table 4. Yellow highlighting indicates HU treatment. 1HU7 has no significant effects. After recovery the exercised group recovers above 1HU7+R2 (+26.99%) and AC level (19.28%). After the second unloading period the 2HU10 group is significantly lower than AC while 2HU10+Ex is above (+11.25%) AC. Pre- to post-HU values for the 9- 10 month period show non-significant changes for all groups.
Values are presented as mean ± SE
*** Indicates significant difference from baseline value; p<0.05**
† Indicates significant difference from age-matched cage control value at same time point; p<0.05
 # Indicates significant difference from pre- to post-HU value within same group; p<0.05
Ψ Indicates significant difference between 1HU7+Ex and 1HU7+2; p<0.05

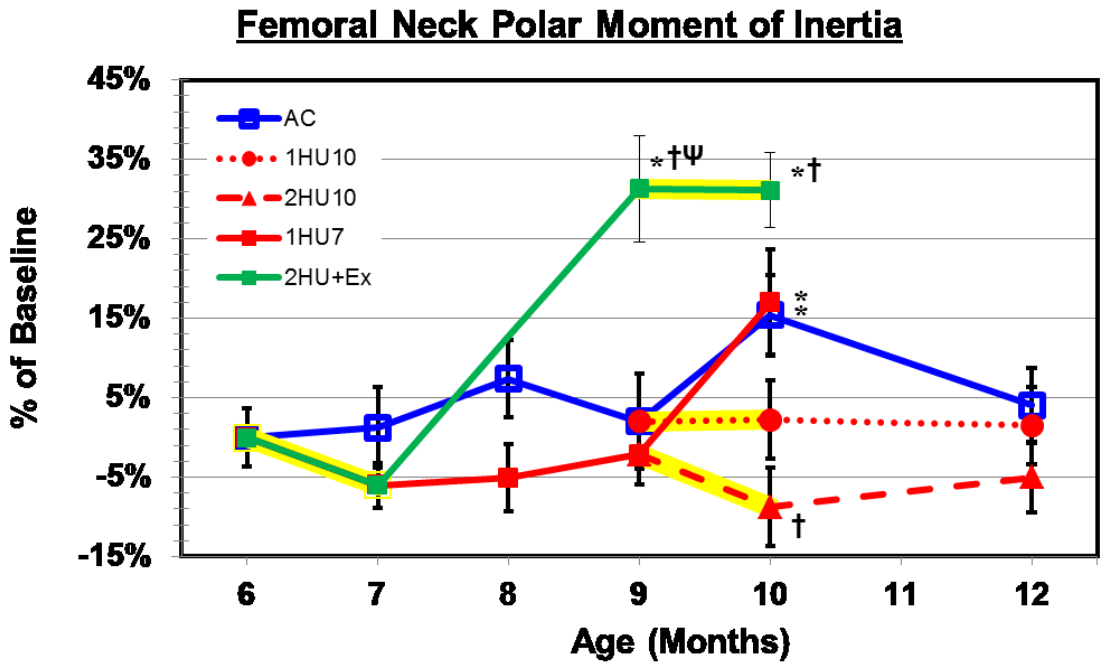

Figure 26: Changes in polar moment of inertia of the right femoral neck. Numerical data are presented in Table 4. Yellow highlighting indicates HU treatment. 1HU7 has no significant effects. After recovery the exercised group recovers above 1HU7+R2 (+34.21%) and AC level (28.76%). After the second unloading period the 2HU10 group is significantly lower than AC while 2HU10+Ex is above (+13.60%) AC. Pre- to post-HU values for the 9- 10 month period show non-significant changes for all groups.
Values are presented as mean ± SE
*** Indicates significant difference from baseline value; $p<0.05$**
† Indicates significant difference from age-matched cage control value at same time point; $p<0.05$
 # Indicates significant difference from pre- to post-HU value within same group; $p<0.05$
Ψ Indicates significant difference between 1HU7+Ex and 1HU7+R2; $p<0.05$

Femoral Neck Calculated Strengths

Table 5 lists absolute values of calculated strengths for the right FN. Structural strength index (SSI) is taken directly from the pQCT scanner. SSI (Figure 27) is a function of polar moment of inertia of the total bone area and the maximum distance to the center. The pattern of change for SSI shows very few differences from that for polar moment of inertia. There are few changes for non–exercised groups. However, after the recovery period 1HU7+Ex exceeds baseline (+29%) and AC9 (+25%). After the second HU, 2HU10+Ex remains above baseline while 2HU10 falls below AC10.

Compressive strength index (CSI) (Figure 28) is a product of the square of total density and total area. 1HU7 decreases substantially from baseline and remains below AC until month 9. Following recovery 1HU7+Ex values increase above BL and AC9. 1HU10 and 2HU10 present significant decreases pre- to post- HU while 2HU10+Ex shows a slight non-significant increase. Following a 2nd HU bout 1HU10 and 2HU10 fall below AC10 while 2HU10+Ex remains above.

Bending strength index (BSI) (Figure 29) has similar trends as polar moment of inertia. There are few changes for non–exercised groups. After recovery period 1HU7+Ex recovers to above baseline and AC9. After the second HU, 2HU10+Ex remains above baseline while 2HU10 falls below AC10.

Table 5: Calculated strengths for right femoral neck from pQCT

	SSI (mm^3)	CSI (mg^2/mm^4)	BSI (mm^3)
6 Months Old			
BL6	2.19 (0.08)	5.52 (0.09)	1.65 (0.04)
7 Months Old			
AC7	2.16 (0.10)	5.75 (0.11)*	1.68 (0.06)
1HU7	2.21 (0.09)	4.80 (0.13)*†	1.55 (0.03)
8 Months Old			
AC8	2.37 (0.12)	5.85 (0.11)*	1.73 (0.05)
1HU7+R1	2.22 (0.14)	5.06 (0.12)*†	1.57 (0.05)†
9 Months Old			
AC9	2.25 (0.14)	5.74 (0.13)	1.68 (0.06)
1HU7+R2	2.05 (0.12)	5.77 (0.11)*	1.66 (0.04)
1HU7+Ex	2.82 (0.19)*Ψ†	6.73 (0.19)*Ψ†	2.01 (0.06)*Ψ†
10 Months Old			
AC10	2.38 (0.11)	6.07 (0.10)*	1.86 (0.05)*
1HU7+R3	2.40 (0.16)	6.17 (0.18)*	1.88 (0.07)*
1HU10	2.18 (0.09)	5.31 (0.08)†#	1.69 (0.06)†
2HU10	1.95 (0.10)†	5.34 (0.12)†#	1.58 (0.06)†
2HU10+Ex	2.70 (0.11)*	6.93 (0.13)*†	2.03 (0.05)*†
12 Months Old			
AC12	2.06 (0.09)	6.16 (0.14)*	1.76 (0.06)
1HU10+R2	2.12 (0.09)	5.75 (0.06)*†	1.71 (0.06)
2HU10+R2	1.91 (0.08)	6.04 (0.14)*	1.65 (0.06)

Values are presented as mean ± SE

*** Indicates significant difference from baseline value, $p < 0.05$**

† Indicates significant difference from age-matched control value at same time point, $p<0.05$

 # Indicates significant difference from pre- to post-HU value within same group, $p<0.05$

Ψ Indicates significant difference from 1HU7+Ex to 1HU7+R2, $p<0.05$

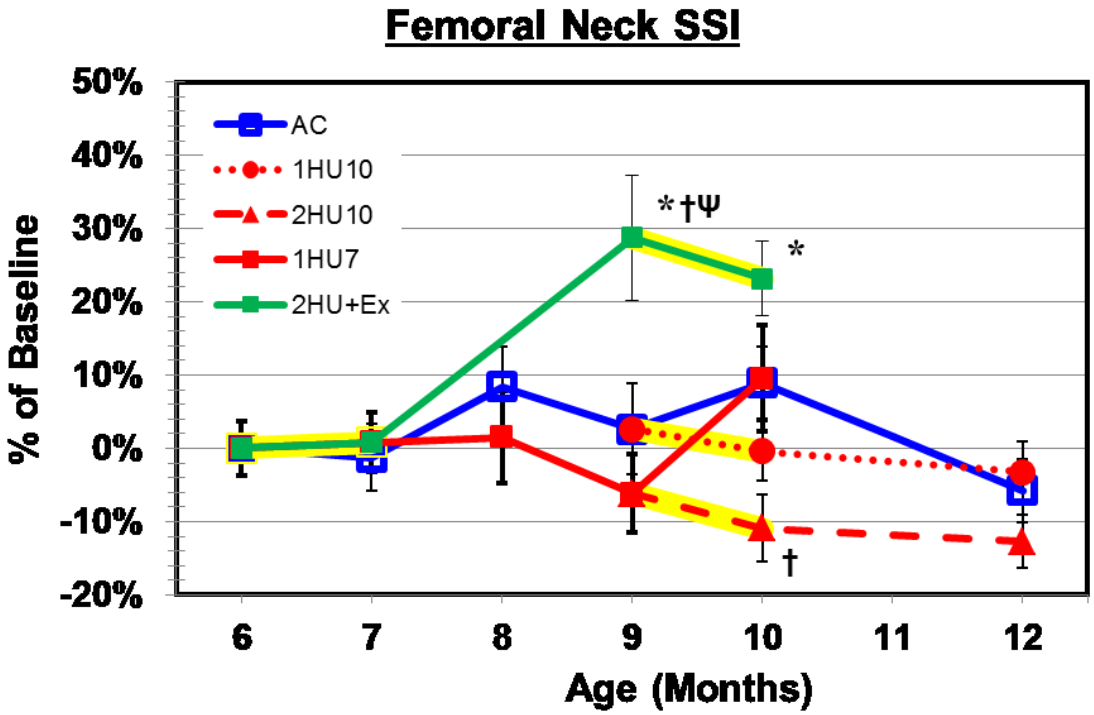

Figure 27: Changes in calculated structural strength index of the right femoral neck. Numerical data are presented in Table 5. Yellow highlighting indicates HU treatment. 1HU7 has no significant effects. After recovery the exercised group recovers above 1HU7+R2 (+37.22%) and AC level (25.44%). After the second unloading period the 2HU10 group is significantly lower than AC while 2HU10+Ex is non-significantly above AC. Pre- to post-HU values for the 9- 10 month period show non-significant changes for all groups.
Values are presented as mean ± SE
*** Indicates significant difference from baseline value; p<0.05**
† Indicates significant difference from age-matched cage control value at same time point; p<0.05
 # Indicates significant difference from pre- to post-HU value within same group; p<0.05
Ψ Indicates significant difference between 1HU7+Ex and 1HU7+R2; p<0.05

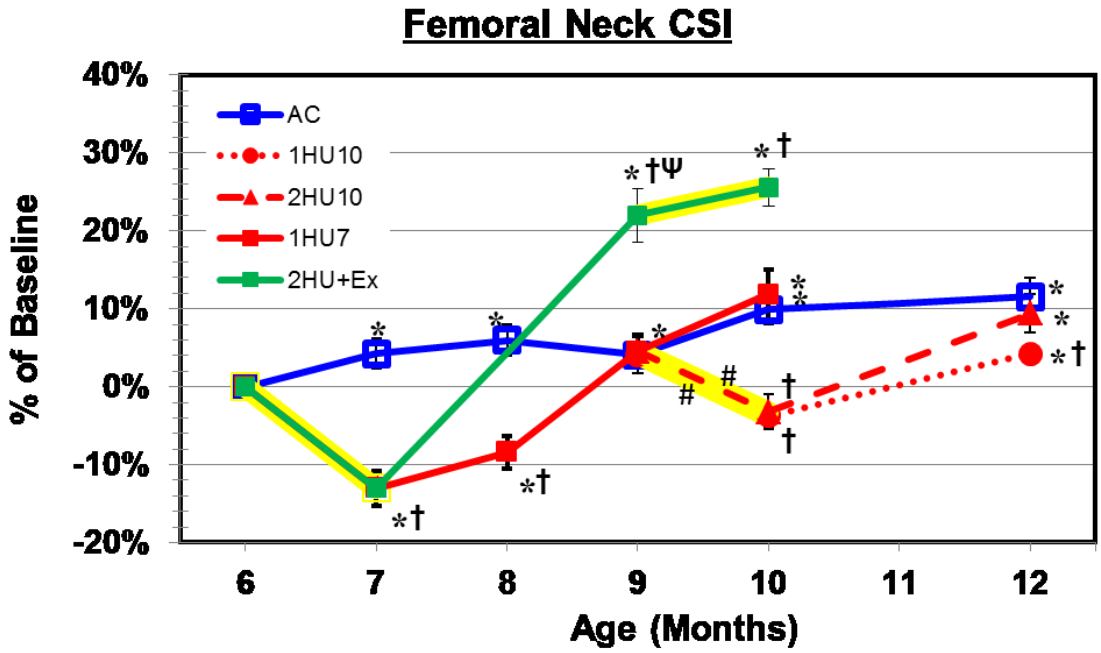

Figure 28: Changes in calculated compressive strength index of right femoral neck. Numerical data are presented in Table 5. Yellow highlighting indicates HU treatment. 1HU7 decreases (-13.05%) from baseline (BL) with a significant difference from AC. After recovery the exercised group recovers above 1HU7+R2 (+16.67%) and AC level (+17.23%). After the second unloading period the 2HU10 and 1HU10 groups are significantly lower than AC while 2HU10+Ex is above AC (+14.27%). Pre- to post-HU values for the 9- 10 month period show significant decreases for the 1HU10 and 2HU10 groups, however, 2HU10+Ex group shows a slight (+2.95%, n.s) increase.
Values are presented as mean ± SE
*** Indicates significant difference from baseline value; $p<0.05$**
† Indicates significant difference from age-matched cage control value at same time point; $p<0.05$
 # Indicates significant difference from pre- to post-HU value within same group; $p<0.05$
Ψ Indicates significant difference between 1HU7+Ex and 1HU7+R2; $p<0.05$

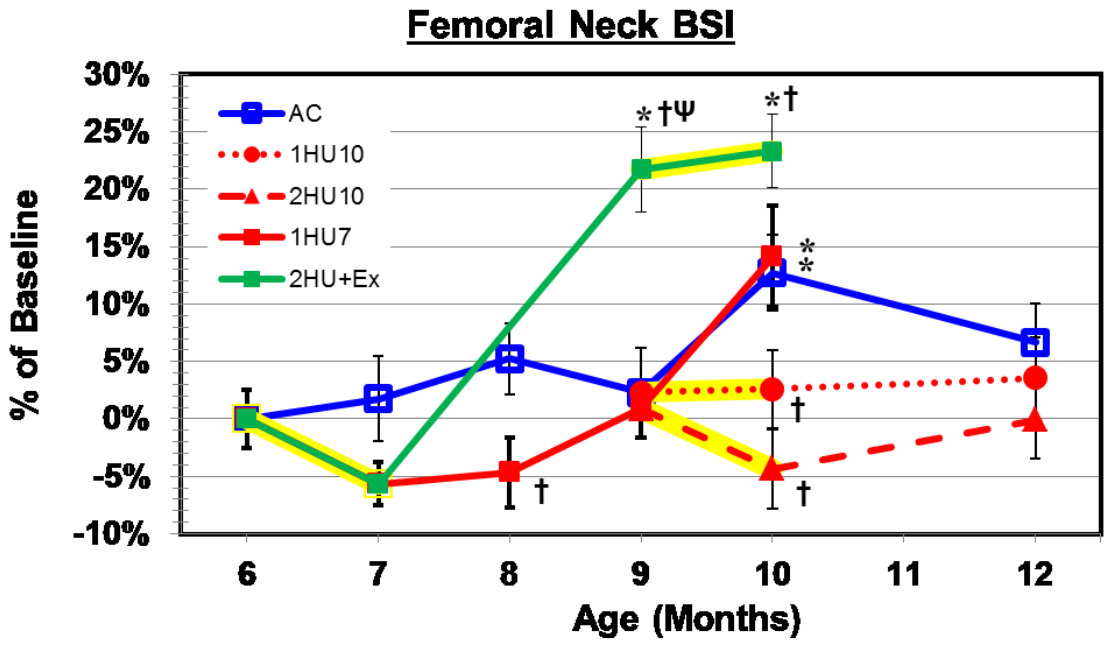

Figure 29: Changes in calculated bending strength index of the right femoral neck. Numerical data are presented in Table 5. Yellow highlighting indicates HU treatment. 1HU7 has no significant effects. After recovery the exercised group recovers above 1HU7+R2 (+20.70%) and AC level (19.03%). After the second unloading period the 2HU10 and 1HU10 groups are significantly lower than AC while 2HU10+Ex is higher than AC (+9.38%). Pre- to post-HU values for the 9- 10 month period show non-significant changes for all groups.
Values are presented as mean ± SE
*** Indicates significant difference from baseline value; p<0.05**
† Indicates significant difference from age-matched cage control value at same time point; p<0.05
 # Indicates significant difference from pre- to post-HU value within same group; p<0.05
Ψ Indicates significant difference between 1HU7+Ex and 1HU7+R2; p<0.05

Femoral Neck Mechanical Properties

Table 6 lists absolute values for mechanical properties for axial and lateral FN testing. Right femoral necks were tested in the axial direction while left femoral necks were tested in the lateral direction. Due to the loading configuration there are several stresses at the femoral neck, including bending, shear, and compressive. Therefore, only ultimate force and stiffness are reported.

Both axial (Figure 30) and lateral (Figure 32) maximum force change in a similar fashion with exercise during recovery, the difference being in the magnitude of change. Maximum force in 1HU7 is significantly lower than in baseline controls (-17.5% axial, -11.9% lateral) and in AC. After exercise 1HU7+Ex recovers above 1HU7+R2 (+30.9% axial, +27.0% lateral) and AC9 (+38.0% axial, +20.6% lateral). 1HU10 and 2HU10 both experience significant decreases in maximum force pre- to post-HU. 2HU10+Ex does not illustrate a significant decrease for the axial testing configuration, whereas the lateral testing maximum force actually reveals an increase pre- to post-HU; however, this increase is not significant. After the second HU bout for both axial and lateral 2HU10+Ex recovers above AC10 and baseline while 1HU10 and 2HU10 remain below.

Axial femoral neck stiffness (Figure 31) reveals no differences among groups until month 9, when all groups' values surpass baseline values. After the second bout of HU, 1HU10 falls below AC12. Lateral femoral neck stiffness (Figure 33) also shows no differences among groups until month 9. Lateral and axial stiffness values at 1HU7+Ex increase above BL. Pre- to post- HU changes are significantly lower for both 2HU10 and

1HU10. After the 2nd bout of HU 2HU10+Ex remains above AC and baseline; however, 2HU remains significantly lower than AC10.

Table 6: Mechanical properties for axial and lateral femoral neck testing

	Axial Maximum Force (N)	Axial Stiffness (N/mm)	Lateral Maximum Force (N)	Lateral Stiffness (N/mm)
6 Months Old				
BL6	95.34 (2.40)	145.53 (6.16)	94.31 (2.10)	56.48 (1.89)
7 Months Old				
AC7	97.55 (2.82)	135.09 (9.61)	97.00 (2.62)	62.12 (2.23)
1HU7	78.69 (2.18)*†	138.12 (10.26)	83.12 (1.73)*†	56.99 (1.75)
8 Months Old				
AC8	99.34 (2.24)	149.77 (9.87)	94.86 (2.75)	63.29 (3.10)
1HU7+R1	95.53 (3.60)	165.81 (8.51)	84.69 (3.79)*†	58.92 (2.86)
9 Months Old				
AC9	97.45 (3.20)	169.81 (5.75)*	93.94 (3.97)	65.45 (2.96)*
1HU7+R2	102.74 (3.20)*	178.93 (8.26)*	89.2 (2.17)	63.41 (3.01)
1HU7+Ex	134.53 (4.63)*†Ψ	195.94 (15.73)*	113.28 (2.85)*†Ψ	67.94 (4.18)*
10 Months Old				
AC10	110.31 (3.17)*	180.48 (6.98)*	95.84 (1.73)	62.37 (2.31)
1HU7+R3	114.85 (3.58)*	162.82 (10.85)	105.56 (6.05)	69.70 (3.79)*
1HU10	84.40 (3.89)*†#	156.92 (9.05)†	83.72 (2.71)*†#	55.72 (3.09)#
2HU10	86.43 (3.63)*†#	162.64 (8.50)	72.33 (5.69)*†#	52.77 (3.82)†#
2HU10+Ex	132.86 (4.15)*†	190.50 (13.56)*	118.39 (4.38)*†	72.74 (3.67)*†
12 Months Old				
AC12	97.2 (4.37)	224.62 (30.57)*	92.94 (3.86)	66.53 (2.92)*
1HU10+R2	102.01 (2.16)*	164.17 (7.94)	86.24 (3.34)*	57.09 (2.78)†
2HU10+R2	98.28 (3.76)	235.39 (31.36)*	93.26 (4.60)	67.22 (4.44)*

Values are presented as mean ± SE

*** Indicates significant difference from baseline value, $p < 0.05$**

† Indicates significant difference from age-matched control value at same time point, $p<0.05$

 # Indicates significant difference from pre- to post-HU value within same group, $p<0.05$

Ψ Indicates significant difference from 1HU7+Ex to 1HU7+R2, $p<0.05$

Axial FN Testing

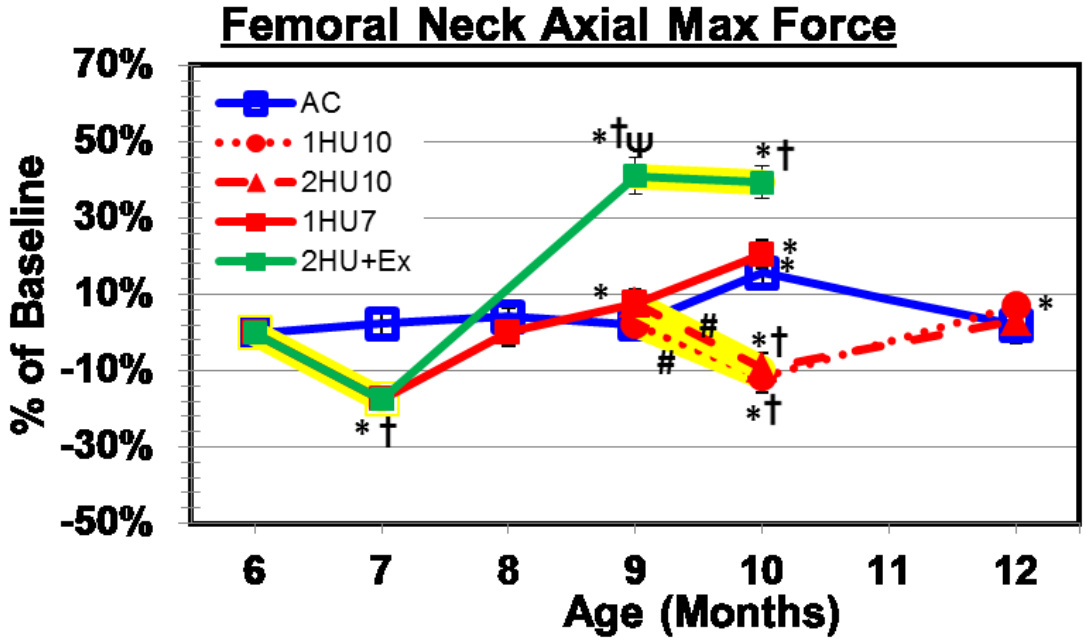

Figure 30: Changes in axial direction mechanical testing maximum force of right femoral neck. Numerical data are presented in Table 6. Yellow highlighting indicates HU treatment. 1HU7 has is significantly lower than BL (-17.47%) and AC. After recovery the exercised group recovers above 1HU7+R2 (+30.94%) and AC level (38.04%). After the second unloading period the 2HU10 and 1HU10 groups are significantly lower than AC while 2HU10+Ex is higher than AC (+20.44%). Pre- to post-HU values for the 9- 10 month period show significant decreases in the 1HU10 and 2HU10 groups while the 2HU10+Ex does not decrease significantly.
Values are presented as mean ± SE
*** Indicates significant difference from baseline value; p<0.05**
† Indicates significant difference from age-matched cage control value at same time point; p<0.05
 # Indicates significant difference from pre- to post-HU value within same group; p<0.05
Ψ Indicates significant difference between 1HU7+Ex and 1HU7+R2; p<0.05

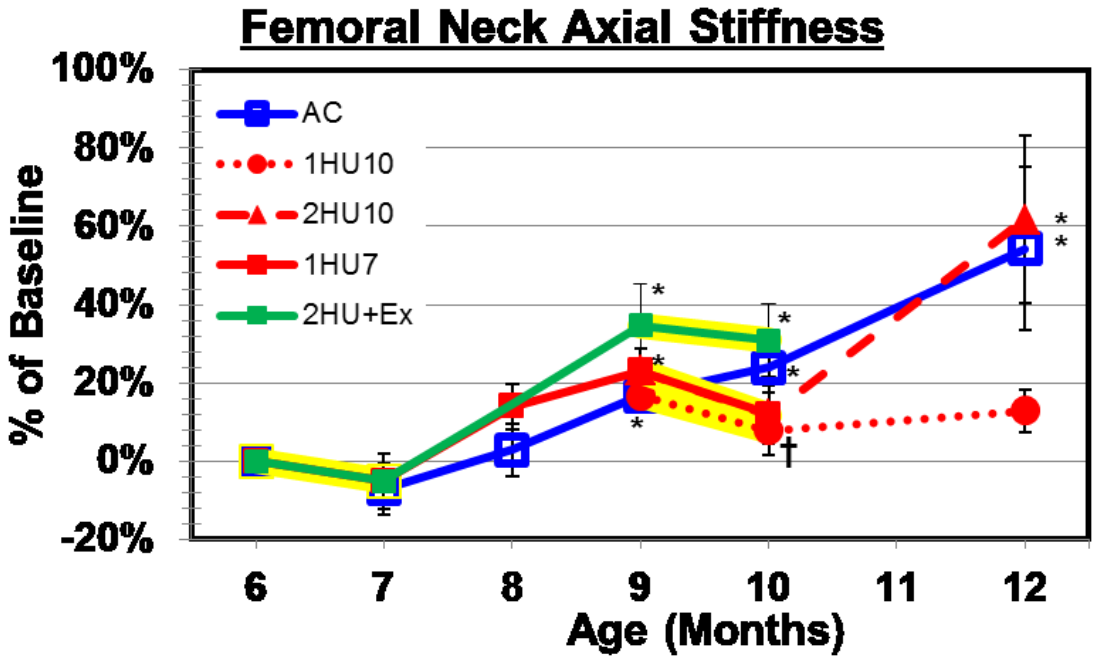

Figure 31: Changes in axial configuration mechanical testing stiffness of right femoral neck. Numerical data are presented in Table 6. Yellow highlighting indicates HU treatment. 1HU7 has no significant effects. After recovery the exercised group recovers to 1HU7+R2 and AC level. After the second unloading period the 1HU10 group is significantly lower than AC while 2HU10+Ex is non-significantly above AC. Pre- to post-HU values for the 9- 10 month period show non-significant changes for all groups.
Values are presented as mean ± SE
*** Indicates significant difference from baseline value; $p<0.05$**
† Indicates significant difference from age-matched cage control value at same time point; $p<0.05$
 # Indicates significant difference from pre- to post-HU value within same group; $p<0.05$
Ψ Indicates significant difference between 1HU7+Ex and 1HU7+R2; $p<0.05$

Lateral FN Testing

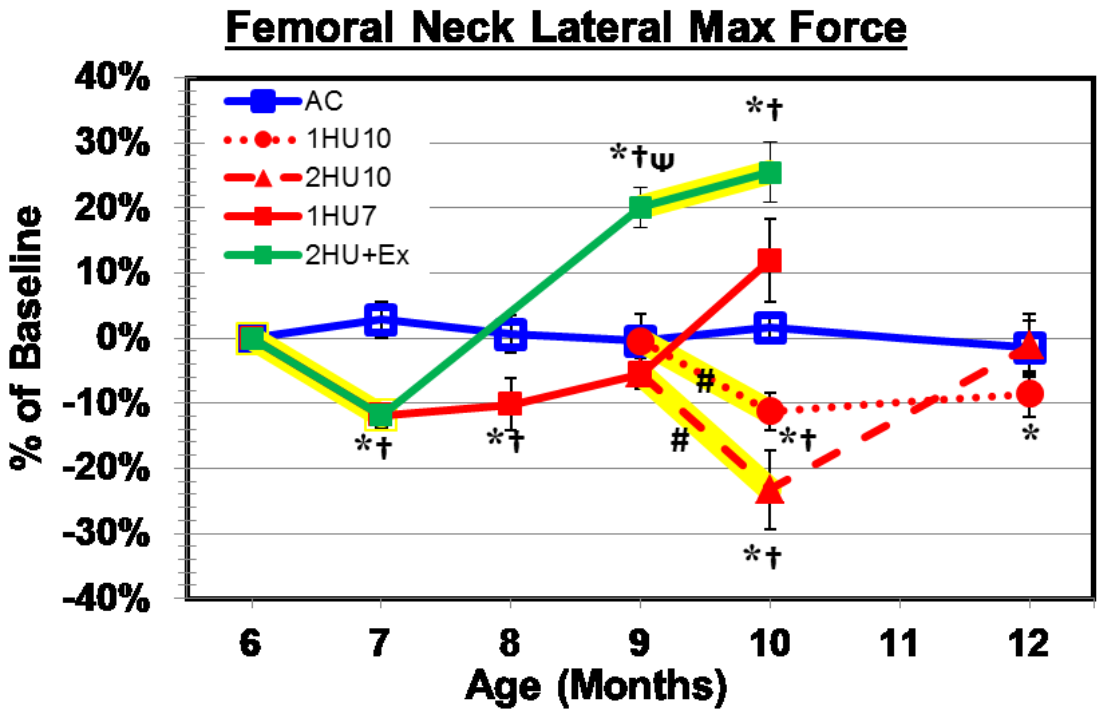

Figure 32: Changes in lateral direction mechanical testing maximum force of left femoral neck. Numerical data are presented in Table 6. Yellow highlighting indicates HU treatment. 1HU7 has is significantly lower than BL (-11.87%) and AC. After recovery the exercised group recovers above 1HU7+R2 (+26.99%) and AC level (20.58%). After the second unloading period the 2HU10 and 1HU10 groups are significantly lower than AC while 2HU10+Ex is higher than AC (+23.53%). Pre- to post-HU values for the 9- 10 month period show significant decreases in the 1HU10 and 2HU10 groups while the 2HU10+Ex group increases slightly (+4.5%, n.s.).
Values are presented as mean ± SE
*** Indicates significant difference from baseline value; p<0.05**
† Indicates significant difference from age-matched cage control value at same time point; p<0.05
 # Indicates significant difference from pre- to post-HU value within same group; p<0.05
Ψ Indicates significant difference between 1HU7+Ex and 1HU7+R2; p<0.05

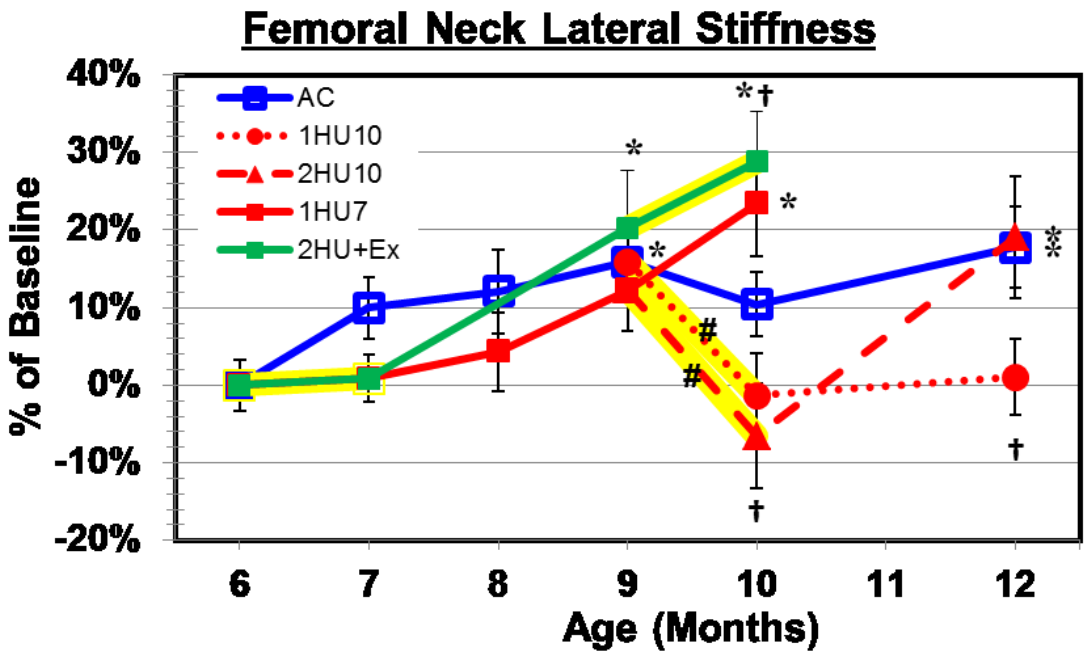

Figure 33: Changes in lateral configuration mechanical testing stiffness of left femoral neck. Numerical data are presented in Table 6. Yellow highlighting indicates HU treatment. 1HU7 has no significant effects. After recovery the exercised group recovers to 1HU7+R2 and AC level. After the second unloading period the 2HU10 group is significantly lower than AC while 2HU10+Ex is significantly above AC (+23.53%). Pre- to post-HU values for the 9- 10 month period show significant decreases in the 1HU10 and 2HU10 groups while the 2HU10+Ex group increases slightly (+7.07%, n.s.).

Values are presented as mean ± SE

*** Indicates significant difference from baseline value; $p<0.05$**

† Indicates significant difference from age-matched cage control value at same time point; $p<0.05$

 # Indicates significant difference from pre- to post-HU value within same group; $p<0.05$

Ψ Indicates significant difference between 1HU7+Ex and 1HU7+R2; $p<0.05$

Femur Diaphysis Densitometric Properties

Table 7 lists absolute values for the densitometric properties of the femur diaphysis. Cortical properties are used because the midshaft diaphysis is composed completely of cortical bone.

Cortical BMC (Figure 34) increases as the animals age. 1HU7 suppresses age-related growth and those values fall below AC. Post recovery there are no differences among groups. Pre- to post-HU vales present non-significant decreases for 2HU10 and 1HU10. 2HU10+Ex experiences a non-significant increase pre- to post-HU. After the second bout of HU 2HU10 and 1HU10 groups have significantly lower cortical BMC than AC10.

Cortical vBMD (Figure 35) also increases as the animal age. 1HU7 has no effect on vBMD. After recovery 1HU7+Ex increases well above BL and AC9 while 1HU7+R2 remains at AC10 level. All three groups show significant increases pre- to post-HU for the second bout of unloading. At month 10, 2HU10+Ex vBMD is significantly greater than AC10 while 2HU10 remains below.

Total area (Figure 36) indicates growth as animals age. All data points are above baseline except for 1HU7. There is a significant increase pre- to post-HU for 2HU10+Ex. Cortical area (Figure 37) reveals similar trends to cortical BMC and to total area. 1HU7 suppresses age related growth and fall below AC. Post recovery there are no differences among groups. Pre-post-HU show non-significant decreases for 2HU10 and 1HU10. 2HU10+Ex experiences a non-significant increase pre- to post-Hu. After the second bout of HU 2HU10 has significantly lower cortical area than AC10.

Cortical thickness (Figure 38) also reveals similar patterns as cortical area. The first HU period (1HU7) suppresses age-related growth and these values fall below AC. Post recovery there are no differences among groups. Pre- to post-HU reveal non-significant decreases for 2HU10+Ex and 1HU10, whereas 2HU10 does have a significant decrease in cortical thickness pre- to post-HU. After the second bout of HU all groups have significantly lower cortical thickness than AC10.

Maximum moment of inertia (Figure 39) also increases as the animals age. There are no differences among groups; the only pre-to post- HU difference is a significant increase for the 2HU10+Ex group. Minimum moment of inertial (Figure 40) also increases with age. The only difference is 2HU10 falls below AC10 value. Polar moment of inertia (Figure 41) trends follow closely with maximum moment of inertia.

Table 7: Femur diaphysis pQCT properties

	Cortical BMC (mg/mm)	Cortical vBMD (mg/cm^3)	Total Area (mm^2)	Cortical Area (mm^2)	Cortical Thickness (μm)	I_{max} (mm^4)	I_{min} (mm^4)	I_p (mm^4)
6 Months Old								
BL6	11.76 (0.15)	1429.3 (2.07)	12.60 (0.16)	8.23 (0.10)	0.82 (0.01)	13.8 (0.34)	9.3 (0.26)	23.08 (0.58)
7 Months Old								
AC7	13.0 (0.22)*	1432.6 (3.01)	13.47 (0.24)*	9.05 (0.15)*	0.89 (0.01)*	15.8 (0.59)*	10.9 (0.33)*	26.8 (0.91)*
1HU7	12.2 (0.23)†	1430.8 (2.37)	13.07 (0.19)	8.54 (0.15)†	0.84 (0.01)†	14.5 (0.48)	10.3 (0.31)*	24.8 (0.77)
8 Months Old								
AC8	13.1 (0.17)*	1442.2 (2.11)*	13.82 (0.20)*	9.10 (0.13)*	0.87 (0.01)*	16.3 (0.48)*	11.5 (0.33)*	27.8 (0.79)*
1HU7+R1	12.6 (0.24)*	1443.8 (2.37)*	13.29 (0.24)*	8.72 (0.16)*	0.85 (0.01)*	14.9 (0.61)	10.7 (0.34)*	25.6 (0.94)*
9 Months Old								
AC9	13.5 (0.31)*	1446.1 (1.68)*	14.06 (0.33)*	9.34 (0.21)*	0.89 (0.01)*	16.8 (0.79)*	12.2 (0.59)*	29.0 (1.35)*
1HU7+R2	13.1 (0.14)*	1447.2 (2.56)*	13.60 (0.20)*	9.07 (0.09)*	0.88 (0.01)*	16.0 (0.52)*	11.1 (0.22)*	27.0 (0.70)*
1HU7+Ex	13.53 (0.24)*	1465.8 (2.51)*Ψ†	13.96 (0.21)*	9.23 (0.16)*	0.88 (0.01)*	16.7 (0.48)*	11.7 (0.41)*	28.4 (0.86)*
10 Months Old								
AC10	13.98 (0.23)*	1465.3 (2.31)*	14.21 (0.23)*	9.54 (0.15)*	0.91 (0.01)*	17.1 (0.54)*	12.5 (0.40)*	29.63 (0.93)*
1HU7+R3	14.1 (0.38)*	1460.8 (2.84)*	14.31 (0.31)*	9.66 (0.26)*	0.92 (0.02)*	17.5 (0.80)*	12.7 (0.52)*	30.2 (1.31)*
1HU10	13.3 (0.21)*†	1458.3 (1.63)*#	13.86 (0.23)*	9.10 (0.15)*	0.87 (0.01)*†	16.4 (0.51)*	11.5 (0.40)*	27.9 (0.89)*
2HU10	12.9 (0.22)*†	1453.9 (1.86)*†#	13.75 (0.26)*	8.86 (0.15)*†	0.85 (0.01)#†	15.9 (0.54)*	11.3 (0.41)*†	27.2 (0.94)*
2HU10+Ex	14.04 (0.20)*	1478.1 (2.47)*†#	14.70 (0.20)*#	9.50 (0.13)*	0.88 (0.01)*†	18.2 (0.50)*#	12.8 (0.38)*	31.03 (0.85)*#
12 Months Old								
AC12	14.6 (0.27)*	1472.5 (2.07)*	14.80 (0.25)*	9.91 (0.18)*	0.92 (0.01)*	18.4 (0.53)*	13.6 (0.54)*	32.0 (1.05)*
1HU10+R2	14.0 (0.28)*	1458.0 (2.17)*†	14.65 (0.24)*	9.59 (0.18)*	0.89 (0.01)*	18.1 (0.63)*	13.0 (0.45)*	31.0 (1.05)*
2HU10+R2	14.1 (0.38)*	1465.3 (1.66)*†	14.49 (0.31)*	9.65 (0.26)*	0.91 (0.02)*	17.5 (0.77)*	13.0 (0.60)*	30.6 (1.34)*

Values are presented as mean ± SE

*** Indicates significant difference from baseline value, $p < 0.05$**

† Indicates significant difference from age-matched control value at same time point, $p<0.05$

 # Indicates significant difference from pre- to post-HU value within same group, $p<0.05$

Ψ Indicates significant difference from 1HU7+Ex to 1HU7+R2, $p<0.05$

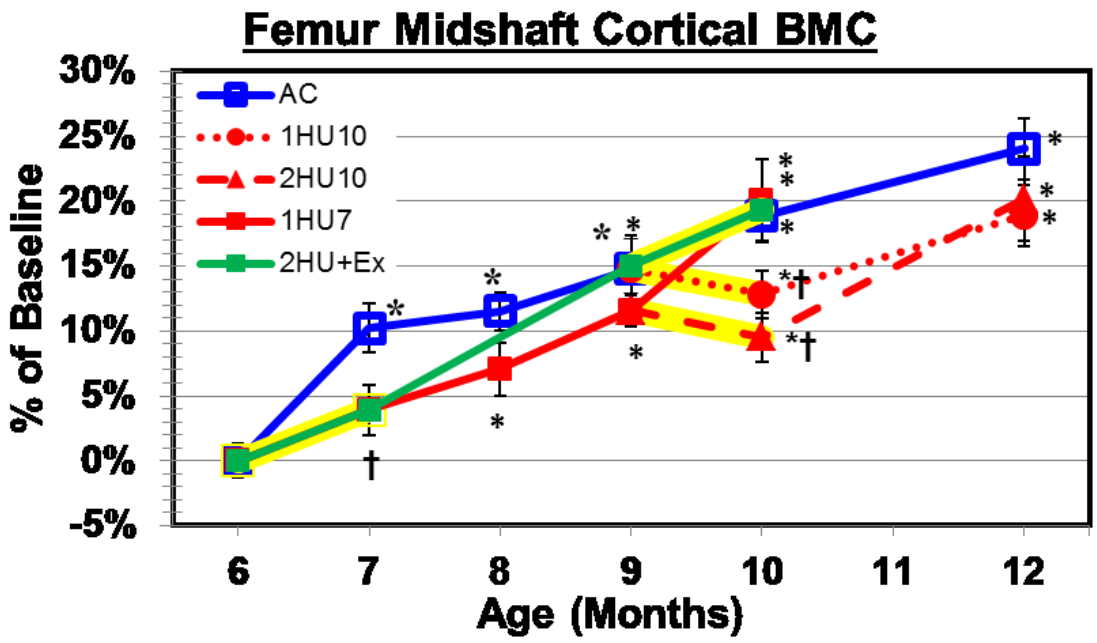

Figure 34: Changes cortical BMC of the femur midshaft. Numerical data are presented in Table 7. Yellow highlighting indicates HU treatment. Cortical BMC increases as the animal ages. 1HU7 suppresses age related growths and animals fall below AC. After recovery the exercised group recovers to 1HU7+R2 and AC level. After the second unloading period the 2HU10 and 1HU10 groups are significantly lower than AC while 2HU10+Ex remains at AC level. Pre- to post-HU values for the 9- 10 month period show non-significant decreases in the 1HU10 and 2HU10 groups while the 2HU10+Ex group increases slightly (+3.76%, n.s.).
Values are presented as mean ± SE
*** Indicates significant difference from baseline value; $p<0.05$**
† Indicates significant difference from age-matched cage control value at same time point; $p<0.05$
 # Indicates significant difference from pre- to post-HU value within same group; $p<0.05$
Ψ Indicates significant difference between 1HU7+Ex and 1HU7+R2; $p<0.05$

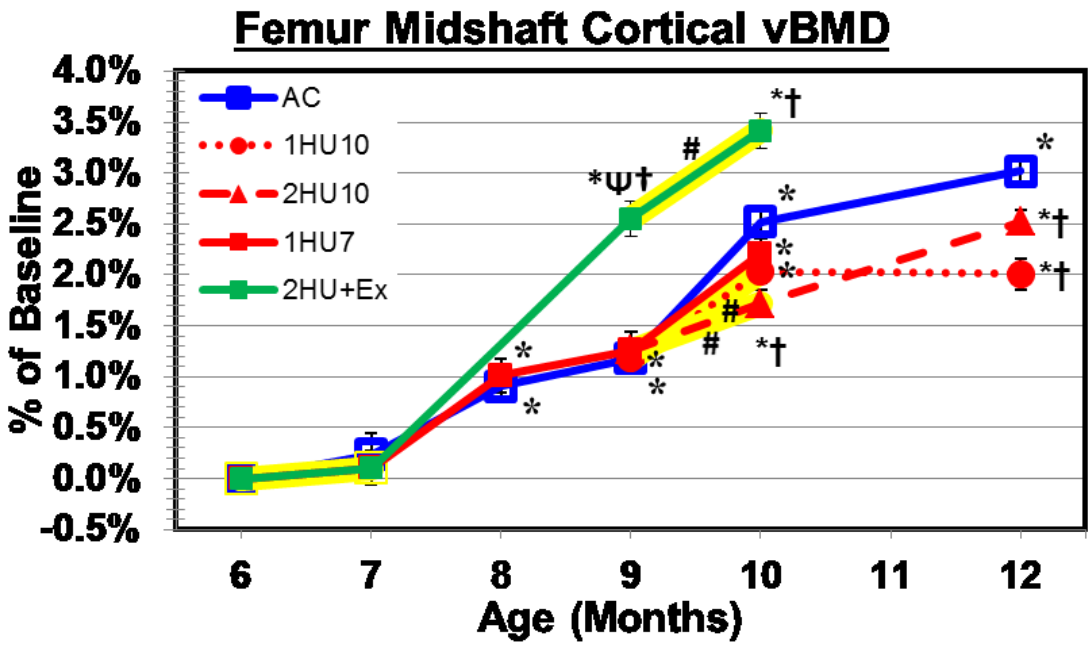

Figure 35: Changes cortical vBMD of the femur midshaft. Numerical data are presented in Table 7. Yellow highlighting indicates HU treatment. Cortical vBMD increases as the animal ages. 1HU7 has no effect on vBMD. After recovery the exercised group recovers above 1HU7+R2 (+1.28%) and AC (+1.36%) level. After the second unloading period the 2HU10 group is significantly lower than AC while 2HU10+Ex remains above (+0.88%) AC. Pre- to post-HU values for the 9- 10 month period show significant increases in all groups.
Values are presented as mean ± SE
*** Indicates significant difference from baseline value; $p<0.05$**
† Indicates significant difference from age-matched cage control value at same time point; $p<0.05$
 # Indicates significant difference from pre- to post-HU value within same group; $p<0.05$
Ψ Indicates significant difference between 1HU7+Ex and 1HU7+R2; $p<0.05$

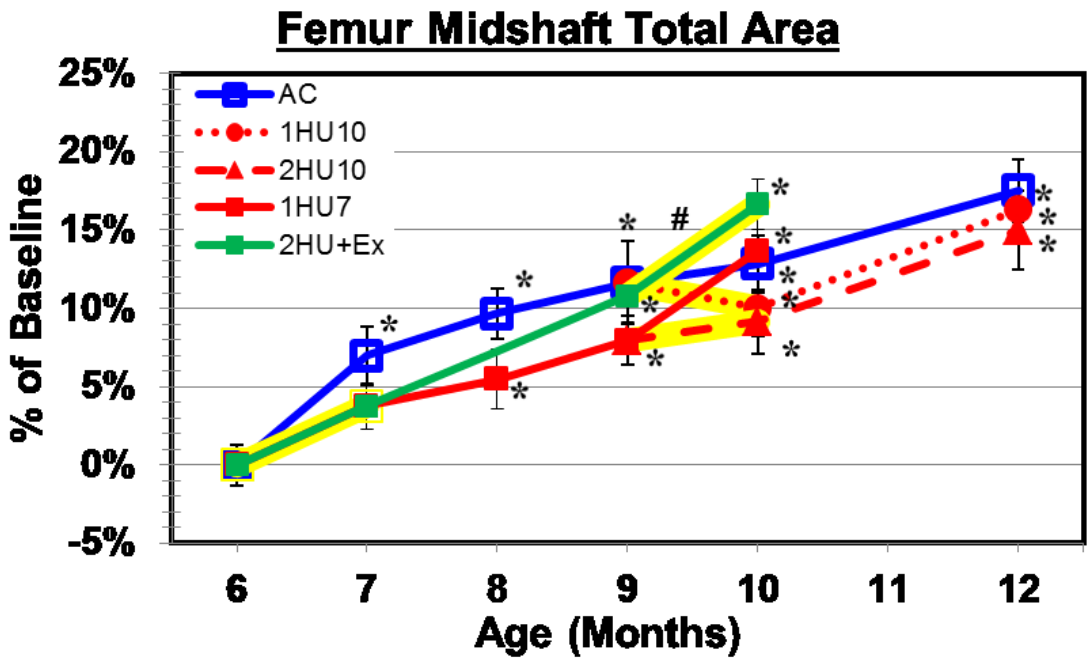

Figure 36: Changes in total area of the femur midshaft. Numerical data are presented in Table 7. Yellow highlighting indicates HU treatment. Total area increases as the animal ages. 1HU7 suppresses growth but total area remains at AC level. After recovery the exercised group (1HU7+Ex) and 1HU7+R2 recover to AC level. After the second unloading period the 2HU10 group is significantly lower than AC while 2HU10+Ex remains at AC level. Pre- to post-HU values for the 9- 10 month period shows a significant increase (+5.3%) in 2HU10+Ex and non-significant changes for 2HU10 and 1HU10.

Values are presented as mean ± SE

*** Indicates significant difference from baseline value; p<0.05**

† Indicates significant difference from age-matched cage control value at same time point; p<0.05

 # Indicates significant difference from pre- to post-HU value within same group; p<0.05

Ψ Indicates significant difference between 1HU7+Ex and 1HU7+R2; p<0.05

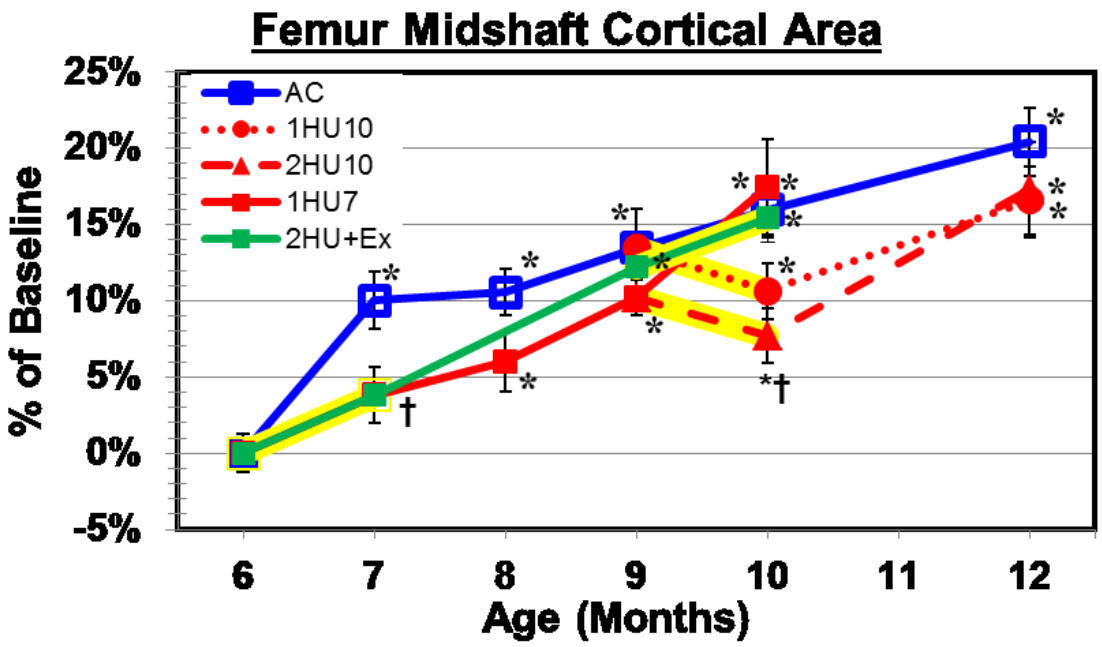

Figure 37: Changes in cortical area of the femur midshaft. Numerical data are presented in Table 7. Yellow highlighting indicates HU treatment. Cortical area increases as the animal ages. 1HU7 suppresses growth at month 7 falling below AC. After recovery the exercised group (1HU7+Ex) and 1HU7+R2 recover to AC level. After the second unloading period the 2HU10 group is significantly lower than AC while 2HU10+Ex remains at AC level. Pre- to post-HU values for the 9- 10 month period shows a non-significant increase in 2HU10+Ex and non-significant decreases in 2HU10 and 1HU10.

Values are presented as mean ± SE

*** Indicates significant difference from baseline value; $p<0.05$**

† Indicates significant difference from age-matched cage control value at same time point; $p<0.05$

 # Indicates significant difference from pre- to post-HU value within same group; $p<0.05$

Ψ Indicates significant difference between 1HU7+Ex and 1HU7+R2; $p<0.05$

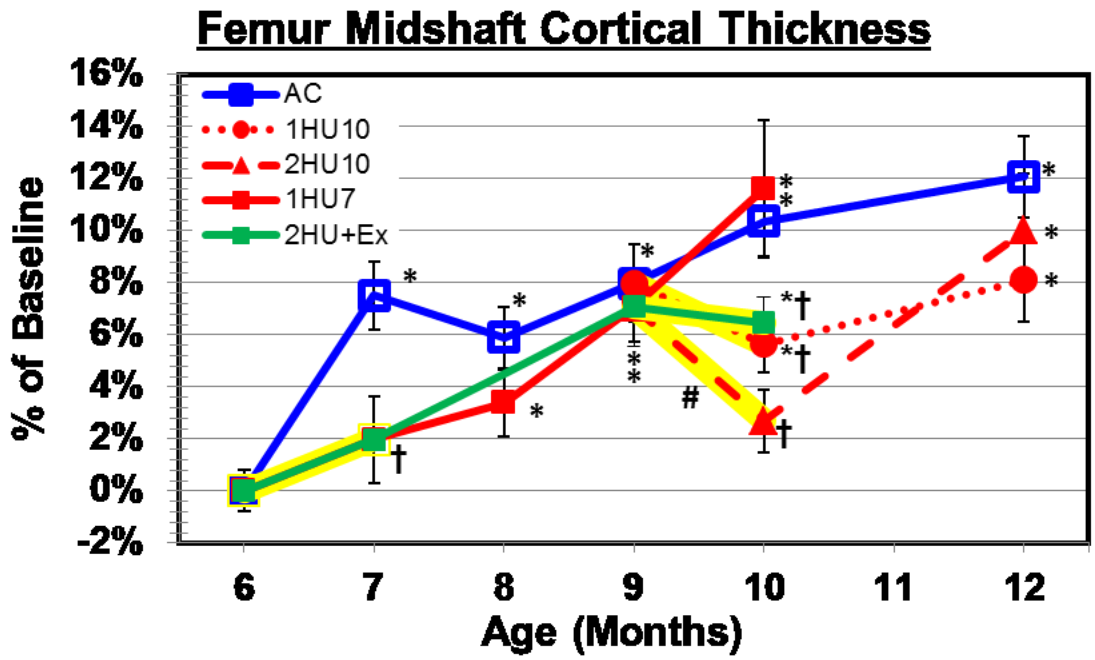

Figure 38: Changes cortical thickness of the femur midshaft. Numerical data are presented in Table 7. Yellow highlighting indicates HU treatment. Cortical thickness increases as the animal ages. 1HU7 suppresses growth at month 7 falling below AC. After recovery the exercised group (1HU7+Ex) and 1HU7+R2 recover to AC level. After the second unloading period all groups are significantly lower than AC. Pre- to post-HU values for the 9- 10 month period shows a non-significant decrease in 2HU10+Ex and 1HU10 while 2HU10 shows significant decrease.
Values are presented as mean ± SE
*** Indicates significant difference from baseline value; $p<0.05$**
† Indicates significant difference from age-matched cage control value at same time point; $p<0.05$
 # Indicates significant difference from pre- to post-HU value within same group; $p<0.05$
Ψ Indicates significant difference between 1HU7+Ex and 1HU7+R2; $p<0.05$

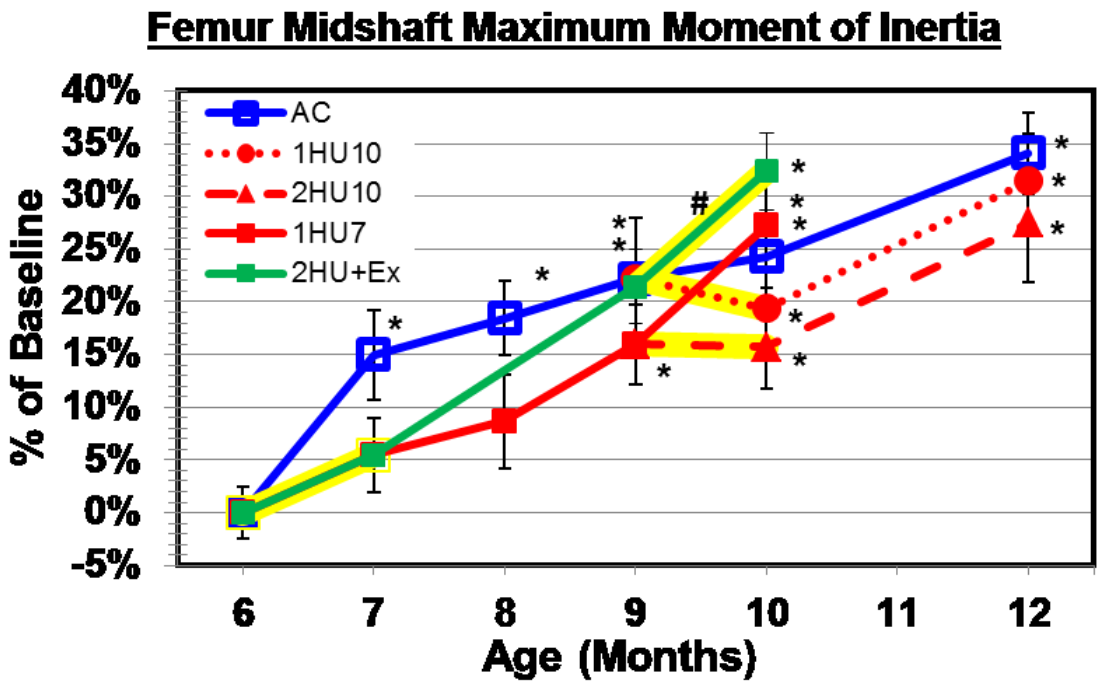

Figure 39: Changes in maximum moment of inertia of the femur midshaft. Numerical data are presented in Table 7. Yellow highlighting indicates HU treatment. Maximum moment of inertia increases as the animal ages. 1HU7 suppresses growth at month 7. After recovery the exercised group (1HU7+Ex) and 1HU7+R2 recover to AC level. After the second unloading period all groups remain at AC level. Pre- to post-HU values for the 9- 10 month period shows a non-significant decrease in 2HU10 and 1HU10 while 2HU10+Ex shows a significant increase (+8.98%).
Values are presented as mean ± SE
*** Indicates significant difference from baseline value; $p<0.05$**
† Indicates significant difference from age-matched cage control value at same time point; $p<0.05$
 # Indicates significant difference from pre- to post-HU value within same group; $p<0.05$
Ψ Indicates significant difference between 1HU7+Ex and 1HU7+R2; $p<0.05$

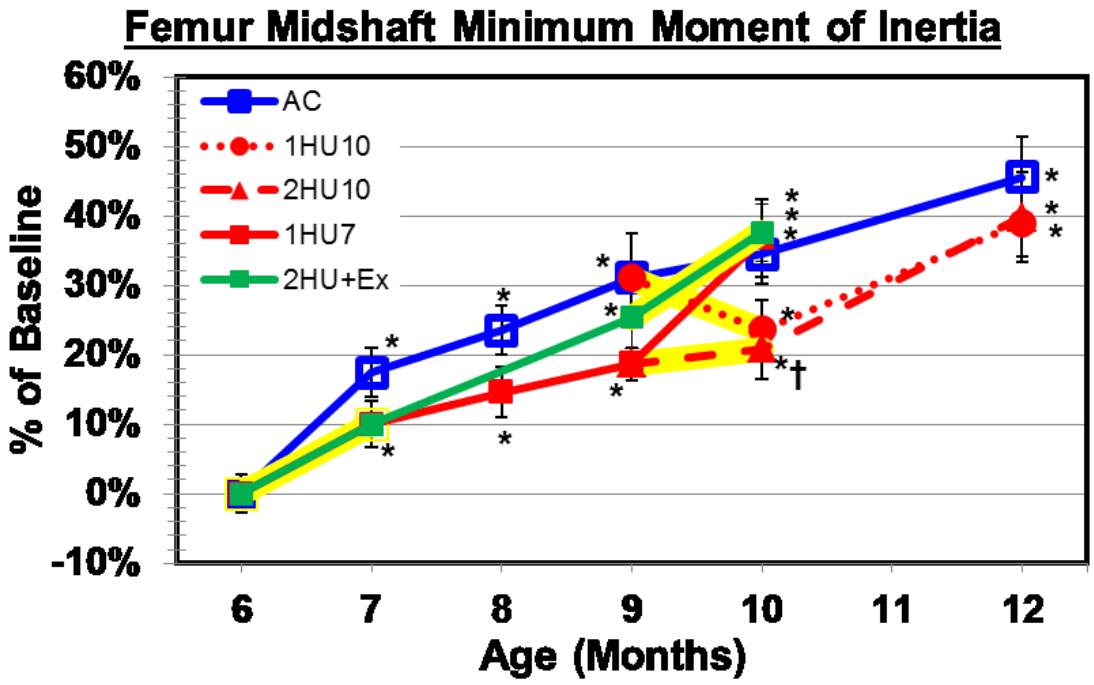

Figure 40: Changes in minimum moment of inertia of the femur midshaft. Numerical data are presented in Table 7. Yellow highlighting indicates HU treatment. Minimum moment of inertia increases as the animal ages. 1HU7 suppresses growth at month 7. After recovery both the exercised group (1HU7+Ex) and 1HU7+R2 recover to AC level. After the second unloading period 1HU10 and 2HU10+Ex remain at AC level while 2HU10 falls below. Pre- to post-HU values for the 9- 10 month period show a non-significant decrease in 1HU10 level. The minimum moment of inertia for the 2HU10 and 2HU10+Ex groups show non-significant increases due to the second HU.
Values are presented as mean ± SE
*** Indicates significant difference from baseline value; $p<0.05$**
† Indicates significant difference from age-matched cage control value at same time point; $p<0.05$
 # Indicates significant difference from pre- to post-HU value within same group; $p<0.05$
Ψ Indicates significant difference between 1HU7+Ex and 1HU7+R2; $p<0.05$

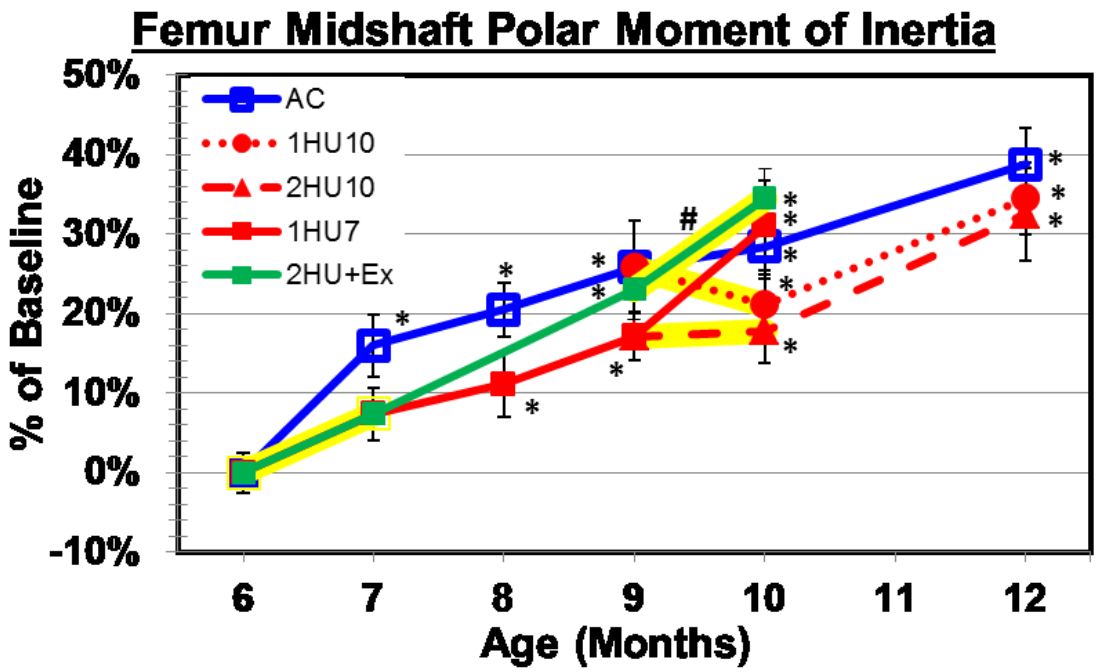

Figure 41: Changes in polar moment of inertia of the femur midshaft. Numerical data are presented in Table 7. Yellow highlighting indicates HU treatment. Polar moment of inertia increases as the animal ages. 1HU7 suppresses growth at month 7. After recovery both the exercised group (1HU7+Ex) and 1HU7+R2 recover to AC level. After the second unloading period all groups remain at AC level. Pre- to post-HU values for the 9- 10 month period show a non-significant decrease in 1HU10 group. The polar moment of inertia for the 2HU10+Ex group shows a significant increases pre- to poast-HU (+9.28%).
Values are presented as mean ± SE
*** Indicates significant difference from baseline value; $p<0.05$**
† Indicates significant difference from age-matched cage control value at same time point; $p<0.05$
 # Indicates significant difference from pre- to post-HU value within same group; $p<0.05$
Ψ Indicates significant difference between 1HU7+Ex and 1HU7+R2; $p<0.05$

Femur Diaphysis Mechanical Properties

Table 8 lists absolute values for the mechanical testing data of the femur diaphysis. The femur midshaft diaphysis results presented are the outcome of three point bending tests.

Maximum force (Figure 42) increases as the animals age. There are no differences between groups, even after the 1st HU period, until month 9. During recovery, the exercised group (1HU7+Ex) maximum force does not increase as do mean values for AC and 1HU7+R and remains lower after the second unloading period. Pre- to post-HU values for the 9- 10 month period show non-significant changes in the exercise and ambulatory recovery groups.

Stiffness (Figure 43) reveals there are no differences between groups until month 9. After recovery the exercised group (1HU7+Ex) maximum force falls below AC and 1HU7+R2 level. After the second unloading 2HU10+Ex remains significantly lower than AC10. Pre- to post-HU values for the 9- 10 month period indicate non-significant changes in the exercise and ambulatory recovery groups.

Elastic modulus (Figure 44) shows similar trends as stiffness. HU increases elastic modulus of the 1HU7, 1HU10, and 2HU10 although this change is not significant, while 2HU10+Ex decreases (n.s.). After recovery period the exercised group's (1HU7+Ex) elastic modulus falls below AC9 and 1HU7+R2 level. After the second unloading period all groups remain at A10C level except 2HU10+Ex is significantly lower.

For pre-yield toughness (Figure 45) and energy to yield (Figure 46), 1HU7 suppresses age related increases and falls below AC. However, after two months of recovery both the exercised group (1HU7+Ex) and 1HU7+R2 recover to AC level. After the second unloading period 2HU10+Ex remains at AC level while 2HU10 (and 1HU10 for pre-yield toughness) fall below. Pre- to post-HU values for the 9- 10 month period show a non-significant changes in all groups. There are large fluctuations in energy to fracture (Figure 47). This may have to do with the data being post-yield. Typically pre-yield data is most valid. Post-yield the bone is in the elastic region of the stress-strain curve and stresses cause permanent damage and deformation to the bone specimen.

Yield stress (Figure 48) reveals no significant differences in groups either after HU or after recovery. The only significant difference is present at 2HU10+Ex which is 20.54% lower when compared to AC. Ultimate stress (Figure 49) presents a few more differences. 1HU7 has no effect on ultimate stress. After recovery, 1HU7+R2 remains at AC level while 1HU7+Ex falls below AC9 and 1HU7+R2. There are no significant changes pre to post HU from 9-10 months. 2HU10+Ex shows a non-significant decrease after the second HU which causes it to fall below AC and baseline level.

Table 8: Femur diaphysis mechanical properties from three-point bending tests

	Maximum Force (N)	Stiffness (N/mm)	Elastic Modulus (MPa)	Pre-Yield Toughness (mJ/mm^3)	Energy to Yield (mJ)	Energy to Fracture (mJ)	Yield Stress (MPa)	Ultimate Stress (MPa)
6 Months Old								
BL6	215.91 (3.80)	678.01 (37.66)	4.17 (0.24)	1.43 (0.13)	25.0 (2.67)	120.4 (6.16)	96.2 (4.61)	132.5 (2.99)
7 Months Old								
AC7	263.87 (5.71)*	722.97 (44.29)	3.87 (0.27)	1.97 (0.16)*	35.9 (3.79)*	133.1 (7.71)	112.0 (3.23)	144.1 (3.29)*
1HU7	247.76 (7.28)*	816.95 (50.03)*	4.68 (0.29)†	1.52 (0.13)†	25.5 (2.24)†	137.1 (8.22)	106.1 (3.95)	144.9 (4.21)*
8 Months Old								
AC8	264.37 (3.90)*	857.71 (94.00)	4.41 (0.49)	1.75 (0.16)	32.1 (3.24)*	144.3 (8.22)*	105.3 (3.04)	140.2 (3.00)
1HU7+R1	257.05 (7.32)*	865.96 (70.72)*	4.71 (0.27)	1.44 (0.13)	24.2 (1.96)†	122.4 (6.98)	107.5 (5.16)	146.0 (2.91)*
9 Months Old								
AC9	269.43 (10.34)*	897.93 (75.62)*	4.35 (0.28)	1.73 (0.25)	32.2 (4.88)	94.6 (12.9)	107.7 (6.38)	137.9 (4.76)
1HU7+R2	266.18 (5.48)*	851.58 (74.81)*	4.44 (0.40)	1.72 (0.32)	31.4 (5.42)	129.9 (6.49)†	107.2 (7.37)	141.1 (4.67)
1HU7+Ex	241.77 (7.20)*Ψ†	571.09 (39.23)Ψ†	2.83 (0.18)*Ψ†	1.92 (0.33)	36.3 (6.20)	134.9 (7.19)†	91.9 (4.75)	124.4 (3.58)Ψ†
10 Months Old								
AC10	274.90 (7.06)*	743.11 (59.53)	3.61 (0.29)*	2.16 (0.22)*	41.5 (4.84)*	129.4 (6.78)	107.5 (3.74)	138.7 (3.55)
1HU7+R3	288.53 (11.88)*	883.96 (53.83)*†	4.09 (0.30)	1.69 (0.25)	33.1 (5.06)	140.7 (15.8)	103.3 (6.39)	139.6 (4.21)
1HU10	259.96 (8.12)*	934.41 (108.41)*	4.77 (0.52)	1.54 (0.26)†	29.2 (4.71)	130.2 (10.5)#	106.7 (6.11)	135.0 (5.05)
2HU10	268.42 (6.82)*	967.56 (121.74)	5.05 (0.62)	1.58 (0.31)†	28.8 (5.61)†	116.0 (8.97)	106.4 (4.29)	143.5 (3.23)*
2HU10+Ex	246.77 (6.23)*†	494.05 (34.04)*†	2.30 (0.20)*†	2.12 (0.35)	41.1 (6.95)*	129.0 (7.11)	85.4 (3.73)†	120.5 (3.39)*†
12 Months Old								
AC12	295.45 (10.70)*	1010.26(107.23)*	4.50 (0.50)	1.35 (0.16)	26.4 (3.02)	141.4 (13.6)	104.2 (3.31)	140.1 (5.28)
1HU10+R2	290.70 (8.32)*	1154.82 (89.54)*	5.41 (0.50)*	1.49 (0.37)	29.8 (8.40)	131.3 (10.4)	96.6 (6.17)	141.3 (2.95)
2HU10+R2	292.00 (11.94)*	1142.84 (73.01)*	5.44 (0.47)*	1.09 (0.09)	20.7 (1.99)◊	141.4 (12.7)	102.9 (3.66)	145.2 (3.99)*

Values are presented as mean ± SE

*** Indicates significant difference from baseline value, $p < 0.05$**

† Indicates significant difference from age-matched control value at same time point, $p<0.05$

 # Indicates significant difference from pre- to post-HU value within same group, $p<0.05$

Ψ Indicates significant difference from 1HU7+Ex to 1HU7+R2, $p<0.05$

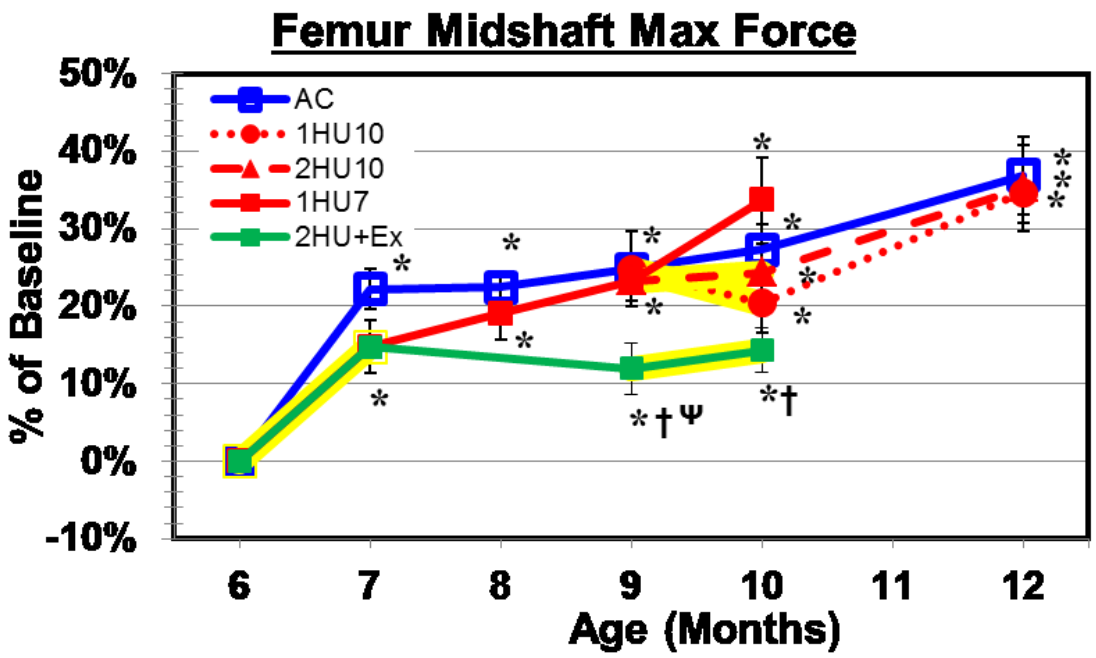

Figure 42: Changes in three-point bending maximum force of the femur midshaft. Numerical data are presented in Table 8. Yellow highlighting indicates HU treatment. Maximum force increases as the animal ages. AC, 1HU10, 2HU10, and 1HU7 all increase and are not significantly different from each other. However, after recovery exercised group (1HU7+Ex) maximum force falls below AC (-10.27%) and 1HU7+R2 (-9.17%) level. After the second unloading period all groups remain at AC level except 2HU10+Ex (-10.23%). Pre- to post-HU values for the 9- 10 month period show a non-significant changes in all groups.
Values are presented as mean ± SE
*** Indicates significant difference from baseline value; p<0.05**
† Indicates significant difference from age-matched cage control value at same time point; p<0.05
 # Indicates significant difference from pre- to post-HU value within same group; p<0.05
Ψ Indicates significant difference between 1HU7+Ex and 1HU7+R2; p<0.05

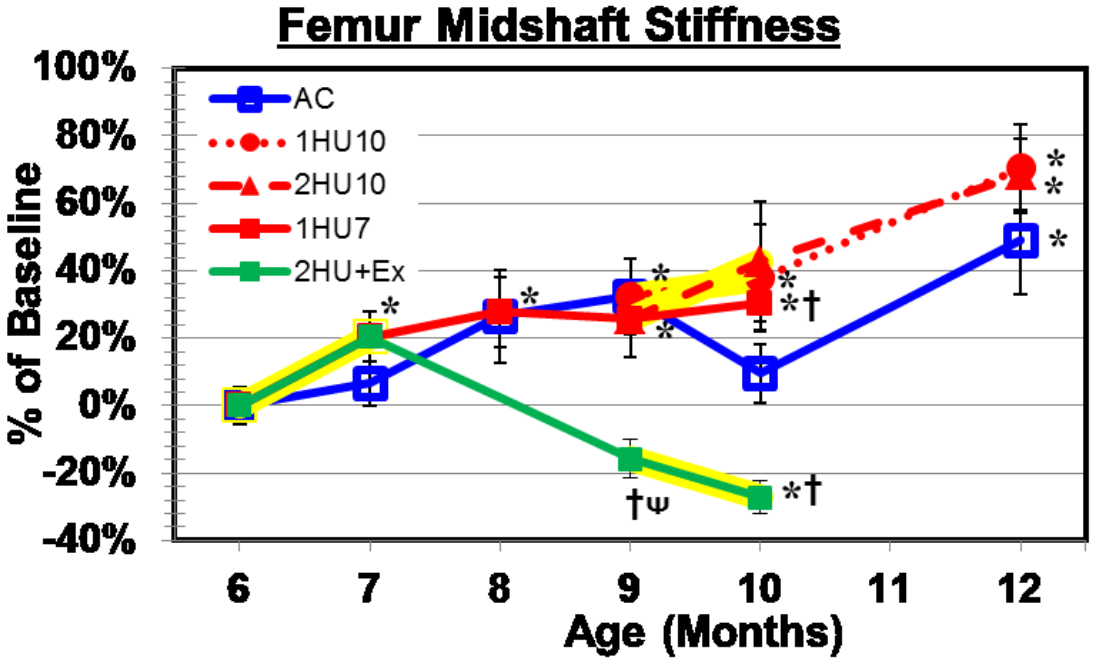

Figure 43: Changes in three-point bending stiffness of the femur midshaft. Numerical data are presented in Table X. Yellow highlighting indicates HU treatment. Stiffness trends upward as the groups age. AC, 1HU10, 2HU10, and 1HU7 all increase and are not significantly different from each other. Only 1HU7+R3 is significantly higher than AC. However, after recovery exercised group (1HU7+Ex) maximum force falls below AC (-36.4%) and 1HU7+R2 (-32.94%) level. After the second unloading period all groups remain at AC level except 2HU10+Ex (-33.52%). Pre- to post-HU values for the 9- 10 month period show a non-significant changes in all groups.
Values are presented as mean ± SE
*** Indicates significant difference from baseline value; p<0.05**
† Indicates significant difference from age-matched cage control value at same time point; p<0.05
 # Indicates significant difference from pre- to post-HU value within same group; p<0.05
Ψ Indicates significant difference between 1HU7+Ex and 1HU7+R2; p<0.05

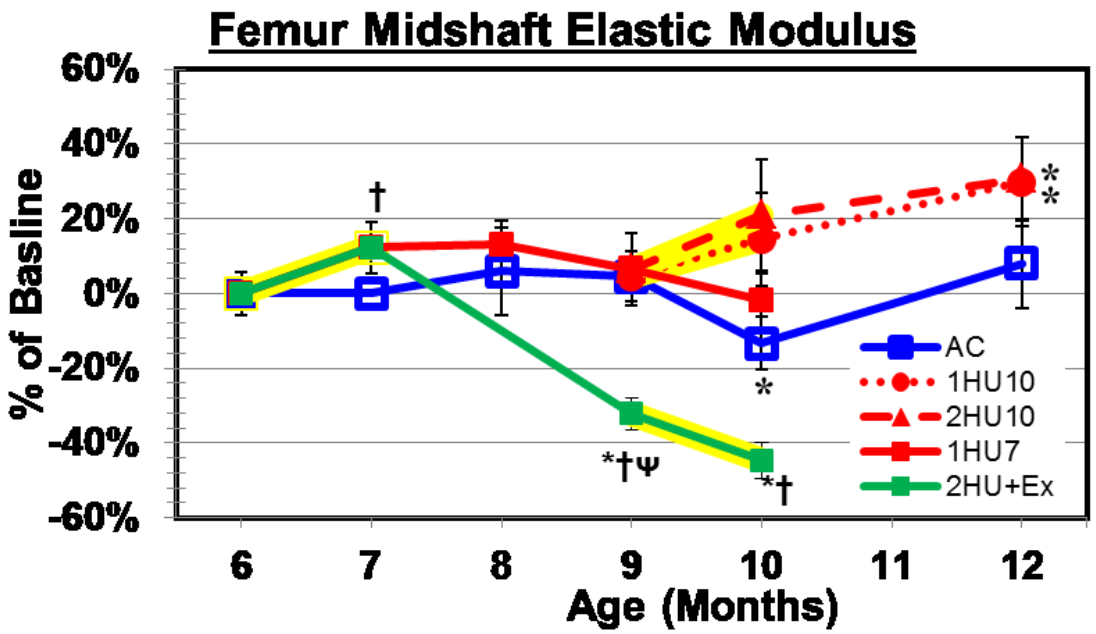

Figure 44: Changes in three-point bending elastic modulus of the femur midshaft. Numerical data are presented in Table 8. Yellow highlighting indicates HU treatment. Elastic modulus shows different trends than maximum force and stiffness. HU increases elastic modulus of the 1HU7, 1HU10, and 2HU10 although this change is not significant while 2HU10+Ex decreases (n.s.). After recovery period exercised group (1HU7+Ex) elastic modulus falls below AC (-35.1%) and 1HU7+R2 (-36.38%) level. After the second unloading period all groups remain at AC level except 2HU10+Ex (-36.18%).

Values are presented as mean ± SE

*** Indicates significant difference from baseline value; $p<0.05$**

† Indicates significant difference from age-matched cage control value at same time point; $p<0.05$

 # Indicates significant difference from pre- to post-HU value within same group; $p<0.05$

Ψ Indicates significant difference between 1HU7+Ex and 1HU7+R2; $p<0.05$

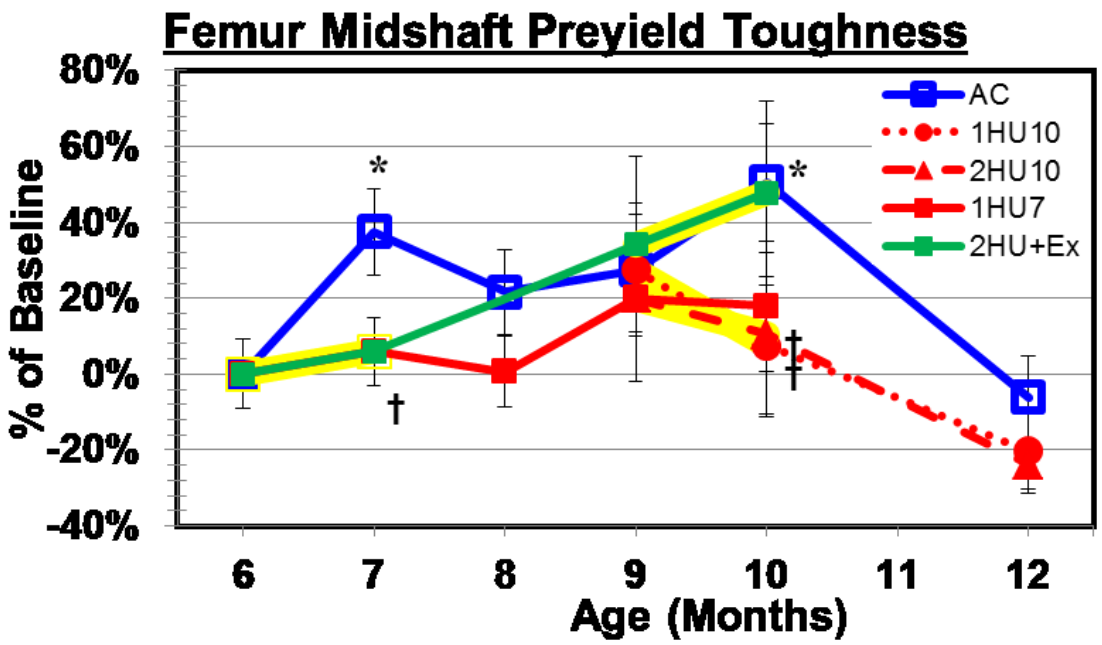

Figure 45: Changes in three-point bending pre-yield toughness of the femur midshaft. Numerical data are presented in Table 8. Yellow highlighting indicates HU treatment. 1HU7 suppresses age related increases and falls below AC. However, after recovery period of both the exercised group (1HU7+Ex) and 1HU7+R2 recover to AC level. After the second unloading period 2HU10+Ex remains at AC level while 1HU10 and 2HU10 fall below. Pre- to post-HU values for the 9- 10 month period show a non-significant changes in all groups, 2HU10+Ex shows an increase (+10.11%, n.s.). Values are presented as mean ± SE

*** Indicates significant difference from baseline value; $p<0.05$**

† Indicates significant difference from age-matched cage control value at same time point; $p<0.05$

 # Indicates significant difference from pre- to post-HU value within same group; $p<0.05$

Ψ Indicates significant difference between 1HU7+Ex and 1HU7+R2; $p<0.05$

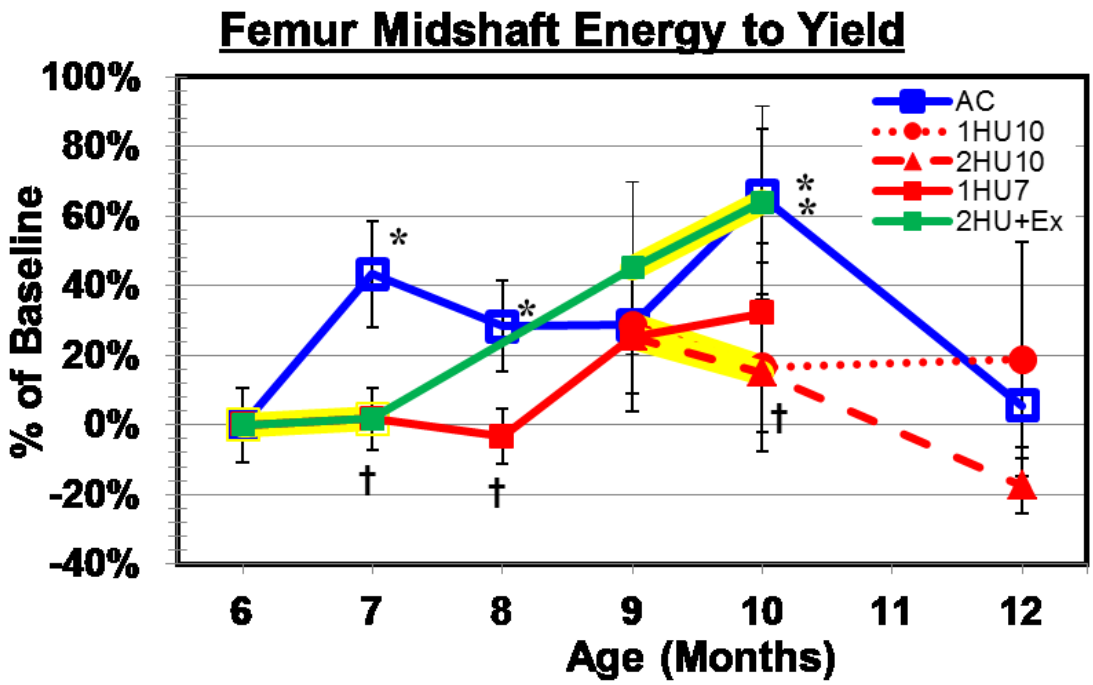

Figure 46: Changes in three-point bending energy to yield of the femur midshaft. Numerical data are presented in Table 8. Yellow highlighting indicates HU treatment. 1HU7 suppresses age related increases and falls below AC. However, after recovery period of both the exercised group (1HU7+Ex) and 1HU7+R2 recover to AC level. After the second unloading period 2HU10+Ex remains at AC level while 2HU10 falls below. Pre- to post-HU values for the 9- 10 month period show a non-significant changes in all groups, 2HU10+Ex shows an increase (+12.97%, n.s.).
Values are presented as mean ± SE
*** Indicates significant difference from baseline value; $p<0.05$**
† Indicates significant difference from age-matched cage control value at same time point; $p<0.05$
 # Indicates significant difference from pre- to post-HU value within same group; $p<0.05$
Ψ Indicates significant difference between 1HU7+Ex and 1HU7+R2; $p<0.05$

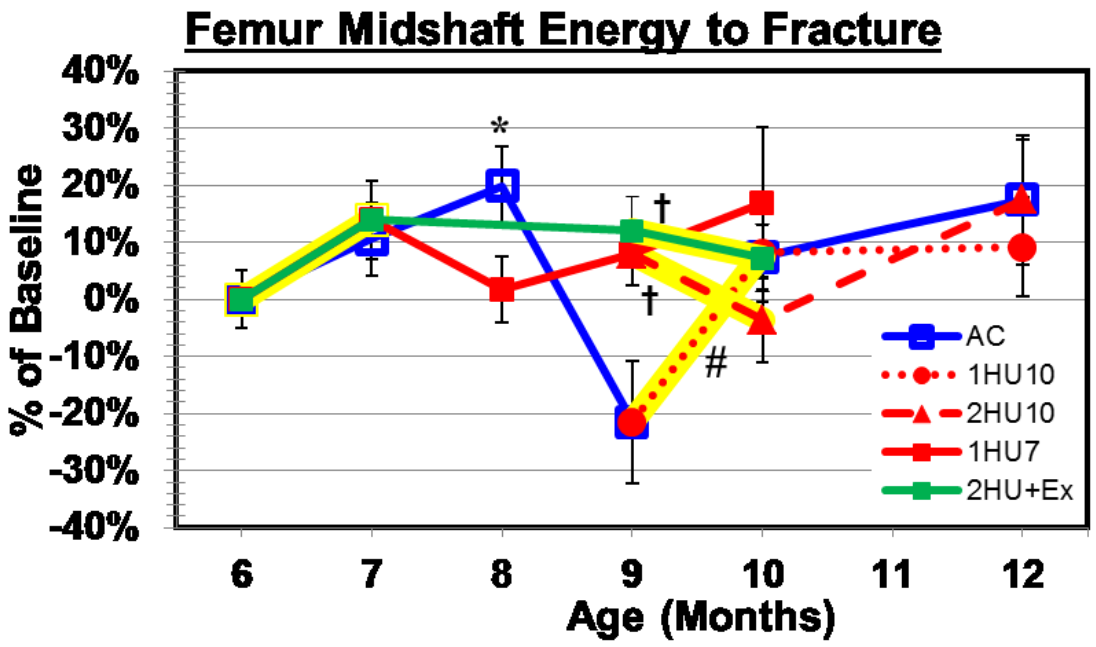

Figure 47: Changes in three-point bending energy to fracture of the femur midshaft. Numerical data are presented in Table 8. Yellow highlighting indicates HU treatment. Fluctuations in energy to fracture do not show trends with HU treatment. This may have to do with the data being post-yield. Typically pre-yield data is most valid.
Values are presented as mean ± SE
*** Indicates significant difference from baseline value; $p<0.05$**
† Indicates significant difference from age-matched cage control value at same time point; $p<0.05$
 # Indicates significant difference from pre- to post-HU value within same group; $p<0.05$
Ψ Indicates significant difference between 1HU7+Ex and 1HU7+R2; $p<0.05$

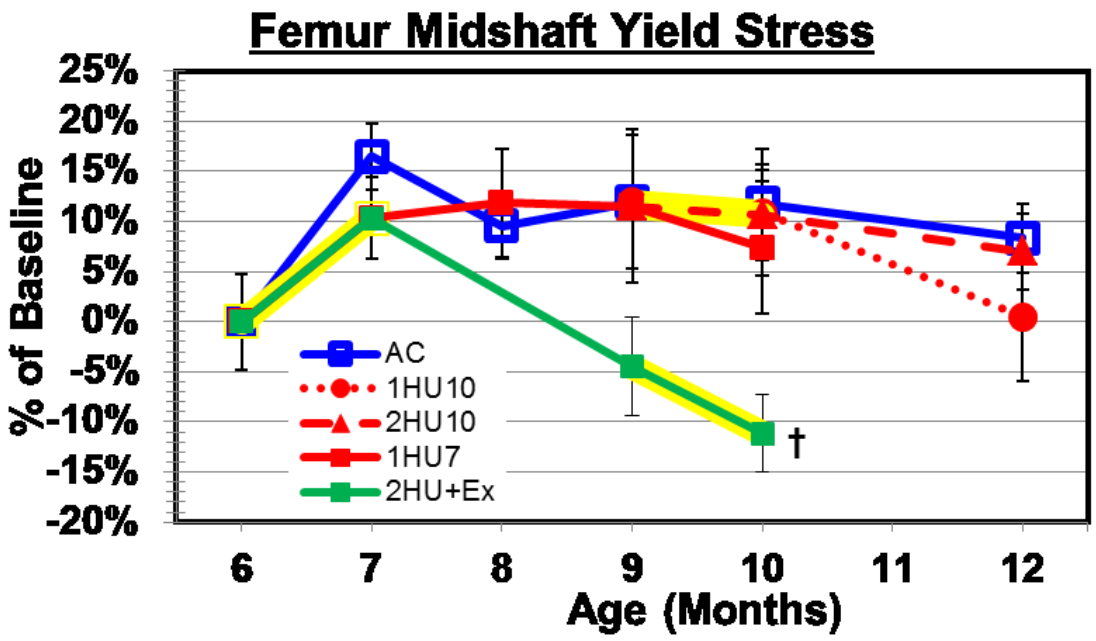

Figure 48: Changes in three-point bending yield stress of the femur midshaft. Numerical data are presented in Table 8. Yellow highlighting indicates HU treatment. There are no significant differences between points. The only significant difference is present at 2HU10+Ex which is -20.54% lower when compared to AC.
Values are presented as mean ± SE
*** Indicates significant difference from baseline value; p<0.05**
† Indicates significant difference from age-matched cage control value at same time point; p<0.05
 # Indicates significant difference from pre- to post-HU value within same group; p<0.05
Ψ Indicates significant difference between 1HU7+Ex and 1HU7+R2; p<0.05

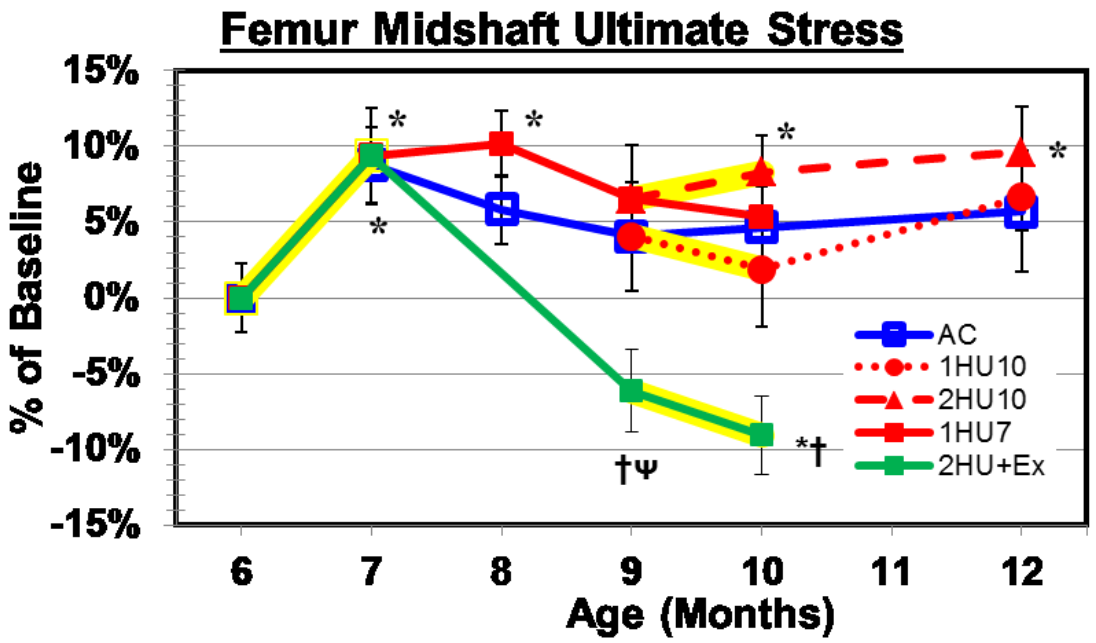

Figure 49: Changes in three-point bending ultimate stress of the femur midshaft. Numerical data are presented in Table 8. Yellow highlighting indicates HU treatment. 1HU7 has no effect on ultimate stress. After recovery, 1HU7+R2 remains at AC level while 1HU7+Ex falls below AC (-9.8%) and 1HU7+R2 (-11.88%). There are no significant changes pre to post HU from 9-10 months. 2HU10+Ex shows a non-significant decrease after the second HU which causes it to fall below AC (-13.11%)and baseline level.
Values are presented as mean ± SE
*** Indicates significant difference from baseline value; p<0.05**
† Indicates significant difference from age-matched cage control value at same time point; p<0.05
 # Indicates significant difference from pre- to post-HU value within same group; p<0.05
Ψ Indicates significant difference between 1HU7+Ex and 1HU7+R2; p<0.05

Distal Femur Metaphysis Densitometric Properties

Table 9 lists absolute values for the pQCT properties of the DFM. The DFM is a mixed bone site and properties reported will include total, cancellous, and cortical compartments of BMC, vBMD, and Area.

Total (Figure 50) and cortical BMC (Figure 51) are affected by 1HU7 and were significantly lower than pre-HU values and AC values at same time point. At month 9, the exercise group BMC values increased to well above AC, while 1HU7+R2 does not fully recover. After the second unloading period, the 1HU10 and 2HU10 groups falls below AC while 2HU10+Ex remains above AC level. Pre- to post-HU values for cortical BMC reveal no changes in the 9 to 10 month period, whereas total BMC values decline significantly for the 1HU10 group. However, 2HU10 shows only a slight non-significant decrease while the 2HU10+Ex groups presents a slight non-significant increase. Recovery characteristics were similar for cancellous BMC (Figure 52); however, there were no significant pre- to post-HU changes.

Total (Figure 53), cortical (Figure 54), and cancellous vBMD (Figure 55) all show significant decreases after the first HU bout. Total and cancellous vBMD illustrate very similar patterns after recovery suggesting the cancellous bone is more affected by exercise than cortical. Aging animals reveal a gradual decline in vBMD at this site. After 1st HU, 1HU7 exhibits significant losses. At month 9, 1HU7+Ex vales are higher than AC while 1HU7+R2 values are within AC values. For total vBMD after the second unloading period the 1HU10 and 2HU10 groups fall below AC10 while 2HU10+Ex remains above AC level. Pre- to post-HU values for the 9 to10 month period present significant decreases for the 2HU10 and 1HU10 groups; however, 2HU10+Ex reveals only a slight non-significant decrease. Cancellous bone trends are similar results after the second HU, except 2HU10 is not different from AC10. Pre- to post-HU values for the 9 to 10 month period illustrate significant decreases (-13.47%) for the 1HU10 group; however, 2HU10 and 2HU10+Ex demonstrate only a slight non-significant decrease.

Cortical vBMD presents a significant loss from pre-HU value for 1HU7. At month 9, the exercised group and ambulatory recovery group both reach AC level. After the second unloading period the 2HU10 group falls below AC, while 2HU10+Ex remains at AC level. Pre- to post-HU values for the 9 to 10 month period reveal significant decreases for the 2HU10 group; however, 1HU10 and 2HU10+Ex values result in only slight non-significant decreases.

Table 9: Properties from pQCT for total, cancellous, and cortical bone of the distal femur metaphysis

	Total BMC (mg/mm)	Total vBMD (mg/cm^3)	Cancellous BMC (mg/mm)	Cancellous vBMD (mg/cm^3)	Cortical BMC (mg/mm)	Cortical vBMD (mg/cm^3)
6 Months Old						
BL6	12.51 (0.19)	657.1 (6.3)	3.76 (0.12)	340.1 (6.9)	8.72 (0.13)	1078.3 (4.8)
7 Month Old						
AC7	12.95 (0.28)	653.6 (11.4)	4.04 (0.19)	349.9 (15.8)	8.91 (0.14)	1067.1 (4.4)
1HU7	11.29 (0.20) *†	573.9 (9.9) *†	3.49 (0.17) †	282.4 (11.8) *†	7.80 (0.13) *†	1045.6 (6.0) *†
8 Months Old						
AC8	12.68 (0.30)	629.8 (10.4) *	4.09 (0.23)	333.6 (14.4)	8.59 (0.15)	1069.3 (6.5)
1HU7+R1	11.10 (0.17) *†	561.3 (8.1) *†	3.49 (0.15) †	277.7 (12.0) *†	7.60 (0.17) *†	1043.8 (6.2) *†
9 Months Old						
AC9	12.51 (0.21)	622.8 (11.6) *	3.73 (0.12)	311.2 (11.5) *	8.78 (0.14)	1077.1 (4.9)
1HU7+R2	11.69 (0.22) *†	596.3 (11.2) *	3.57 (0.18)	294.9 (12.4) *	8.12 (0.15) *†	1065.8 (6.8)
1HU7+Ex	13.90 (0.29) *†Ψ	656.0 (9.7) †Ψ	4.20 (0.15) †Ψ	348.8 (8.5) †Ψ	9.71 (0.28) *†Ψ	1053.3 (10.4) *
10 Months Old						
AC10	12.63 (0.16)	606.3 (7.4) *	3.73 (0.12)	311.2 (11.6) *	8.88 (0.11)	1049.3 (9.0) *
1HU7+R3	12.52 (0.28)	617.5 (11.9) *	3.85 (0.14)	314.5 (12.0)	8.67 (0.19)	1073.8 (4.1)
1HU10	11.98 (0.15) *#†	572.8 (9.0) *†#	3.53 (0.12)	269.2 (7.0) *†#	8.45 (0.14) †	1063.8 (7.6)
2HU10	11.47 (0.22) *†	555.2 (8.1) *†#	3.72 (0.14)	279.2 (5.4) *	7.75 (0.17) *†	1037.5 (8.2) *†
2HU10+Ex	14.25 (0.20) *†	642.6 (6.4)	4.43 (0.10) *†	344.1 (8.2)	9.83 (0.17) *†	1043.3 (10.4) *
12 Months Old						
AC12	12.75 (0.24)	610.0 (7.6) *	3.72 (0.20)	290.5 (12.4) *	9.03 (0.14)	1091.7 (7.0)
1HU10+R2	12.45 (0.23)	574.4 (6.0) *†	3.82 (0.17)	278.6 (7.9) *	8.63 (0.16)	1062.6 (5.9) †
2HU10+R2	12.02 (0.25)	576.3 (5.7) *†	3.63 (0.18)	276.6 (8.1) *	8.39 (0.15) †	1066.2 (6.2) †

Values are presented as mean ± SE

* Indicates significant difference from baseline value, $p < 0.05$

† Indicates significant difference from age-matched control value at same time point, $p<0.05$

# Indicates significant difference from pre- to post-HU value within same group, $p<0.05$

Ψ Indicates significant difference from 1HU7+Ex to 1HU7+R2, $p<0.05$

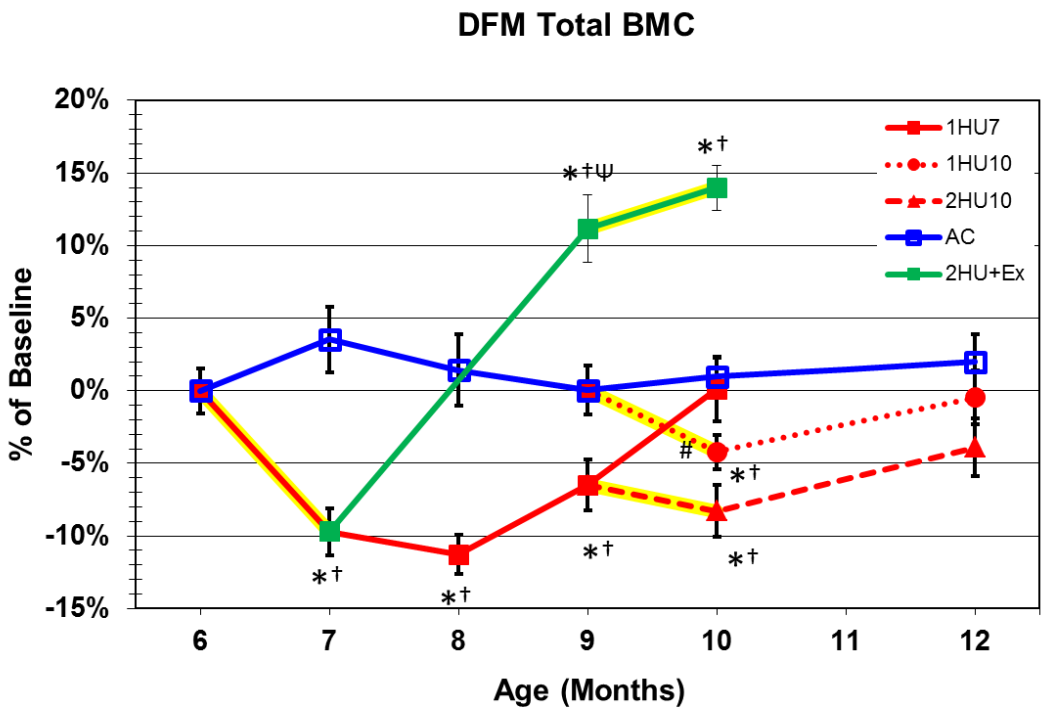

Figure 50: Changes in total BMC of the distal femur metaphysis. Numerical data are presented in Table 9. Yellow highlighting indicates HU treatment. 1HU7 lost 9.71% from pre HU value and was significantly lower than AC. At month 9, the exercised group recovers to above BL level and AC (+12.08%), while 1HU7+R2 does not fully recover. After the second unloading period the 1HU10 and 2HU10 groups falls below AC while 2HU10+Ex remains above AC level (+11.12%). Pre- to post-HU values for the 9- 10 month period show significant decreases for the 1HU10 (-4.25%) group; however, 2HU10 shows only a slight non-significant decrease while the 2HU10+Ex groups shows a slight non-significant increase (+2.53%).
Values are presented as mean ± SE
*** Indicates significant difference from baseline value; $p<0.05$**
† Indicates significant difference from age-matched cage control value at same time point; $p<0.05$
 # Indicates significant difference from pre- to post-HU value within same group; $p<0.05$
Ψ Indicates significant difference between 1HU7+Ex and 1HU7+R2; $p<0.05$

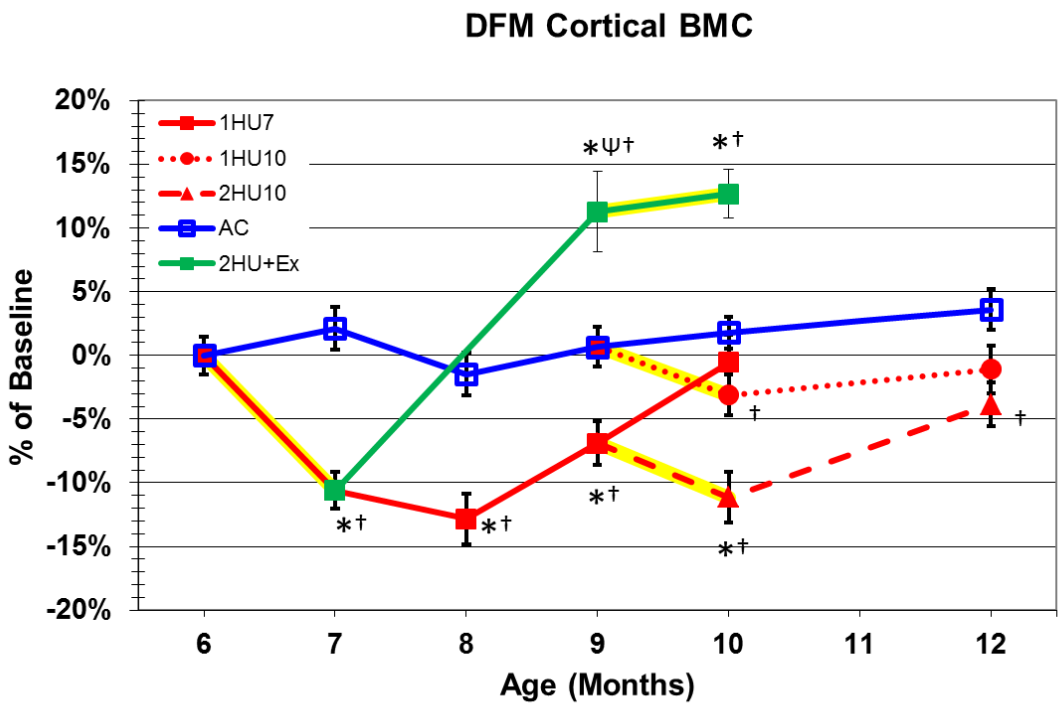

Figure 51: Changes in cortical BMC of the distal femur metaphysis. Numerical data are presented in Table 9. Yellow highlighting indicates HU treatment. 1HU7 lost 10.59% from pre HU value and was significantly lower than AC. At month 9, the exercised group recovers to above BL, AC (+10.56%), and 1HU7+R2 (+19.52%) while 1HU7+R2 does not fully recover. After the second unloading period the 1HU10 and 2HU10 groups fall below AC while 2HU10+Ex remains above AC level (+10.72%). Pre- to post-HU values for the 9- 10 month period show no significant changes for any groups.

Values are presented as mean ± SE

*** Indicates significant difference from baseline value; p<0.05**

† Indicates significant difference from age-matched cage control value at same time point; p<0.05

 # Indicates significant difference from pre- to post-HU value within same group; p<0.05

Ψ Indicates significant difference between 1HU7+Ex and 1HU7+R2; p<0.05

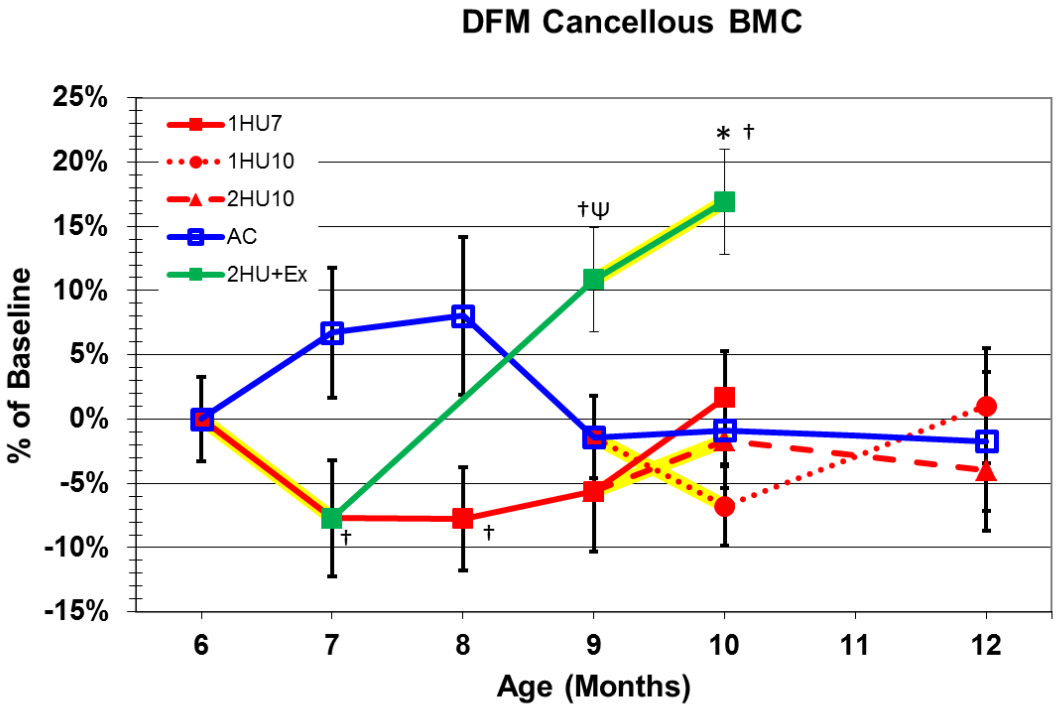

Figure 52: Changes in cancellous BMC of the distal femur metaphysis. Numerical data are presented in Table 9. Yellow highlighting indicates HU treatment. 1HU7 did not have significant losses compared to pre HU value but it was significantly lower than AC7. At month 9, the exercised group recovers to above 1HU7+R2 (+17.46%) and AC (+12.45%). After the second unloading period the 1HU10 and 2HU10 groups remain at AC10 level while 2HU10+Ex remains above AC level (+17.97%). Pre- to post-HU values for the 9- 10 month period show non-significant changes for all groups.

Values are presented as mean ± SE

*** Indicates significant difference from baseline value; $p<0.05$**

† Indicates significant difference from age-matched cage control value at same time point; $p<0.05$

 # Indicates significant difference from pre- to post-HU value within same group; $p<0.05$

Ψ Indicates significant difference between 1HU7+Ex and 1HU7+R2; $p<0.05$

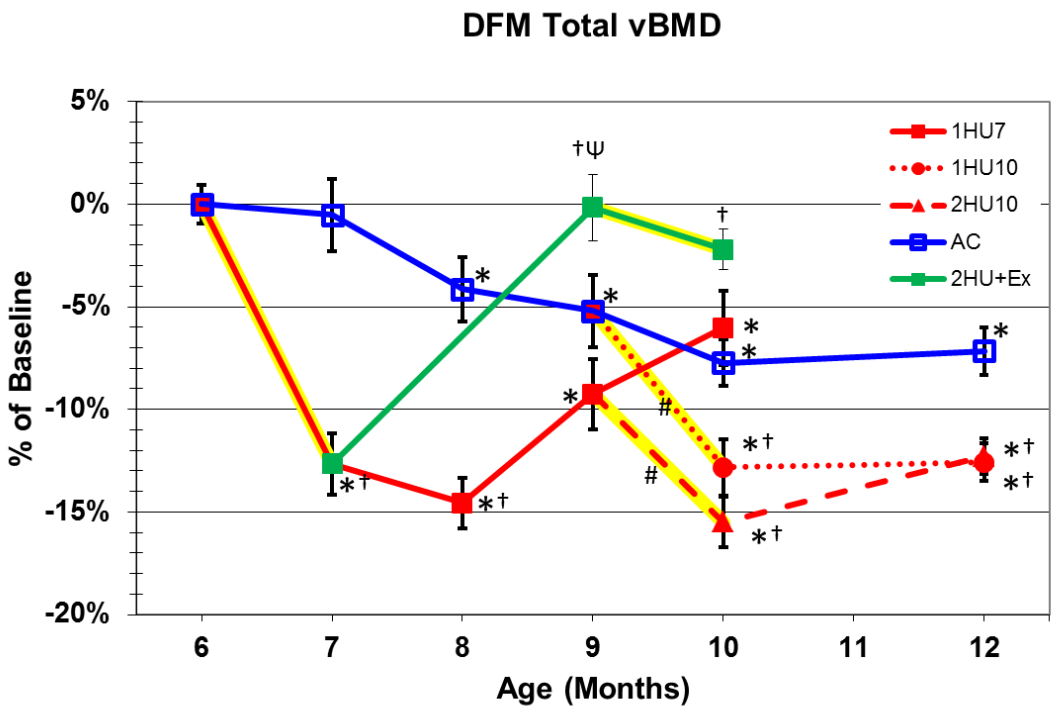

Figure 53: Changes in total vBMD of the distal femur metaphysis. Numerical data are presented in Table 9. Yellow highlighting indicates HU treatment. Aging AC animals show gradual declines in total vBMD. 1HU7 lost 12.65% from pre HU value and was significantly lower than AC. At month 9, the exercised group recovers to BL level and higher than AC (+5.32%), while 1HU7+R2 reaches only AC9 level. After the second unloading period the 1HU10 and 2HU10 groups fall below AC while 2HU10+Ex remains above AC level (+5.98%). Pre- to post-HU values for the 9- 10 month period show significant decreases for the 2HU10 (-6.88%) and 1HU10 (-8.02%) groups however 2HU10+Ex shows only a slight non-significant decrease (2.04%).
Values are presented as mean ± SE
*** Indicates significant difference from baseline value; $p<0.05$**
† Indicates significant difference from age-matched cage control value at same time point; $p<0.05$
 # Indicates significant difference from pre- to post-HU value within same group; $p<0.05$
Ψ Indicates significant difference between 1HU7+Ex and 1HU7+R2; $p<0.05$

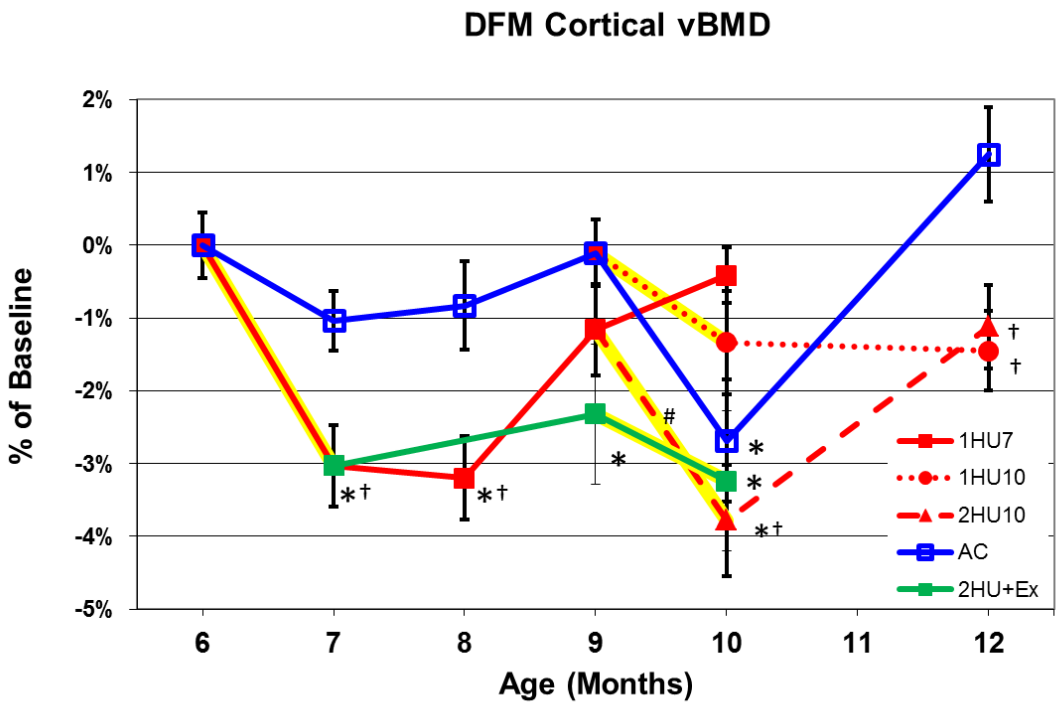

Figure 54: Changes in cortical vBMD of the distal femur metaphysis. Numerical data are presented in Table 9. Yellow highlighting indicates HU treatment. 1HU7 lost 3.03% from pre HU value and was significantly lower than AC. At month 9, the exercised group recovers to AC but remains lower than BL while 1HU7+R2 reaches both BL and AC level. After the second unloading period the 2HU10 group falls below AC while 2HU10+Ex remains at AC level. Pre- to post-HU values for the 9- 10 month period show significant decreases for the 2HU10 (-2.66%) group; however, 1HU10 and 2HU10+Ex groups show only a slight non-significant decrease.
Values are presented as mean ± SE
*** Indicates significant difference from baseline value; p<0.05**
† Indicates significant difference from age-matched cage control value at same time point; p<0.05
 # Indicates significant difference from pre- to post-HU value within same group; p<0.05
Ψ Indicates significant difference between 1HU7+Ex and 1HU7+R2; p<0.05

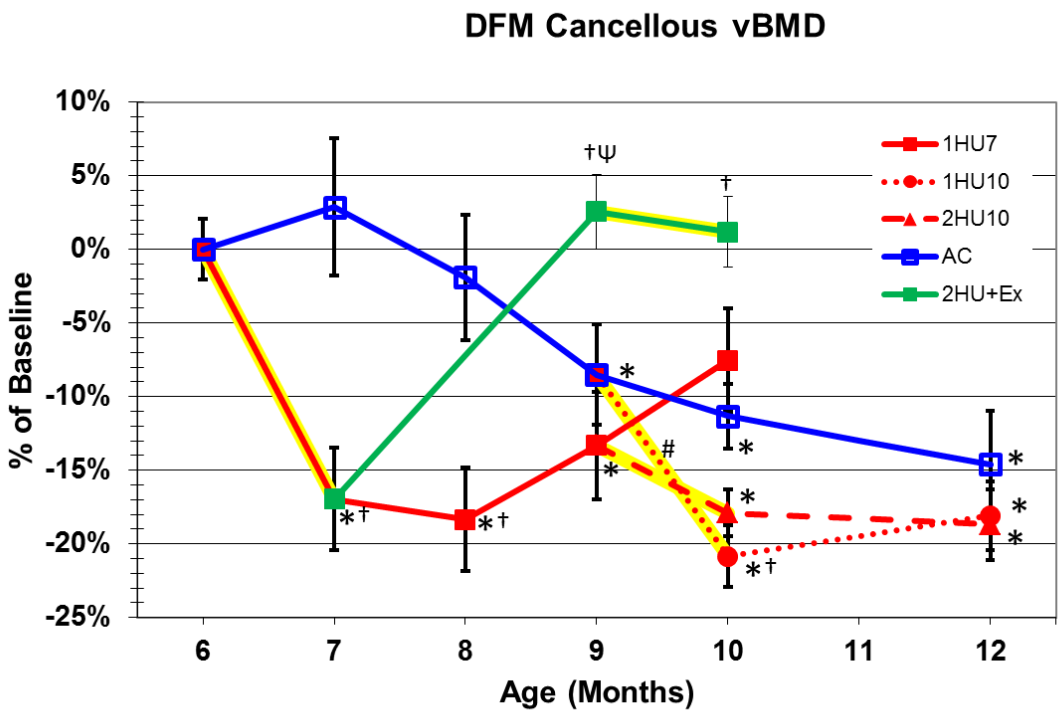

Figure 55: Changes in cancellous vBMD of the distal femur metaphysis. Numerical data are presented in Table 9. Yellow highlighting indicates HU treatment. Aging AC animals show gradual declines in cancellous vBMD after month 7. 1HU7 lost 16.95% from pre HU value and was significantly lower than AC. At month 9, the exercised group recovers to BL level and higher than AC (+12.08%), while 1HU7+R2 reaches only AC9 level. After the second unloading period the 1HU10 group falls below AC while 2HU10+Ex remains above AC level (+14.11%). Pre- to post-HU values for the 9- 10 month period show significant decreases for the 1HU10 (-13.47%) group; however, 2HU10 and 2HU10+Ex show only a slight non-significant decrease.
Values are presented as mean ± SE
*** Indicates significant difference from baseline value; p<0.05**
† Indicates significant difference from age-matched cage control value at same time point; p<0.05
 # Indicates significant difference from pre- to post-HU value within same group; p<0.05
Ψ Indicates significant difference between 1HU7+Ex and 1HU7+R2; p<0.05

Distal Femur Metaphysis Geometric Properties

Table 10 lists absolute values for the geometric properties of the DFM. Total area (Figure 56) increased as the animal aged, indicating periosteal apposition, with no apparent effect of the 1st HU. At month 9, the exercised group values increase to well above BL level and AC9, with continuing gains even during the 2nd HU period. Pre- to post-HU values for the 9 to10 month period show no significant changes despite recovery.

Cortical area (Figure 57) was significantly lower after the first HU. 1HU7+Ex recovered above AC and baseline while 1HU7+R2 remained below AC9. The second HU had no effect on any group's values. Endocortical area (Figure 58) increased during the first HU period, indicating endocortical resorption. Following the second HU the ambulatory recovery group shows increased endocortical area implying endocortical resorption. Cortical thickness (Figure 59) also had similar trends as cortical area. However there were significant changes pre- to post- HH for all groups except 2HU10+Ex.

Moments of inertia (Figure 60 - Figure 62) indicated almost no pre- to post- HU differences. The only differences were in a significant decrease after the 1st HU for maximum moment of inertial and a significant increase in minimum moment of inertia after the 2nd HU. 1HU7+Ex and 2HU10+Ex remained above AC for all inertial parameters.

Table 10: Geometric properties of the distal femur metaphysis

	Total Area (mm^2)	Endocortical Area (mm^2)	Cortical Area (mm^2)	Cortical Thickness (μm)	I_{MAX} (mm^4)	I_{MIN} (mm^4)	I_p (mm^4)
6 Months Old							
BL6	19.09 (0.32)	11.00 (0.25)	8.09 (0.11)	594.95 (6.8)	33.35 (0.92)	16.66 (0.56)	50.01 (1.44)
7 Month Old							
AC7	19.85 (0.34)	11.5 (0.27)	8.35 (0.14)	600.9 (8.7)	35.53 (1.16)	17.57 (0.56)	53.10 (1.63)
1HU7	19.73 (0.28)	12.28 (0.27) *†	7.45 (0.10) *†	529.8 (7.9) *†	29.99 (0.85) *†	16.96 (0.45)	46.94 (1.24) †
8 Months Old							
AC8	20.18 (0.41)	12.14 (0.33) *	8.04 (0.14)	569.3 (7.7) *	35.45 (1.27)	17.75 (0.69)	53.21 (1.86)
1HU7+R1	19.82 (0.38)	12.54 (0.28) *	7.28 (0.15) *†	513.8 (7.9) *†	29.80 (0.89) *†	16.84 (0.63)	46.64 (1.48) †
9 Months Old							
AC9	20.16 (0.36)	12.01 (0.30) *	8.15 (0.12)	578.5 (7.2)	35.37 (0.92)	17.72 (0.55)	53.09 (1.43)
1HU7+R2	19.68 (0.40)	12.07 (0.34) *	7.62 (0.12) *†	544.2 (8.4) *†	32.22 (1.09) †	16.66 (0.56)	48.89 (1.60)
1HU7+Ex	21.22 (041) *Ψ	11.98 (0.37) *	9.24 (0.30) *†Ψ	647.7 (21.1) *†Ψ	39.01 (1.30) *Ψ†	20.98 (0.84) *Ψ†	59.99 (2.04) *Ψ†
10 Months Old							
AC10	20.91 (0.34) *	12.43 (0.27) *	8.48 (0.13) *	591.7 (8.4)	36.62 (0.95) *	19.07 (0.55) *	55.69 (1.44) *
1HU7+R3	20.32 (0.35) *	12.13 (0.28) *	8.08 (0.17)	569.5 (10.7)	34.89 (1.13)	18.08 (0.62)	52.97 (1.68)
1HU10	21.00 (0.30) *	12.07 (0.29) *#	7.93 (0.10) †	547.3 (8.0) *†#	35.20 (0.76)	18.40 (0.44) *	53.60 (1.08) *
2HU10	20.73 (0.41) *	12.21 (0.36) *#	7.46 (0.13) *†	514.4 (8.6) *†#	32.50 (1.00) †	17.66 (0.67)	50.17 (1.63) †
2HU10+Ex	22.20 (0.29) *†	12.78 (0.28) *	9.43 (0.15) *†	643.2 (11.6) *†	40.34 (1.14) *†	23.45 (0.52) *†	63.79 (1.56) *†
12 Months Old							
AC12	20.94 (0.36) *	12.67 (0.31) *	8.27 (0.11)	574.5 (6.7)	38.36 (1.01) *	18.80 (0.61) *	57.16 (1.57) *
1HU10+R2	21.71 (0.41) *	11.86 (0.33) *	8.11 (0.13)	549.0 (7.7) *†	38.19 (1.33) *	19.77 (0.68) *	57.97 (1.94) *
2HU10+R2	20.88 (0.41) *	12.13 (0.33) *	7.86 (0.13) †	543.1 (6.8) *†	34.93 (1.20) *	18.63 (0.65) *	53.55 (1.80)

Values are presented as mean ± SE

* Indicates significant difference from baseline value, $p < 0.05$

† Indicates significant difference from age-matched control value at same time point, $p<0.05$

# Indicates significant difference from pre- to post-HU value within same group, $p<0.05$

Ψ Indicates significant difference from 1HU7+Ex to 1HU7+R2, $p<0.05$

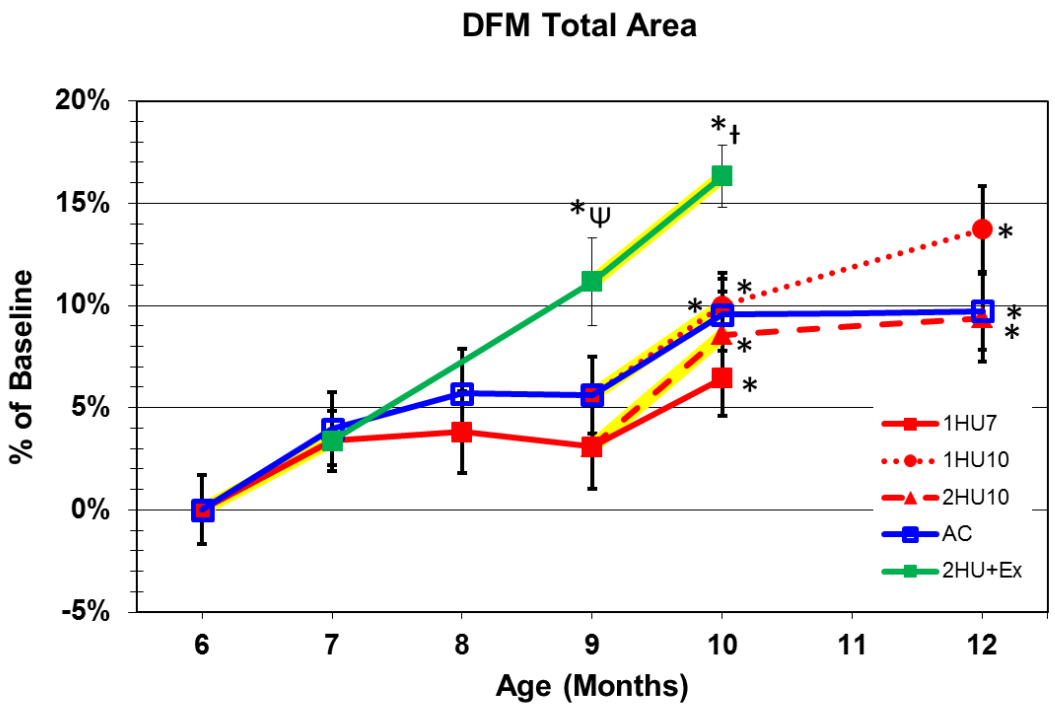

Figure 56: Changes in total area of the distal femur metaphysis. Numerical data are presented in Table 10. Yellow highlighting indicates HU treatment. Aging AC animals show gradual growth in total area. 1HU7 had no effect on total area. At month 9, the exercised group recovers above BL level and AC (+5.26%), while 1HU7+R2 reaches only AC9 level. After the second unloading period 2HU10+Ex remains above AC level (+6.18%). Pre- to post-HU values for the 9- 10 month period show significant changes for any group.
Values are presented as mean ± SE
*** Indicates significant difference from baseline value; $p<0.05$**
† Indicates significant difference from age-matched cage control value at same time point; $p<0.05$
 # Indicates significant difference from pre- to post-HU value within same group; $p<0.05$
Ψ Indicates significant difference between 1HU7+Ex and 1HU7+R2; $p<0.05$

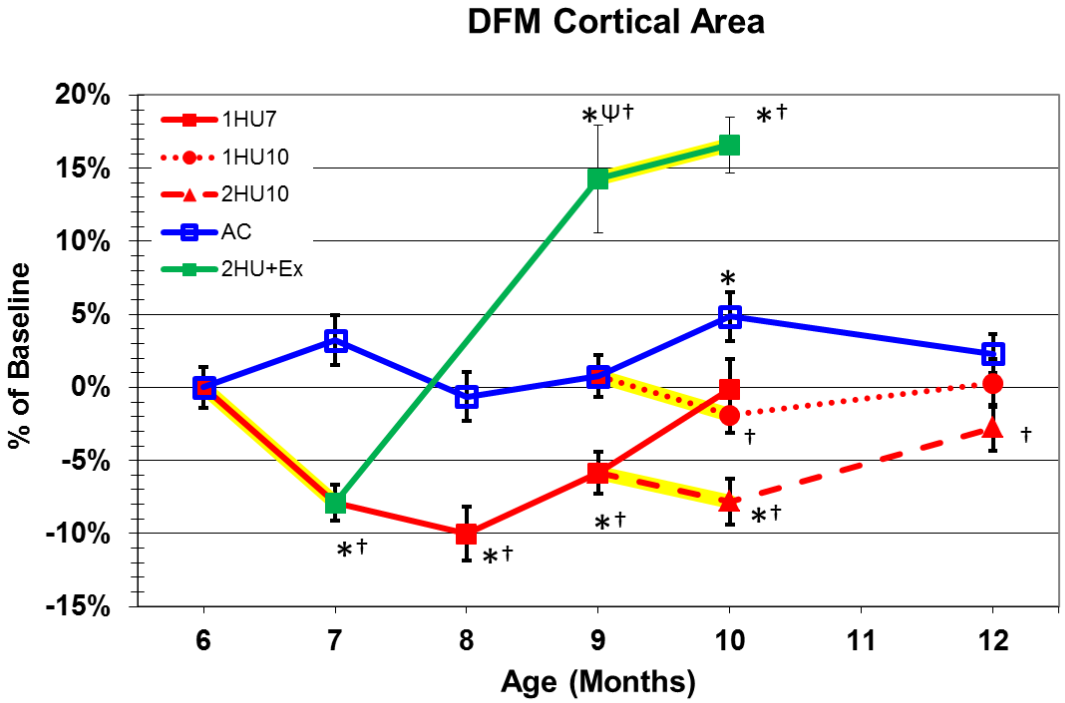

Figure 57: Changes in cortical area of the distal femur metaphysis. Numerical data are presented in Table 10. Yellow highlighting indicates HU treatment. 1HU7 lost 7.9% from pre HU value and was significantly lower than AC. At month 9, the exercised group recovers to above BL, AC (+13.41%), and 1HU7+R2 (+21.35%) while 1HU7+R2 does not fully recover. After the second unloading period the 1HU10 and 2HU10 groups fall below AC while 2HU10+Ex remains above AC level (+11.2%). Pre- to post-HU values for the 9- 10 month period show no significant changes for any groups.
Values are presented as mean ± SE
*** Indicates significant difference from baseline value; $p<0.05$**
† Indicates significant difference from age-matched cage control value at same time point; $p<0.05$
 # Indicates significant difference from pre- to post-HU value within same group; $p<0.05$
Ψ Indicates significant difference between 1HU7+Ex and 1HU7+R2; $p<0.05$

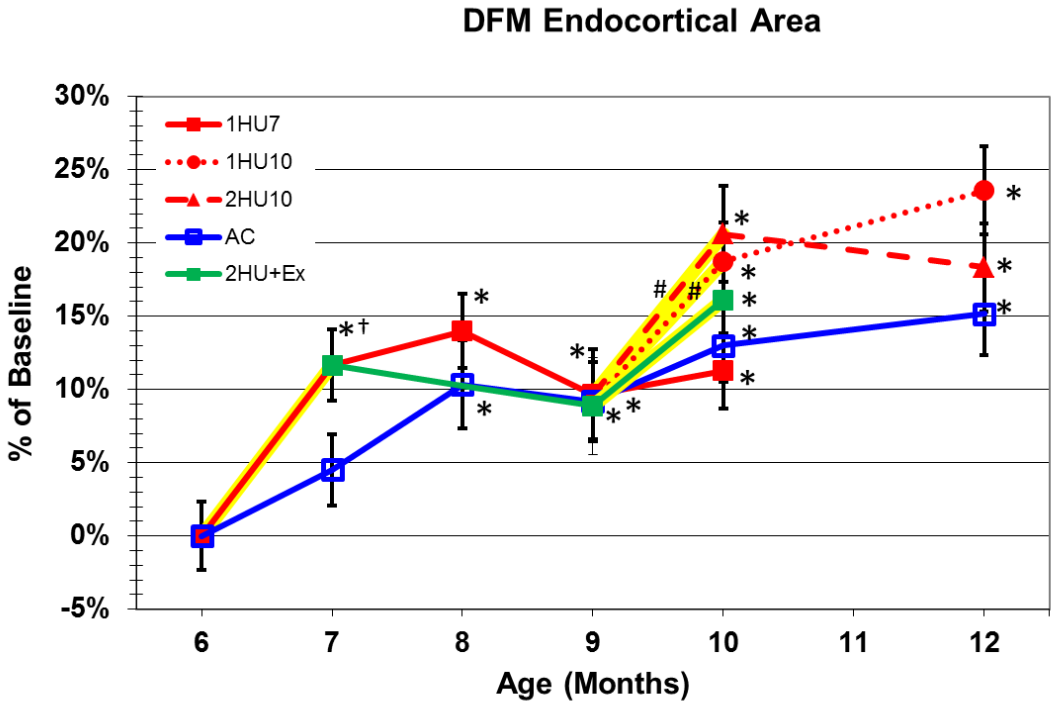

Figure 58: Changes in total area of the distal femur metaphysis. Numerical data are presented in Table 10. Yellow highlighting indicates HU treatment. Aging AC animals show gradual growth in endocortical area. 1HU7 increased 11.65% from pre-HU value. Pre- to post-HU values for the 9- 10 month period show significant increases for the 1HU10 and 2HU10 groups while 2HU10+Ex has only a slight non-significant increase.
Values are presented as mean ± SE
*** Indicates significant difference from baseline value; p<0.05**
† Indicates significant difference from age-matched cage control value at same time point; p<0.05
 # Indicates significant difference from pre- to post-HU value within same group; p<0.05
Ψ Indicates significant difference between 1HU7+Ex and 1HU7+R2; p<0.05

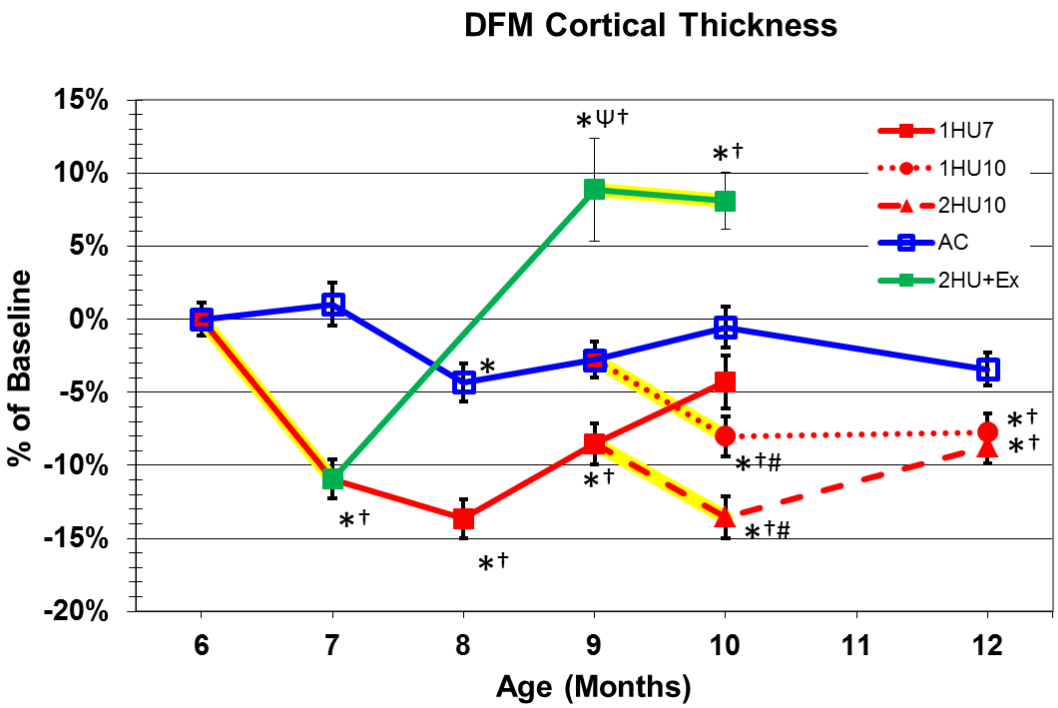

Figure 59: Changes in cortical thickness of the distal femur metaphysis. Numerical data are presented in Table 10. Yellow highlighting indicates HU treatment. 1HU7 lost 10.94% from pre HU value and was significantly lower than AC. At month 9, the exercised group recovers to above BL, AC (+11.96%), and 1HU7+R2 (+19.02%) while 1HU7+R2 does not fully recover. After the second unloading period the 1HU10 and 2HU10 groups falls below AC while 2HU10+Ex remains above AC level (+8.71%). Pre- to post-HU values for the 9- 10 month period show significant decreases for the 1HU10 (-5.4%) and 2HU10 (-5.48%) groups while the 2HU10+Ex group shows a slight non-significant decrease.

Values are presented as mean ± SE

*** Indicates significant difference from baseline value; $p<0.05$**

† Indicates significant difference from age-matched cage control value at same time point; $p<0.05$

 # Indicates significant difference from pre- to post-HU value within same group; $p<0.05$

Ψ Indicates significant difference between 1HU7+Ex and 1HU7+R2; $p<0.05$

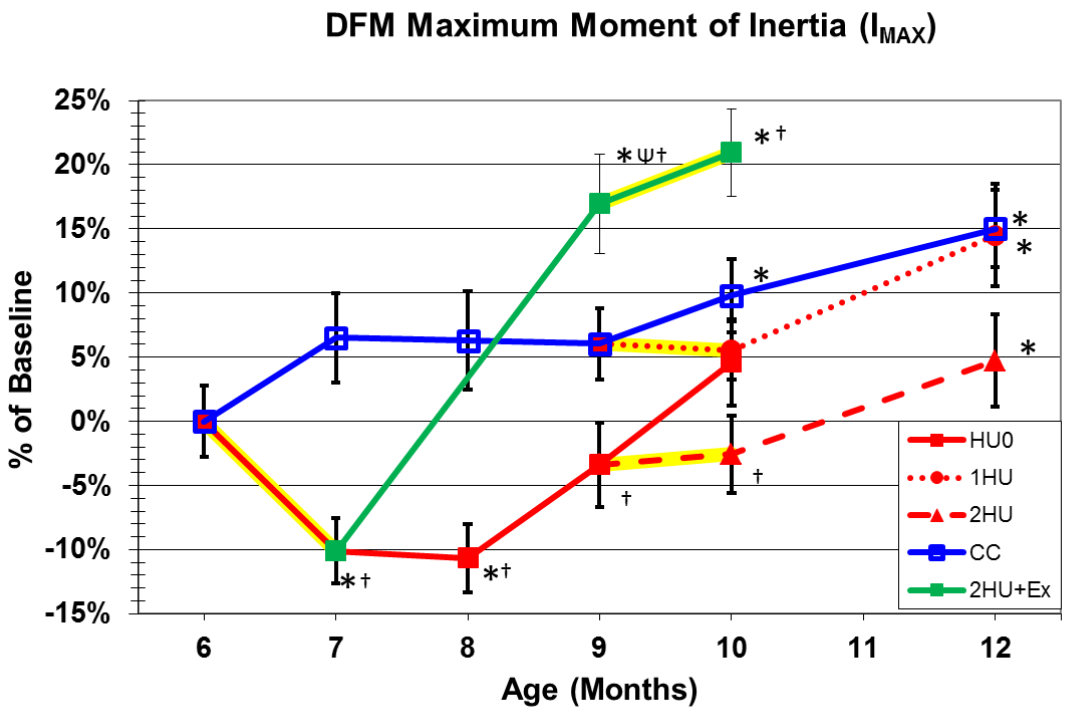

Figure 60: Changes in maximum moment of intertia of the total cross section of the distal femur metaphysis. Numerical data are presented in Table 10. Yellow highlighting indicates HU treatment. 1HU7 lost 10.09% from pre HU value and was significantly lower than AC. At month 9, the exercised group recovers to above BL, AC (+10.31%), and 1HU7+R2 (+21.06%) while 1HU7+R2 does not fully recover to AC9. After the second unloading period the 2HU10 groups remains below AC while 2HU10+Ex remains above AC level (+10.14%). Pre- to post-HU values for the 9- 10 month period show no significant changes for any groups.
Values are presented as mean ± SE
*** Indicates significant difference from baseline value; p<0.05**
† Indicates significant difference from age-matched cage control value at same time point; p<0.05
 # Indicates significant difference from pre- to post-HU value within same group; p<0.05
Ψ Indicates significant difference between 1HU7+Ex and 1HU7+R2; p<0.05

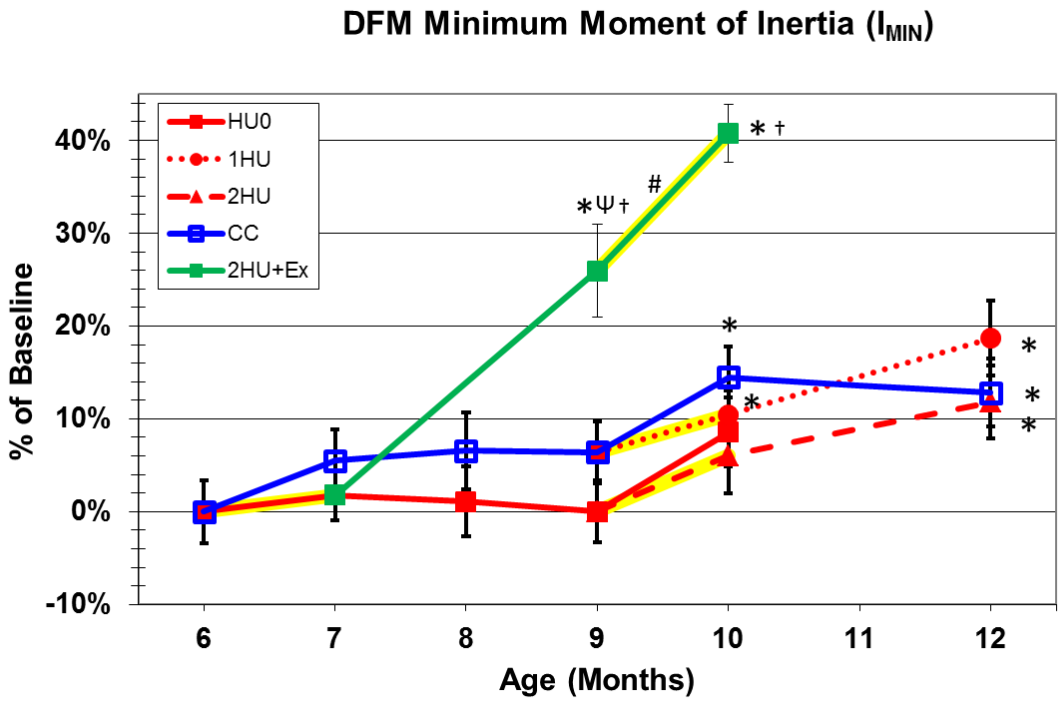

Figure 61: Changes in minimum moment of intertia of the total cross section of the distal femur metaphysis. Numerical data are presented in Table 10. Yellow highlighting indicates HU treatment. HU only has an effect at 2HU10+Ex. Pre to post HU shows an increase of 11.76% in minimum moment of inertia. The exercised group at month 9 and 10 also remains above age matched cage controls.

Values are presented as mean ± SE

*** Indicates significant difference from baseline value; $p<0.05$**

† Indicates significant difference from age-matched cage control value at same time point; $p<0.05$

 # Indicates significant difference from pre- to post-HU value within same group; $p<0.05$

Ψ Indicates significant difference between 1HU7+Ex and 1HU7+R2; $p<0.05$

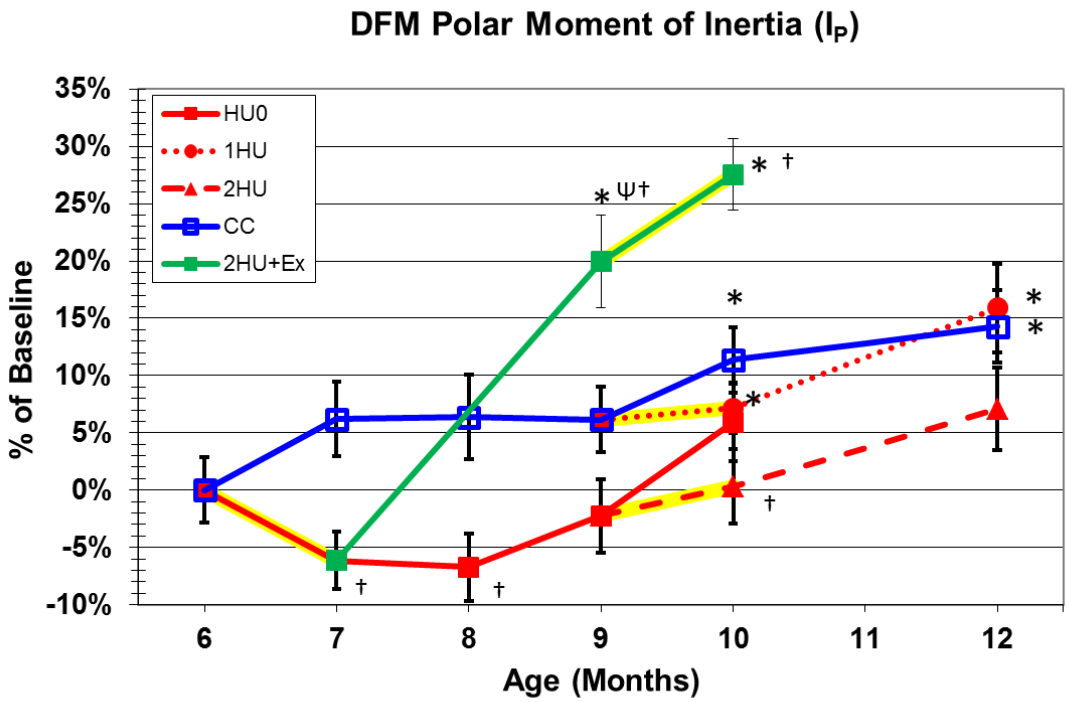

Figure 62: Changes in polar moment of intertia of the total cross section of the distal femur metaphysis. Numerical data are presented in Table 10. Yellow highlighting indicates HU treatment. 1HU7 suppressed age related growths and was significantly lower than AC. At month 9, the exercised group recovers above BL, AC (+13.01%), and 1HU7+R2 (+22.71%). After the second unloading period the 2HU10 groups remains below AC while 2HU10+Ex remains above AC level (+15.54%). Pre- to post-HU values for the 9- 10 month period show no significant changes for any groups.

Values are presented as mean ± SE

*** Indicates significant difference from baseline value; p<0.05**

† Indicates significant difference from age-matched cage control value at same time point; p<0.05

 # Indicates significant difference from pre- to post-HU value within same group; p<0.05

Ψ Indicates significant difference between 1HU7+Ex and 1HU7+R2; p<0.05

Distal Femur Metaphysis Strength Indices

Table 11 lists absolute values for calculated strengths of the distal femur metaphysis. Pattern of change for structural strength index (Figure 63) is identical to I_P. 1HU7 suppressed age related increases and was significantly lower than AC. At month 9, the exercised group exhibits a large increase above AC and 1HU7+R2. After the second unloading period the 2HU10 group remains below AC while 2HU10+Ex remains above AC level. Pre- to post-HU values for the 9- 10 month period show no significant changes for any groups.

Total CSI (Figure 64) and cancellous CSI (Figure 65) both had significant hindlimb unloading related declines for the first HU period. At month 9, the exercised group recovers above BL, AC, and 1HU7+R2. After the second unloading period the 2HU10 and 1HU10 groups remains below AC while 2HU10+Ex remains above AC level. Pre- to post-HU values for the 9- 10 month period reveal significant decreases for only 1HU10.

Table 11: Calculated strength indices for total and cancellous bone of the distal femur metaphysis

	SSI (mm^3)	Total CSI (mg^2/mm^4)	Cancellous CSI (mg^2/mm^4)
6 Months Old			
BL6	15.43 (0.33)	7.74 (0.15)	1.17 (0.06)
7 Month Old			
AC7	16.23 (0.38) *	8.03 (0.28)	1.31 (0.10)
1HU7	14.65 (0.27) †	6.16 (0.19) *†	0.92 (0.08) *†
8 Months Old			
AC8	16.18 (0.43)	7.59 (0.27)	1.27 (0.13)
1HU7+R1	14.65 (0.34) †	5.96 (0.15) *†	0.91 (0.08) *†
9 Months Old			
AC9	16.23 (0.34) *	7.39 (0.22)	1.06 (0.07)
1HU7+R2	15.18 (0.36) †	6.65 (0.21) *†	0.98 (0.08)
1HU7+Ex	17.73 (0.44) *Ψ†	8.65 (0.28) *†Ψ	1.37 (0.08) *†Ψ
10 Months Old			
AC10	16.73 (0.34) *	7.31 (0.15) *	1.05 (0.05)
1HU7+R3	16.23 (0.39)	7.37 (0.28)	1.12 (0.08)
1HU10	16.09 (0.25) *	6.57 (0.15) *†#	0.88 (0.06) *#†
2HU10	15.12 (0.40) †	6.13 (0.18) *†	0.97 (0.06) *
2HU10+Ex	18.83 (0.35) *†	8.72 (0.17) *†	1.427 (0.08) *†
12 Months Old			
AC12	16.96 (0.35) *	7.39 (0.20)	1.01 (0.09)
1HU10+R2	17.12 (0.46) *	6.84 (0.19) *	1.00 (0.08)
2HU10+R2	16.18 (0.41) *	6.66 (0.18) *†	0.96 (0.08) *

Values are presented as mean ± SE

* Indicates significant difference from baseline value, $p < 0.05$

† Indicates significant difference from age-matched control value at same time point, $p<0.05$

# Indicates significant difference from pre- to post-HU value within same group, $p<0.05$

Ψ Indicates significant difference from 1HU7+Ex to 1HU7+R2, $p<0.05$

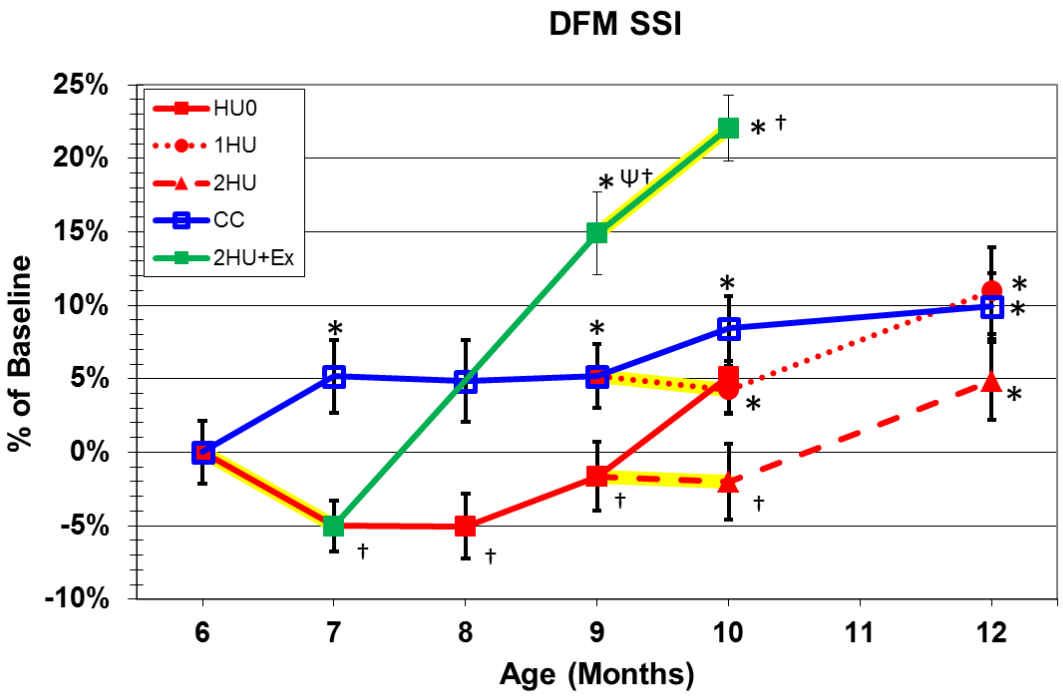

Figure 63: Changes in stress-strain index of the distal femur metaphysis. Numerical data are presented in Table 11. Yellow highlighting indicates HU treatment. 1HU7 suppressed age related growths and was significantly lower than AC. At month 9, the exercised group recovers above BL, AC (+9.25%), and 1HU7+R2 (+16.82%). After the second unloading period the 2HU10 groups remains below AC while 2HU10+Ex remains above AC level (+15.56%). Pre- to post-HU values for the 9- 10 month period show no significant changes for any groups.
Values are presented as mean ± SE
*** Indicates significant difference from baseline value; p<0.05**
† Indicates significant difference from age-matched cage control value at same time point; p<0.05
 # Indicates significant difference from pre- to post-HU value within same group; p<0.05
Ψ Indicates significant difference between 1HU7+Ex and 1HU7+R2; p<0.05

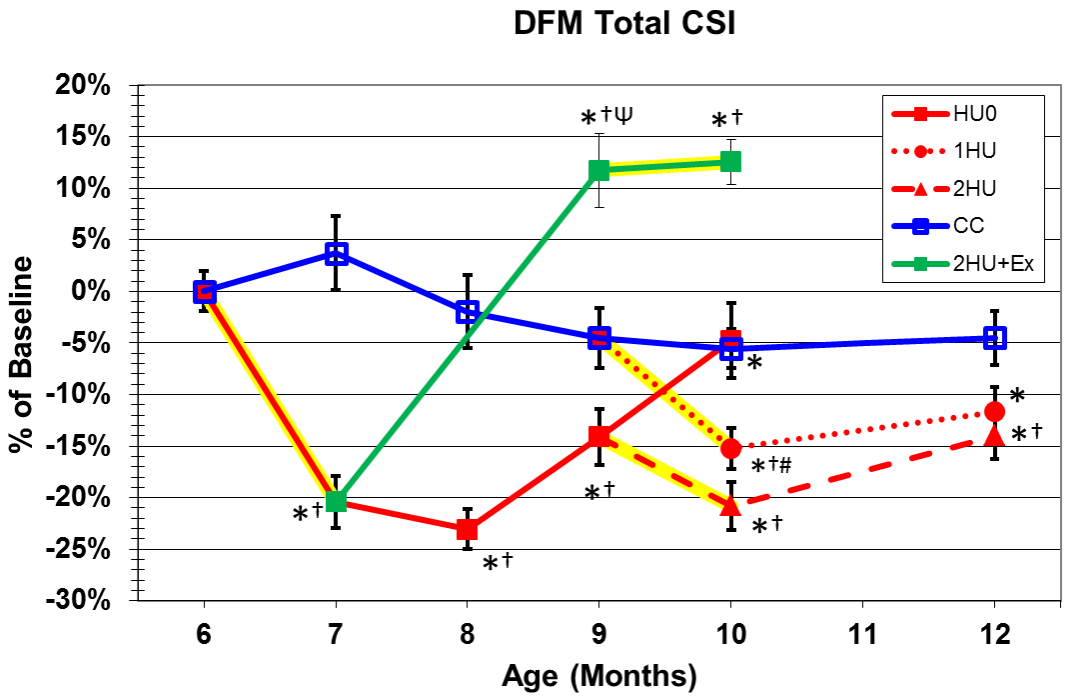

Figure 64: Changes in compressive strength index of the total cross-section of the distal femur metaphysis. Numerical data are presented in Table 11. Yellow highlighting indicates HU treatment. 1HU7 decreases CSI by -20.41% and was significantly lower than AC. At month 9, the exercised group recovers above BL, AC (+17.01%), and 1HU7+R2 (+30.09%). After the second unloading period the 2HU10 groups remains below AC while 2HU10+Ex remains above AC level (+19.18%). Pre- to post-HU values for the 9- 10 month period show significant changes only for 1HU10 which decreased 11.18%.
Values are presented as mean ± SE
*** Indicates significant difference from baseline value; p<0.05**
† Indicates significant difference from age-matched cage control value at same time point; p<0.05
 # Indicates significant difference from pre- to post-HU value within same group; p<0.05
Ψ Indicates significant difference between 1HU7+Ex and 1HU7+R2; p<0.05

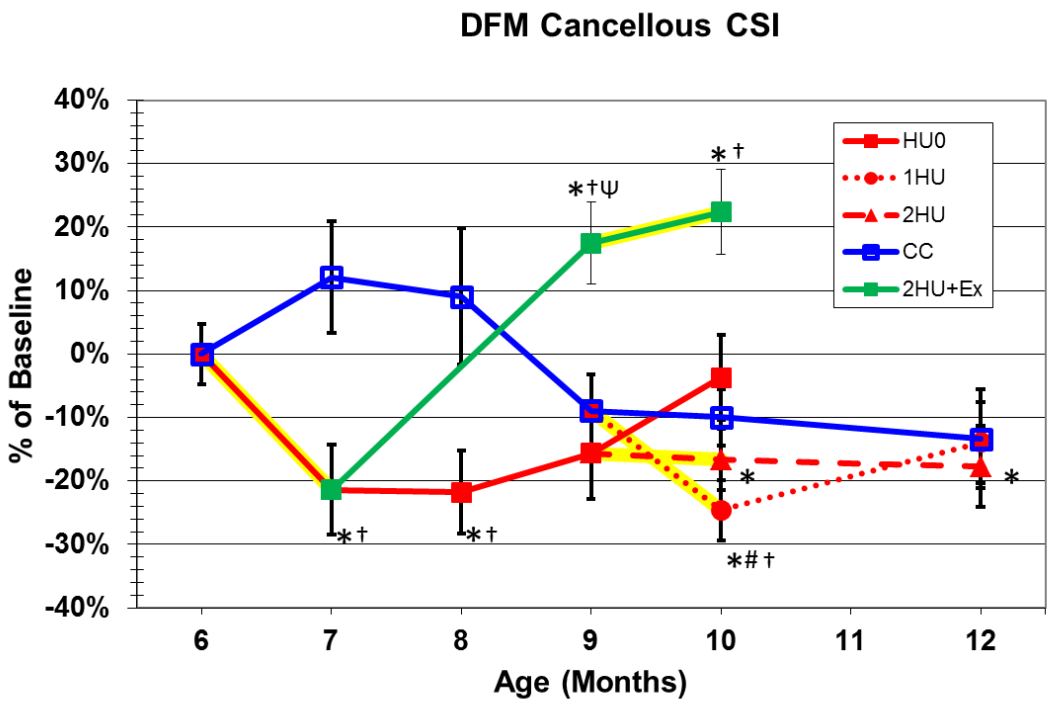

Figure 65: Changes in compressive strength index of the cancellous cross-section of the distal femur metaphysis. Numerical data are presented in Table 11. Yellow highlighting indicates HU treatment. 1HU7 decreases cancellous CSI by 21.38% and was significantly lower than AC. At month 9, the exercised group recovers above BL, AC (+29.05%), and 1HU7+R2 (+39.33%). After the second unloading period the 1HU10 group remains below AC while 2HU10+Ex remains above AC level (+35.9%). Pre- to post-HU values for the 9- 10 month period show significant changes only for 1HU10 which decreased 17.22%.

Values are presented as mean ± SE

*** Indicates significant difference from baseline value; $p<0.05$**

† Indicates significant difference from age-matched cage control value at same time point; $p<0.05$

 # Indicates significant difference from pre- to post-HU value within same group; $p<0.05$

Ψ Indicates significant difference between 1HU7+Ex and 1HU7+R2; $p<0.05$

Distal Femur Metaphysis Mechanical Properties

Table 12 lists the absolute values for mechanical properties of the distal femur metaphysis. Reduced platen compression testing was conducted at the DFM. Ultimate stress (Figure 66) does not reveal significant declines for the 1st HU or 2nd HU for either ambulatory or exercise recovery groups. Energy to ultimate (Figure 67) also does not present significant declines for the 1st HU but the ambulatory recovery group values decrease significantly after a 2nd HU. Interestingly, exercised animals exhibit non-significant increases after a 2nd HU bout. Elastic modulus (Figure 68) showed the same patterns as ultimate stress. One unique observation is that Elastic modulus actually increased significantly (+108%) for the exercise recovery group following a 2nd bout of HU.

Ultimate strain (Figure 69) exhibited no differences from pre- to post-HU, although there was a steep decline in 2HU10+Ex animals. After recovery 1HU+Ex was significantly higher than all other groups.

Table 12: Estimated mechanical properties of cancellous bone of the distal femur metaphysis

	Elastic Modulus (MPa)	Ultimate Stress (MPa)	Yield Stress (MPa)	Energy to Ultimate (mJ)	Energy to Yield (mJ)	Strain at Ultimate (%)	Strain at Yield (%)
6 Months Old							
BL6	27.26 (4.50)	0.80 (0.15)	0.71 (0.15)	143.7 (29.7)	101.5 (26.1)	6.66 (1.02)	5.82 (1.22)
7 Month Old							
AC7	48.05 (7.87)	1.52 (0.36) *	1.36 (0.35)	244.9 (79.0)	171.9 (72.4)	4.46 (0.56)	3.63 (0.50)
1HU7	16.66 (3.30) †	0.37 (0.07) †	0.32 (0.06) *†	49.7 (11.1) †	26.4 (6.0) †	4.70 (0.41)	3.63 (0.31)
8 Months Old							
AC8	46.37 (6.51)	1.21 (0.27)	0.99 (0.24)	177.2 (59.1)	118.2 (51.1)	3.88 (0.63)	3.14 (0.61)
1HU7+R1	27.65 (5.09) †	0.67 (0.18)	0.53 (0.14)	118.0 (29.7)	40.8 (13.2)	3.97 (0.56)	2.59 (0.33)
9 Months Old							
AC9	28.44 (6.24)	0.74 (0.15)	0.56 (0.13)	111.6 (26.7)	50.4 (14.1)	5.27 (0.70)	3.43 (0.63)
1HU7+R2	30.84 (7.28)	0.80 (0.19)	0.64 (0.15)	105.7 (27.4)	55.1 (14.7)	4.27 (0.42)	3.27 (0.43)
1HU7+Ex	29.98 (6.58)	1.19 (0.23)	1.17 (0.31) †	450.9 (112.4) *†Ψ	356.4 (145.5) *†Ψ	13.65 (2.79) *†Ψ	10.87 (2.52) *†Ψ
10 Months Old							
AC10	22.49 (3.22)	0.68 (0.11)	0.76 (0.13)	235.2 (47.3)	169.1 (36.9)	9.92 (1.29) *	8.90 (1.29) *
1HU7+R3	36.99 (8.31)	1.00 (0.21)	0.84 (0.18)	158.5 (44.2)	84.7 (23.5)	4.68 (0.51) †	3.51 (0.48) †
1HU10	11.22 (3.73) *†#	0.24 (0.11) *†#	0.18 (0.08) *#†	45.8 (32.2) *#†	12.1 (6.5) *†#	4.36 (0.64) †	3.11 (0.60) †
2HU10	22.26 (4.79)	0.43 (0.10)	0.37 (0.09) †	44.0 (13.2) †	26.1 (6.1) †	4.42 (0.51) †	3.78 (0.43) †
2HU10+Ex	62.32 (9.65) *†#	1.92 (0.28) *†	1.63 (0.25) *†	526.2 (100.9) *†	329.0 (98.0) *	8.48 (1.69)	7.70 (1.94)
12 Months Old							
AC12	34.13 (10.38)	1.01 (0.34)	0.70 (0.21)	152.2 (48.7)	54.9 (14.5)	6.23 (0.73)	4.57 (0.69)
1HU10+R2	19.22 (4.03)	0.36 (0.07)	0.32 (0.06)	34.1 (7.2) *†	20.3 (4.2)	4.17 (0.55) †	3.33 (0.49)
2HU10+R2	36.26 (5.49)	0.82 (0.13)	0.65 (0.10)	106.1 (23.0)	44.7 (9.5)	4.26 (0.41) †	3.05 (0.32)

Values are presented as mean ± SE

* Indicates significant difference from baseline value, $p < 0.05$

† Indicates significant difference from age-matched control value at same time point, $p<0.05$

# Indicates significant difference from pre- to post-HU value within same group, $p<0.05$

Ψ Indicates significant difference from 1HU7+Ex to 1HU7+R2, $p<0.05$

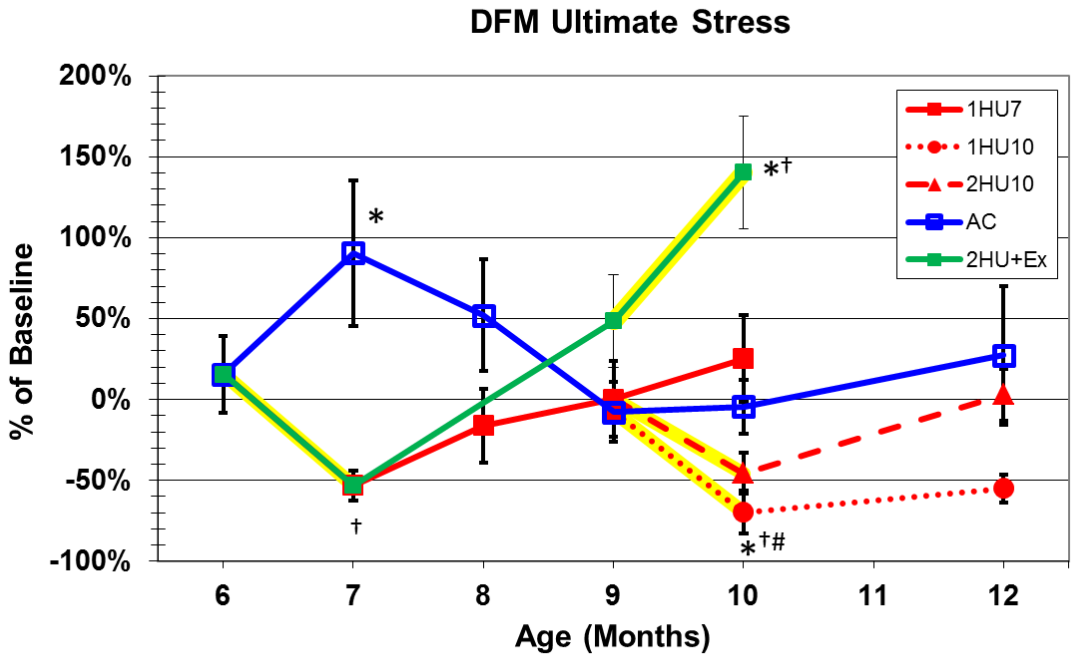

Figure 66: Changes in estimated ultimate stress of the distal femur metaphysis. Numerical data are presented in Table 12. Yellow highlighting indicates HU treatment. 1HU7 shows a non-significant decrease in ultimate stress of 53.13% and was significantly lower than AC. At month 9, 1HU7+R2 and 1HU7+Ex groups recover to BL and AC. After the second unloading period the 1HU10 falls below AC and BL while 2HU10+Ex experiences gains above BL and AC level (+183.18%). Pre- to post-HU values for the 9- 10 month period show significant changes only for 1HU10 which decreased 67.2%. 2HU10+Ex experienced a non-significant increase pre to post HU of 61.86%.
Values are presented as mean ± SE
*** Indicates significant difference from baseline value; $p<0.05$**
† Indicates significant difference from age-matched cage control value at same time point; $p<0.05$
 # Indicates significant difference from pre- to post-HU value within same group; $p<0.05$
Ψ Indicates significant difference between 1HU7+Ex and 1HU7+R2; $p<0.05$

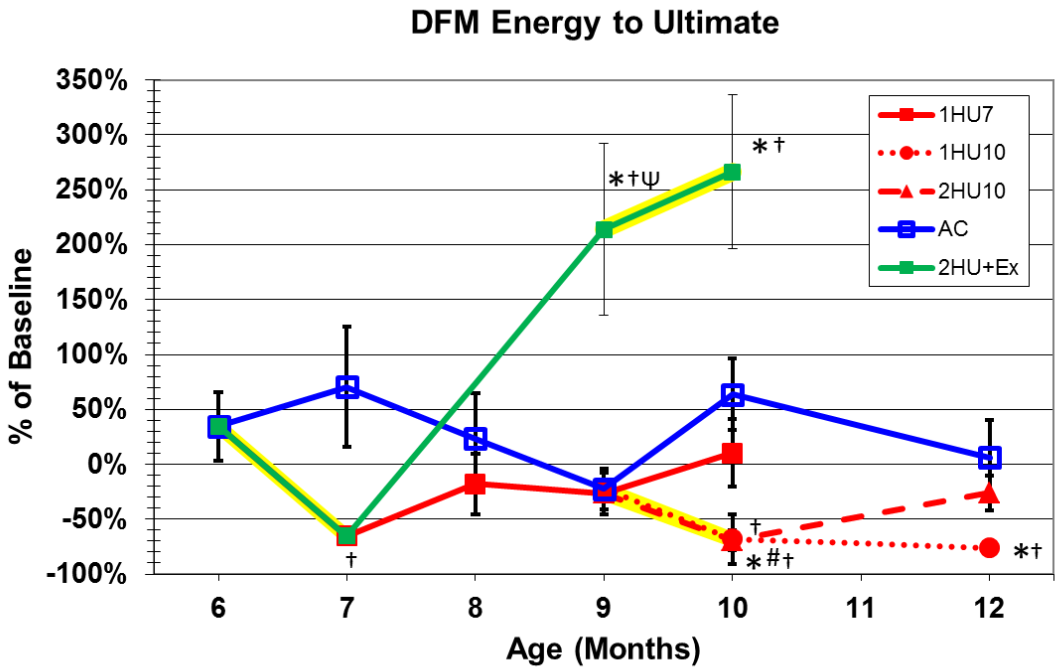

Figure 67: Changes in energy to ultimate of the distal femur metaphysis. Numerical data are presented in Table 12. Yellow highlighting indicates HU treatment. 1HU7 shows a non-significant decrease in energy of 65.40% and was significantly lower than AC. At month 9, 1HU7+R2 recovers to BL and AC while 1HU7+Ex shows significant gains above BL, AC9 (+304.1%), and 1HU7+R2 (+326.4%). After the second unloading period 1HU10 and 2HU10 fall below AC while 2HU10+Ex experiences gains above BL and AC level (+123.7%). Pre- to post-HU values for the 9- 10 month period shows a significant decrease for 1HU10 of 58.9%. 2HU10+Ex experienced a non-significant increase in energy pre to post HU of 16.7%.
Values are presented as mean ± SE
*** Indicates significant difference from baseline value; $p<0.05$**
† Indicates significant difference from age-matched cage control value at same time point; $p<0.05$
 # Indicates significant difference from pre- to post-HU value within same group; $p<0.05$
Ψ Indicates significant difference between 1HU7+Ex and 1HU7+R2; $p<0.05$

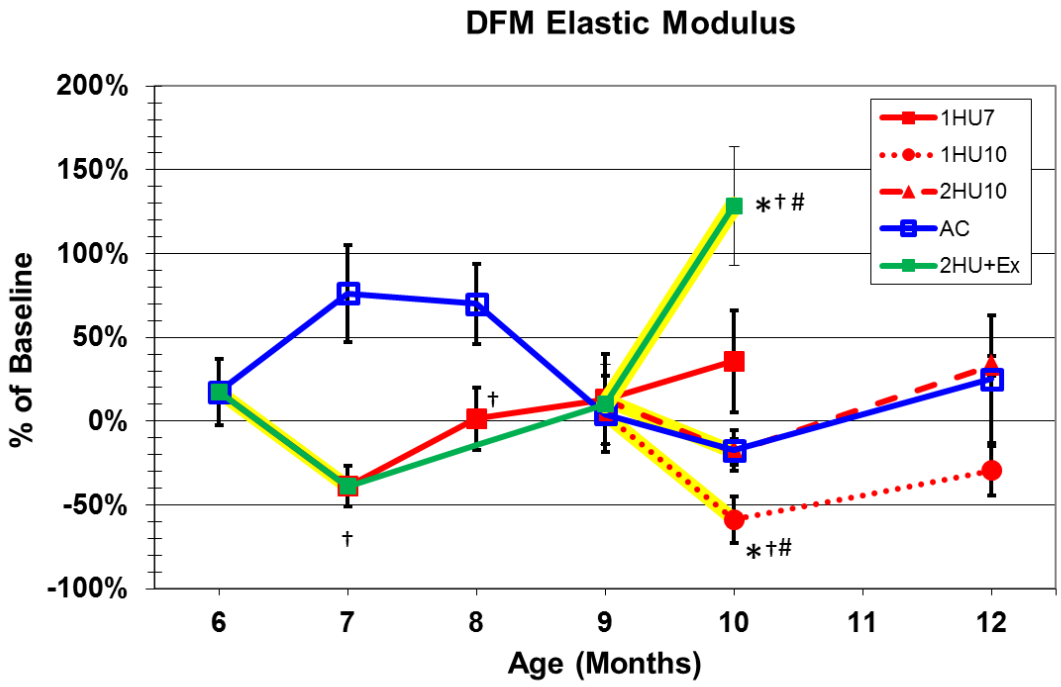

Figure 68: Changes in elastic modulus of the distal femur metaphysis. Numerical data are presented in Table 12. Yellow highlighting indicates HU treatment. 1HU7 shows a non-significant decrease in elastic modulus of 38.9% and was significantly lower than AC. At month 9, 1HU7+R2 and 1HU7+Ex groups recover to BL and AC. After the second unloading period the 1HU10 falls below AC and BL while 2HU10+Ex experiences gains above BL and AC level (+177.2%). Pre- to post-HU values for the 9- 10 month period shows a significant decrease for 1HU10 of 60.5%. However, 2HU10+Ex experienced a significant increase in elastic modulus pre to post HU of 107.9%.
Values are presented as mean ± SE
*** Indicates significant difference from baseline value; $p<0.05$**
† Indicates significant difference from age-matched cage control value at same time point; $p<0.05$
 # Indicates significant difference from pre- to post-HU value within same group; $p<0.05$
Ψ Indicates significant difference between 1HU7+Ex and 1HU7+R2; $p<0.05$

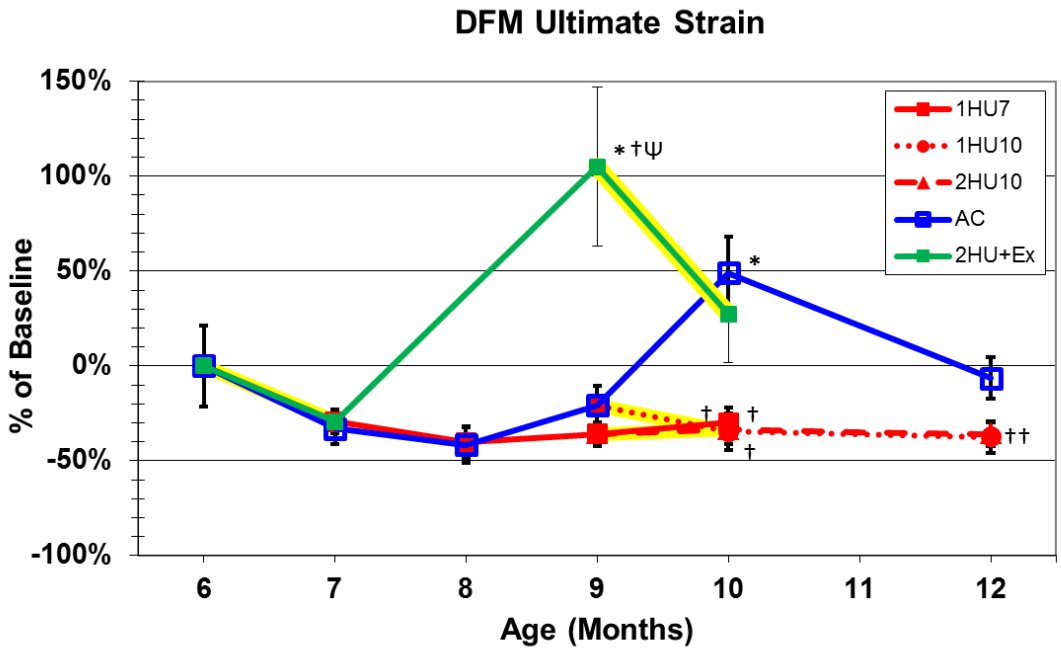

Figure 69: Changes in energy to ultimate strain femur metaphysis. Numerical data are presented in Table 12. Yellow highlighting indicates HU treatment. 1HU7 shows non-significant changes. At month 9 1HU7+Ex shows significant gains above BL, AC9 (+158.8%), and 1HU7+R2 (+219.6%). After the second unloading period 1HU10 and 2HU10 fall below AC while 2HU10+Ex remains at AC level. Pre- to post-HU values for the 9- 10 month period show no significant changes for any group.

Values are presented as mean ± SE

*** Indicates significant difference from baseline value; p<0.05**

† Indicates significant difference from age-matched cage control value at same time point; p<0.05

 # Indicates significant difference from pre- to post-HU value within same group; p<0.05

Ψ Indicates significant difference between 1HU7+Ex and 1HU7+R2; p<0.05

DISCUSSION

The objective of this study was to examine the effects of resistance exercise during recovery in-between two bouts of simulated microgravity. Recovery of animals undergoing simulated microgravity can be defined in two ways. To determine if an animal is fully recovered, the animals undergoing treatment can be compared to either baseline controls (at start of experiment) or age-matched cage control. In this study animals will be considered fully recovered if they are within age-matched cage control value. The discussion will focus on addressing HU and recovery characteristics of individual sites beginning with the femoral neck, followed by the femur midshaft diaphysis, and finally the distal femur metaphysis. The three sites will then be compared to each other. The discussion will conclude with comparing these data to other studies.

As mentioned previously, this experiment, focusing on exercise during recovery in-between two microgravity simulations, is the final component of a three-part study. The other experiments were conducted to assess the effects of cage activity or ambulatory recovery between two unloading bouts and also the effects of a single HU for older animals starting at 9 months of age and ending at 10 months of age. This discussion will build on what was previously reported by Josh Kupke in "Characterization of the femoral neck regions response to the rat hindlimb unloading model through tomographic scanning, mechanical testing and estimated strengths" [15], Scott Morgan in "The effects of multiple unloading exposures on bone properties in the femur of adult male rats" [14], and Josh Davis in "Characterization of the bone loss and

recovery response at the distal femur metaphysis of the adult hindlimb unloaded rat" [13]. Josh Kupke reported on the first HU with three recovery periods at the FN, Scott Morgan focused on the first two experiments FN and FD data, and Josh Davis focused on the first two experiments at the DFM. Results from these studies will also be summarized for context and reference. Furthermore, these data include additional animals which were added to BL and AC10 for this experiment.

Femoral Neck

FN AC: Cortical BMC of aging controls animals increases as the study progresses. Cancellous BMC decreases. Total BMC fluctuates, neither showing trends of increasing or decreasing. Similarly, cortical vBMD increases as animals grow older while cancellous vBMD decreases throughout the study. As a result total vBMD remains relatively steady. Cortical BMC and cortical vBMD of aging controls increases throughout the study above BL levels. Cancellous BMC and vBMD decreases to lower than BL values by month 12. These changes indicate that, while the animals are considered skeletally mature, cancellous bone is decreasing while cortical bone is increasing. Cortical area presents significant increases after month 8 while endocortical area illustrates significantly lower values than BL only at month 12 suggesting endosteal apposition. Total area does not indicate any fluctuations with BL throughout the study. Moments of inertia do not trend upward or down for increasing age. This implies that age has less of an effect on these properties.

FN Response to HU Treatment

FN 1HU7: Cortical BMC decreased significantly from BL while cancellous BMC only decreased slightly (n.s.). This results in a significant decrease for total BMC. Cortical vBMD shows a non-significant increase from BL while cancellous vBMD presents a significant, 15%, decrease. This results in a significant decrease for total vBMD from BL. These data indicate that HU treatment affects cancellous density more severely than cortical density. Cortical area and cortical thickness decrease significantly from BL while endocortical area slightly increases. Total area, in turn does not present a significant change. This trend may indicate endocortical resorption due to HU. There are no significant changes in moments of inertia. Moments of inertia are used as predictors of resistance to bending or torsion.

FN 1HU10: Cortical BMC for single HU for older age animals indicate no difference from pre-HU value. Cancellous BMC reveals a non-significant decrease. As a result, total BMC demonstrates a non-significant decrease. Cortical vBMD shows a slight n.s. decrease while cancellous vBMD illustrates a large significant decrease. Total vBMD reveals a decrease for the 1HU10 animals; however, this decrease is not significantly different from its pre-HU value. Like the 1HU7 group these data also indicate that cancellous density is affected more so than cortical vBMD. Areas, cortical thickness, and moments of inertia remain steady post-HU with no significant differences from pre-HU. There are no effects of unloading on geometry of this older HU group. Similar to 1HU7, cancellous density and bone mineral content are more affected by HU than cortical bone.

FN 2HU10: Cortical BMC presents a significant decrease from pre-HU value while cancellous BMC indicates a non-significant decrease. Total BMC also reveals a non-significant decrease. Cortical vBMD illustrates a non-significant increase, while cancellous vBMD a non-significant decrease. This results in a non-significant decrease in total vBMD. The effect of a 2nd HU for total vBMD is less severe in terms of rate of loss pre- to post-HU when compared to 1HU7. This is explained by the change in cortical vBMD for 2nd HU bout being about same as the 1st HU while cancellous vBMD decreased for the 2nd HU at a lower rate of loss compared to the 1st HU.

Cortical area illustrates a significant decrease similar in magnitude as 1HU7 while endocortical area reveals a non-significant decrease (1HU7 indicated a non-significant increase). This results in a non-significant decrease in total area. While this decrease is not significant it is still at a higher rate of loss than the 1st HU which remained relatively constant. These data indicates that a 2nd bout of HU affects the geometric properties of the FN more so than 1HU7. Cortical thickness and moments of inertia show non-significant decreases from pre-HU value for 2HU10.

FN 2HU10+Ex: These data are for changes seen from 1HU7+Ex to 2HU10+Ex. Cortical BMC indicates a non-significant increase for animals with an exercise recovery in between unloading periods. Cancellous BMC shows a non-significant decrease from pre-HU value. As a result, total BMC illustrates no change from pre-HU for this group. 2HU10 reveals a non-significant decrease. The protective effect seen for BMC for 2HU10+Ex could be attributed to extended benefits of exercise. Cortical vBMD indicates a non-significant increase from pre-HU value while cancellous vBMD

demonstrates no change. Total vBMD presents a non-significant increase while 2HU10 vBMD illustrates a non-significant decrease. Again exercise demonstrates extended benefit in the response to the 2nd HU. Compared to 1HU7, total BMC and total vBMD reveal clear benefits of exercise. 1HU7 groups decrease significantly from pre-HU values while 2HU10+Ex indicate no significant changes. For BMC, this can be attributed to the increase seen in cortical BMC (-5.5% 1HU7 and +5.2% 2HU10+Ex) while vBMD shows benefits of exercise for cancellous vBMD (-15.0% 1HU7 and -0.5% 2Hu10+Ex).

Cortical area presents a non-significant increase while endocortical area illustrates a non-significant decrease. Total area data reveal non-significant decrease. The rate of decrease is higher than 1HU7 but lower than 2HU10. However, neither of these changes is significant, so there are no added benefits of exercise to total area compared to 1HU7 or 2HU10. HU treatment on exercised rats demonstrates increases from pre-HU value in cortical area and cortical thickness while 2HU10 and 1HU7 have significant decreases. Exercise benefits can be observed for cortical bone. Moments of inertia also reveal similar trends of exercise benefits.

Overall we see extended benefits of exercise in cortical BMC, cortical area, and CSI into the 2nd HU. Exercise groups indicate no significant changes pre- to post-HU, while ambulatory recovery groups show significant declines due to 2nd HU.

FN Recovery

1HU7 causes a decrease in total BMC and by month 9 1HU7+R2 has recovered to AC9. 1HU7+Ex shows “super recovery” above AC9 (+17%) and 1HU7+R2 (+20%).

"Super recovery" is defined as 1HU7+Ex value being significantly higher than AC9 and 1HU7+R2. Cortical BMC and cancellous BMC recover above AC9 (+13.7%, +26%) and 1HU7+R2 (10.2%, 48.9%). The data indicate that cancellous BMC is more affected by exercise than cortical BMC. Total vBMD presents recovery for both 1HU7+Ex and 1HU7+R2 to AC level. Cortical vBMD reveals 1HU7+Ex to recover to AC but it remains lower than 1HU7+R2. Cancellous vBMD demonstrates 1HU7+Ex to recover to AC but it recovers above (n.s.) 1HU7+R2. Therefore, total vBMD illustrates no difference between 1HU7+Ex and 1HU7+R2.

Total area, cortical area, and moments of inertia show recovery for 1HU7+Ex above AC9 and 1HU7+R2. 1HU7+R2 recovers to AC9 level. Endocortical area reveals 1HU7+Ex recovering above 1HU7 but within AC9 value. 1HU7+Ex and 1HU7+R2 both recover to AC levels. However, 1HU7+Ex recovers significantly above 1HU7+R2. Cortical thickness indicates recovery at AC values for both groups. From the geometric data, we can conclude that there is periosteal apposition after recovery for the exercised group. The ambulatory recover group geometric data indicates endosteal apposition.

FN Mechanical Testing

Axial maximum force and lateral maximum force both follow trends similar to total BMC. Axial maximum force reveals significant pre- to post-HU decreases for all groups except 2HU10+Ex. It is clear that HU affects mechanical strength for all non-exercised groups. The non-significant decrease for 2HU10+Ex could be attributed to the added benefits to strength of exercise. Recovery of maximum force for 1HU7+Ex is also higher than AC9 (+38%) and 1HU7+R2 (+30.1%). 1HU7+R1 recovers to AC by month

8. Lateral maximum force follows the same trends as axial; however, it reveals a slight (n.s.) increase after a 2nd bout of unloading. Differences between axial and lateral testing only lie in the magnitude. Recovery of lateral maximum force is 21% above AC9 and 27% above 1HU7+R2. Effects were more dramatic in terms of biomechanical strength than for densitometric properties. Exercise during recovery illustrates clear benefits for maximum force after recovery and extends into the response of the 2nd HU. Exercise groups present non-significant changes in maximum force after 2nd HU while ambulatory recovery groups show significant decreases due to 2nd HU.

Axial stiffness reveals no significant differences due to HU or recovery periods. Only 1HU10 has a significant decrease when compared AC10 which was due to a non-significant suppression of age related increases pre- to post-HU. In lateral stiffness there are significant pre- to post-HU decreases in 2HU10 and 1HU10 while 2HU10+Ex indicates a slight increase. There is no difference in recovery for 1HU7+Ex and 1HU7+R2.

SSI is used to provide an indicator of mechanical strength. In general, SSI does not follow the same patterns as max force data. There are some similarities for the exercised group recovery. CSI more closely follows the trends for maximum force, especially lateral configuration. Maximum force recovers to AC9 for 1HU7+R2 and above all groups for 1HU7+Ex as indicated in CSI. HU effects seen for maximum force are predicted by CSI (significant pre- to post-HU values, except for 2HU10+Ex). BSI shows better trends than SSI but the decreases of HU effect seen for mechanical testing are not predicted with BSI.

Femur Diaphysis

FD AC: Femur diaphysis cortical BMC, vBMD, area, cortical thickness, and moments of inertia all increase throughout the study for the aging control animals. Cortical bone shows trends of increases at both the FN and FD as animals age.

FD Response to HU Treatment

FD 1HU7: FD shows non-significant increase for cortical BMC, vBMD, area, and cortical thickness compared to BL. In this purely cortical site, HU only suppresses age related increases of cortical bone.

FD 1HU10: Cortical BMC, area, cortical thickness, and moments of inertia reveal non-significant decreases from pre-HU value. Cortical vBMD shows a significant increase, however, this increase is due to animal growth. HU merely mitigates growth.

FD 2HU10: Cortical BMC, cortical area, and moments of inertia reveal non-significant decreases. Cortical thickness demonstrates a significant decrease. 1HU7 illustrated a non-significant increases indicating animal growth suppression. These data present a 2^{nd} HU affects animals more than the 1^{st} HU. Cortical vBMD shows very similar rate of increase for the 1^{st} and 2^{nd} HU so density is not as affected by treatment as other parameters. 2HU10 decreases are similar to 1HU10 decreases for cortical area and cortical BMC so age effects may play a part in decreases rather than treatment.

FD 2HU10+Ex: Cortical BMC and area presents non-significant increases from pre-HU value similar to AC increases. 2HU10 reveals decreases for each of these parameters. Moments of inertia demonstrate significant increases while 2HU10 has

relatively constant pre- to post-HU values. There is a slight decrease in cortical thickness, while in 2HU10 there is a significant decrease (-4.1%). Cortical vBMD shows a significant increase for 2HU10+Ex and 2HU10. While 2HU10 reveals suppression of age related increases, 2HU10+Ex data indicate higher rate of increase similar to age related increase for AC9 to AC10. It is clear that each of these properties show a positive response related to the exercise recovery.

FD Recovery

Recovery of cortical BMC, area, cortical thickness and moments of inertia reveal no difference from AC9 or between 1HU7+Ex and 1HU7+R2. Total and cortical areas show no significant differences from AC so bone growth can only be associated with normal growth due to aging. Cortical vBMD does show recovery of 1HU7+Ex above AC9 and 1HU7+R2. An exercise recovery shows benefits to maintaining cortical density at the midshaft when compared to ambulatory recovery without exercise.

FD Mechanical Testing

Maximum force of the femur diaphysis follows closely with densitometric and geometric trends. 1HU7 shows suppression of age related increases while there is not much of an effect for the 2nd HU or older single HU. The surprising aspect of the maximum force for the diaphysis is the recovery for the 1HU7+Ex group. This group does not recover to AC9 while 1HU7+R2 does. Stiffness shows similar results. There are no effects of HU for stiffness, however 1HU7+Ex does not recover to AC9 while 1HU7+R2 does. Densitometric parameters did not give any indication that the 2HU+Ex

group would not recover. These parameters indicate that 1HU7+Ex does completely recover.

Elastic modulus also shows incomplete recovery for 1HU7+Ex. Pre-yield toughness and energy to yield show few differences between groups. Yield stress shows only a significantly lower value for 2HU10+Ex when compared to BL. Ultimate stress also does not show any benefits of exercise during recovery. For biomechanical properties at femur midshaft exercise appears to have had a negative effect.

Distal Femur Metaphysis

DFM AC: Observing the aging controls throughout the experiment at the DFM total vBMD shows decreases as the animals age. Cancellous vBMD also shows decreases after month 7. Cortical vBMD shows no true increasing or decreasing trend. For the most part, total vBMD shows decreasing trend due to the cancellous vBMD. BMC on the other hand does not have any increasing or decreasing trends as the study progresses and most time points remain at BL value.

Total area shows increasing trends with values significantly above BL at AC10 after month 10. Endocortical area also shows an increasing trend with values being significantly higher than BL after month 8. Neither cortical area nor cortical thickness show an increasing or decreasing trend as the animals age.

DFM Response to HU treatment

DFM 1HU7: Total vBMD shows a significant decrease from BL due to 1HU7. Cancellous vBMD shows a significant decrease of 17% while cortical vBMD also shows

a significant decrease of 3%. Cancellous BMC shows a decrease from pre-HU values but this decrease is not significant. Cortical BMC shows a significant decrease of 10.6%. Total BMC in turn also has a significant decrease in total BMC after HU of 9.7%. Endocortical area shows a significant increase while cortical area shows a significant decrease. These data indicate endocortical resorption due to HU. In addition, an increase in endocortical area also contributes to a decrease in cancellous vBMD since vBMD is inversely related to the endocortical area. Cortical thickness also shows a significant decrease due to HU but total area shows no differences. This indicates that normal bone periosteal growth seen in AC is still occurring despite HU, but there is thinning of the cortical shell.

DFM 1HU10: Cancellous vBMD shows a significant decrease post HU. Cortical vBMD shows a decrease but it is not significant. Total vBMD in turn shows a significant decrease. Neither cancellous nor cortical BMC show significant decreases but the combined effect of total BMC does show a significant decrease. These data show that at this bone site cancellous bone is more affected by HU than cortical. Similar to 1HU7 cortical thickness shows thinning while endocortical area increases.

DFM 2HU10: Cortical vBMD shows a significant decrease similar to 1HU7 decreases. Cancellous vBMD shows a non-significant decrease. The combination of these effects results in a significant loss in total vBMD. The decrease was similar to that experienced by 1HU10. This indicates that the 1st HU did not affect the response of the 2nd HU in total vBMD. Neither cancellous nor cortical BMC show any significant

changes pre- to post- HU. Similar to 1HU10 cortical thickness shows thinning while endocortical area increases.

DFM 2HU10+Ex: Cortical, cancellous, and total vBMD show decreases but none are significant. Cortical, cancellous, and total BMC all show slight non-significant increases. This conservation of pre-HU values is not seen in the 2HU10 group. This can be explained in the differences in the recovery period. Exercise has clear benefits that extend into the 2nd unloading bout. Endocortical, cortical, and total area show non-significant increases. Exercise prevents cortical thinning and endocortical resorption due to HU.

DFM Recovery

Response to 1HU7 causes a decrease in total vBMD, and by month 9, 1HU7+R2 has recovered to AC9 but remains below baseline. 1HU7+Ex shows recovery above AC9 and 1HU7+R2. Cancellous vBMD shows the same trend, while cortical vBMD shows that both groups recover to AC9 level. Exercise has more of an effect on cancellous vBMD, exceeding AC9 value by +12.1%. Cancellous and cortical BMC show the benefits of exercise for bone. Cancellous BMC for 1HU7+R2 falls within AC9 while 1HU7+Ex exceeds AC9 (+12.5%). Cortical BMC shows incomplete recovery for 1HU7+R2. It remains below AC9, while 1HU7+Ex exceeds AC9 (+11%). Total BMC in turn shows complete recovery of 1HU7+Ex group above AC9 and 1HU7+R2. 1HU7+R2 does not recover to AC9.

Endocortical area of 1HU7+Ex does not show any differences compared to AC9, both 1HU7+R2 and 1HU7+Ex decrease to AC9 level. Exercise recovery shows a greater

impact on cortical area. 1HU7+Ex recovers above all groups while 1HU7+R2 never fully recovers to AC9 value. Total area as a result shows complete recovery for 1HU7+Ex and 1HU7+R2 within AC level, however 1HU7+Ex recovers above 1HU7+R2. Cortical thickness shows recovery above AC9 for 1HU7+Ex while 1HU7+R2 does not completely recover. In summary, 1HU7+Ex shows periosteal expansion and increased cortical thickness due to exercise recovery. Exercise has no additional effect on the endosteal surface.

DFM Mechanical Testing

Ultimate stress was calculated and followed trends of cancellous BMC. 1HU7 suppressed age related ultimate stress increases. 2HU10 showed a non-significant decrease while 1HU10 showed a significant decrease pre- to post-HU. 1HU10 fell below AC10. Both 1HU7+Ex and 1HU7+R2 fully recovered within AC9 levels. 2HU10+Ex shows a non-significant increase in ultimate stress pre- to post-HU, which can be attributed to benefits in cancellous bone due to exercise. 2HU10+Ex is significantly higher than AC10. Elastic modulus shows very similar trends, 1HU7 suppressed age related increases. Both 1HU7+R2 and 1HU7+Ex recover to AC9. 2HU10 shows a non-significant decrease while 1HU10 shows significant decrease, which also causes elastic modulus to fall below AC10. 2HU10+Ex shows a significant increase in elastic modulus pre- to post-HU. 2HU10+Ex is significantly higher than AC10. Energy to Ultimate Stress and ultimate strain both also show the benefits of an exercise recovery at the DFM. 1HU7+Ex shows recovery above AC9 and 1HU7+R2 which protects the animals through a 2nd bout of unloading.

Comparison of Multiple Sites

The femoral neck and the distal femur metaphysis are sites with both cancellous and cortical bone. Both types of bone contribute to mineral properties and mechanical strengths. The femur midshaft diaphysis is a site made up of exclusively cortical bone. From the makeup of the site it would seem that the femoral neck and distal femur metaphysis would yield similarities while the diaphysis would probably differ from the other sites.

The femoral neck and distal femur metaphysis show similar changes in in BMC with treatment for all compartments. Total BMC lost for the first HU at the femoral neck was -6.8% while the distal femur metaphysis lost -9.7%. After recovery, the femoral neck recovered to 17.4% above AC9 and distal femur metaphysis recovered 12.1% above AC9. The second bout of HU loss was not significant for either site. Since both sites are mixed, the losses due to HU and the recovery after exercise show similar changes in BMC at each site. Cortical and cancellous BMC also had similar response to exercise recovery in pattern and percent change at the distal femur metaphysis and femoral neck. Changes in vBMD were different for each site; however, the distal femur metaphysis had "super recovery" after exercise in cancellous and total vBMD while the femoral neck showed no true benefits in any vBMD parameters.

The diaphysis showed few significant differences pre- to post-HU. The only significant difference was in cortical vBMD, which recovered +1.4% above AC9 and had a significant pre- to post-HU increase for the 2nd HU. The femur diaphysis shows opposite effects of recovery in densitometric properties when compared to the femoral

neck. At the femur diaphysis we see that exercise shows "super recovery" in cortical vBMD while at the femoral neck there are no real benefits to vBMD after exercise recovery. The distal femur metaphysis shows significant recovery effects in total and cancellous vBMD but not so in cortical vBMD. The percent change for the femur diaphysis properties are much smaller than those for the distal femur metaphysis and the femur diaphysis. This could be attributed to the diaphysis being composed of cortical bone and being less affected by treatment.

Geometric changes in the femoral neck and distal femur metaphysis were similar in that exercise recovery led to increases in total area, which indicated periosteal apposition. Femur diaphysis had no geometric changes related to treatment, only increase in cortical and total area due to aging.

Mechanical properties of the three sites cannot be directly compared. The femoral neck test is a bending, shear, and compressive test. The diaphysis is a cortical site tested with a pure bending test. The distal femur metaphysis was tested using a compressive test (RPC) of only cancellous bone specimen. Despite the difference in testing, the benefits of exercise are clear at the femoral neck and distal femur metaphysis. Femoral neck axial maximum force of 1HU7+Ex is 38% above AC9 level and there was no significant decrease due to the 2^{nd} HU. Lateral testing showed similar "super recovery" benefits, but with smaller magnitude, and the 2^{nd} HU showed a non-significant increase. The femoral neck strength shows clear benefits of exercise post recovery and into the 2^{nd} HU. The distal femur metaphysis ultimate stress also shows benefits of exercise post recovery, but these benefits are more apparent after the 2^{nd} HU.

After exercise recovery ultimate stress was above AC9 and 1HU+R2; however, the three groups were not statistically different. The 2nd HU actually reveals a non-significant increase pre- to post-exposure for 2HU10+Ex. While the increase is not statistically significant the upward trend after recovery shows extended benefits of exercise into the 2nd HU bout. The diaphysis, on the other hand, does not show any benefits of exercise. Post exercise recovery the maximum force of the femur diaphysis falls below AC9 and 1HU7+R2 and no benefits from exercise are seen during the 2nd HU.

It is important to note that, while it appears that exercise in this study did not show benefits at the femur diaphysis, this does not negate the benefits seen at the femoral neck and distal femur metaphysis. These mixed bone sites are most important because they are the most clinically relevant, since most osteoporotic related fractures occur at the hip and spine in humans. The distal femur metaphysis results are equally important since the distal femur metaphysis can be used as a model for a human femoral neck which is comprised of a higher cancellous to cortical bone ratio than a rat femoral neck.

Comparison to Other Studies

Several studies have demonstrated that recovery does not lead to complete restoration of bone even after a recovery period exceeding the disuse period [3, 4, 36, 37] Carpenter et al. [4] found that crewmembers with six months aboard the ISS showed incomplete recovery even after four years of returning to weight bearing on Earth. In the cancellous compartment of the femoral neck, BMD did not fully recover to pre-flight

values. After one year of returning to Earth cancellous BMD was only 89% of preflight value and after 2-4.5 years cancellous BMD was at 81% of pre-flight value, showing a further decrease. There were also increases in bone structure several years after recovery including increases in total and cortical volume. Our data indicate cancellous vBMD of the distal femur metaphysis showed "super recovery" after the 1st HU in the exercised group. This suggests that an exercise regimen can promote full recovery of bone, although the current exercise regimen undertaken by astronauts does not effect a complete recovery.

Our results indicate that resistance exercise training during recovery following disuse was beneficial to mechanical and densitometric properties of the femoral neck and distal femur metaphysis. This is in agreement with several studies that showed the benefits of exercise on bone [38-42]. A study conducted by Ju et al. [38] compared the effects of a jump exercise versus treadmill running during recovery period after tail suspension. Unlike our study they used growing rats five weeks of age, which have a higher potential for recovery since their bones are rapidly changing. They found that both jump and running exercises following unloading had beneficial effects at the femur. BMD data obtained from DXA indicated that recovery was achieved by the animals undergoing ambulatory recovery and the exercised animals had recovered above control in agreement with vBMD in this study at the distal femur metaphysis. We observed vBMD of 1HU7+Ex at the distal femur metaphysis recovered above AC while 1HU7+R2 recovered to AC. At the midshaft, cortical vBMD showed the same pattern. Interestingly the non-exercised group of the Ju et al. [38] study showed complete

recovery, but further examination of trabecular microarchitecture via micro CT showed that the femur metaphysis had not completely recovered. They observed lower values for trabecular number and trabecular bone volume and an increase in trabecular spacing. They attributed incomplete recovery to rapid trabecular bone loss resulting from a decrease in bone formation sites. The exercised groups did show full recovery in trabecular architecture, specifically, increases in trabecular bone mass through increases of trabecular thickness in jump trained rats and increases in trabecular number for treadmill trained rats. Unfortunately, they did not show any data for mechanical testing. However, since they showed increases in trabecular bone micro architecture such as trabecular thickness, trabecular number, and connectivity, an increase in strength would be expected. These data are consistent with effects we saw from our resistance exercise protocol during recovery. It may also be true that our exercise recovery leads to positive micro architectural changes; however, further analysis would have to be made using micro CT imaging to support this statement.

Another study conducted by Shimano et al. [43] used female rats four months of age with one 28 day unloading bout and 21 days of recovery. The recovery period consisted of either an ambulatory or a treadmill running group. In agreement with our data, mechanical testing of the femoral neck showed a significantly lower value in strength for the HU group compared to AC. However, there were no differences in HU plus twenty-one days of ambulatory or exercise recovery groups when compared to AC. These data show there is no benefit of treadmill exercise for femoral neck strength.

Comparing this with our resistance exercise data would indicate that a resistance exercise regimen provides greater osteogenic effect than endurance exercise.

Growing rats have more of a potential for bone recovery after remobilization since they exhibit rapid response to treatments, so it is more appropriate for our study to compare the similarities of mature adult rats. A study by Vico et al. [37] utilized six month old rats to observe the effects of a 14 day HU and 28 day recovery. At the femur they showed a non-significant decrease in BMC as measured by DXA, but significant losses were observed at the tibia. The changes they observed in BMC due to HU and recovery show that effects of treatment are time dependent. This would also indicate that recovery time is dependent on duration of disuse. Their re-ambulation results indicated the tibia was not fully recovered despite a recovery period twice the length of suspension. However, they did not subject the rats to any type of exercise. It is not clear from their data what compartment of bone contributed to incomplete recovery because of the imaging method used. DXA is not sensitive enough to be able to discern differences from cancellous and cortical bone. Our densitometric properties were measured using pQCT. This imaging method allowed us to discover what compartment contributed to the losses at each site. For example, the distal femur metaphysis and femoral neck, showed significant losses due to HU in cancellous vBMD, which contributed to most of the significant loss in total vBMD. In contrast for this current study, the femur diaphysis, an exclusively cortical site, showed non-significant increase in cortical vBMD that indicated suppressed growth. This is in agreement with

Bloomfield et al. [22] who showed that there were few changes in cortical bone mass and geometry while mixed sites showed clear adverse effects of HU.

One concern of the benefits we found for exercised animals is whether or not the recovery would persist after the exercise program had discontinued or whether it was necessary to continue exercise in order to maintain bone strength. A study by Honda et al. [41] showed that high impact jump training induced increases in bone mass and strength and these benefits remained even after six months of detraining in adult male rats. These data are in agreement with the benefits of exercise recovery we see extended into a 2nd bout of unloading (the animal does not exercise from 1HU7+Ex to 2HU10+Ex). Despite a 2nd period of disuse, the exercise recovery protects the rats from showing significant declines in strength. Lateral femoral neck maximum force and distal femur metaphysis ultimate stress actually show non-significant increases pre- to post-HU. This could be due to delayed effect of increases in bone formation rate. In comparison, the 2nd HU of the ambulatory recovery groups at both sites show decreases. Exercise recovery also allows for post-2nd HU strength to remain above AC10 at the femoral neck and distal femur metaphysis.

The femur diaphysis showed significantly lower values in strength for 1HU7+Ex and 2HU10+Ex compared to AC despite the indications of the densitometric data, which showed "super recovery" of cortical vBMD and recovery to AC in cortical BMC and geometric parameters. A study by Ju et al. [40] showed that treadmill exercise in young rats resulted in values of Imax, Imin, cortical area, strength, and stiffness above values of control rats at the femur diaphysis. The strength and stiffness data were not in agreement

with our diaphysis results. This could have to do with the exercise modality, which affects bone based on strain magnitude, cycle number, and loading direction [44]. The exercise type for Ju et al. [40] was an endurance exercise. They showed increases in cortical area and moments of inertia that were more drastic than what we saw after our resistance exercise recovery. Our resistance exercise group did not show any differences from AC or 1HU7+R2 for these parameters. They indicated that periosteal bone apposition was primarily responsible for geometric changes of cortical bone. Our exercise area data did not indicate periosteal bone apposition due to exercise. The difference in our results in addition to exercise modality could be explained by the age of the animals. We used mature 6-month-old adult rats whereas Ju et al. [40] used young growing rats 4 weeks of age. The young growing rat is quicker to adapt to mechanical loading and age may be a major contributor to increases they saw in cortical area and moments of inertia. In contrast to our data, they also saw less exercise effects in BMD at the proximal and distal ends of the femur, which is where we see more effects of resistance exercise.

At the femoral neck, the exercised group showed periosteal expansion while the ambulatory group showed sign of endosteal apposition or medullary contraction after recovery. The geometric data suggest that the femoral neck bone adapted to increased loading from resistance exercise with bone formation on the periosteal surface. This is in agreement with Bass et al. [45], who found that increased strains showed geometric changes resulting in periosteal expansion and as a result a higher resistance to bending in humans. Endocortical bone apposition does not have as much of an effect on resistance

to bending. Periosteal apposition is also consistent with astronaut data obtained by Lang et al. [3] after recovery. However, they point out that the increase in bone size did not lead to increases in bone strength measures. They concluded that the geometric bone changes are beneficial to normal stance loading but may not protect against fracture in a lateral fall. While they were unable to obtain mechanical testing data, it is interesting to note that our maximum force data indicated "super recovery" in the exercise group in the axial and lateral direction. This suggests that exercise, although increasing total area by periosteal apposition, does indeed protect against fracture in both loading directions. In addition, this resistance exercise regimen could have benefits, as indicated previously, in trabecular micro architecture such as increases in trabecular thickness or number.

The benefits of exercise in maximum force for both axial and lateral directions could also be supported by distribution of trabeculae in regions of the femoral neck that protect against multiple loading conditions. Lang et al. [3] mention that during spaceflight there is loss of cancellous BMC in both the inferior and supero-lateral cortex of the femoral neck. Upon resuming ambulation on Earth there is cancellous replacement in the inferior cortex due to adaptation to ambulatory loading, while there is no replacement of bone in the supero-lateral cortex. This incomplete recovery at the supero-lateral cortex makes astronauts susceptible to fracture during a lateral fall. After recovery we see cancellous BMC at the femoral neck is significantly higher than AC and 1HU7+R2. "Super recovery" of maximum force in both lateral and axial directions may suggest that the distribution of the increases in cancellous BMC is in both the inferior and more importantly the supero-lateral cortex. The resistance exercise recovery showed

clear benefits of bone adaptation, which protected the femoral neck from fracture during both stance and lateral fall.

LIMITATIONS

There are several limitations in this study that are important to point out. First, direct extension of quadruped data to humans is not appropriate. The bone structure and remodeling patterns in the rat are different than those of human bone. First, rats have much more cortical bone at the femoral neck than humans and structural differences in cancellous bone. The femoral neck geometry is also different between the two. Rats also do not have osteons or Haversian systems as found in humans, which take part in the continuous remodeling process in cortical bone

In this study, we wanted to use mature adult rats so we chose the 6-month-old animal to model the adult human. At six months of age rats are considered to be skeletally mature and can provide a basis for comparison with adult human. However, it is apparent from the data generated that there was still growth in aging controls as the experiment progressed for several parameters. Choosing an older rat, possibly at 7 months of age, could show more effects due to HU rather than suppression of age-related growths.

RPC testing also has some limitations that should be pointed out. First, the test is dependent on the organization of the cancellous bone within the cortical shell. Density and porosity of cancellous bone within each specimen varied. Since cancellous bone is not evenly distributed throughout the cross section then there will be some discrepancies in the calculation of stress which assumed homogeneity of cancellous bone throughout the platen area. The RPC test also has effects from the cortical shell which is not isolated

from cancellous bone. As a result, the stress calculated is not an indicator of pure cancellous bone stress.

FUTURE WORK

Further investigations would prove to be beneficial to obtaining insight into the benefits of this exercise modality. Analysis via micro CT would prove to be useful in order to determine if exercise caused micro-architectural changes such as: increases in trabecular thickness, number, or orientation. It would also be interesting to implement exercise during the HU period since astronauts exercise during spaceflight. Utilizing a combined drug and exercise countermeasure may also prove to be beneficial to recovery of bone. Further, it would reveal more information about extended benefits of exercise to run a recovery period after the 2nd HU bout in order to determine if detraining would preserve the benefits we found during this study.

CONCLUSIONS

Long duration spaceflight superimposed on aging bone loss poses increased risk of fracture during reloading for astronauts. Exercise has been proposed as a potential method of accelerating recovery; however, current exercise regimens used aboard ISS have not proved to be effective in protecting bone. In this study, we used a rodent model to investigate the effects of resistance exercise recovery in-between two bouts of HU.

We have demonstrated that a bout of HU, one month in duration, results in significant losses in a number of bone parameters. Resistance exercise during recovery produced positive gains in densitometric and biomechanical properties. Most notably, at the femoral neck all BMC parameters showed recovery above AC and ambulatory recovered group. The 2nd HU did not indicate any significant changes. Geometric changes in the exercised group suggest periosteal apposition due to exercise, which contributes to higher resistance to bending. Maximum force assessed in both the axial and lateral loading configurations in exercised rats also recovered to higher values than all other groups and were protected against decreases due to a 2nd HU bout. These data were similar to changes seen in total BMC; however, the magnitude of changes in maximum force was much greater. At the femur diaphysis, the exercised animals exhibited recovery of cortical vBMD above all other groups and a significant increase after the 2nd HU. Contrary to the benefits seen in cortical vBMD, maximum force did not indicate benefits to exercise at the midshaft. There were no changes due to treatment in total or cortical area at the femur diaphysis. This may be due to the diaphysis

consisting exclusively of cortical bone. At the distal femur metaphysis, cancellous and total vBMD as well as all BMC data show clear benefits of exercise recovery with higher values in the exercised group as compared to all other groups within the same time point. Geometric data illustrate that at the distal femur metaphysis there was a gain in total area (periosteal apposition) similar to that seen at the femoral neck. Ultimate stress data indicate exercise recovery benefits extended into the 2nd HU, similar to cancellous BMC. There was a non-significant increase pre- to post-HU in ultimate stress, which placed exercised animals significantly higher than all other groups.

The data obtained were partially in agreement with the hypothesis that exercise during recovery would improve bone structural and mechanical properties further than ambulatory weight bearing during recovery. This was true for the most part, except for biomechanical properties at the femur diaphysis. The hypothesis that exercise would have no effect on the 2nd HU was proven incorrect. We saw clear benefits of exercise, especially in the lateral femoral neck maximum force and distal femur metaphysis ultimate stress, which exhibited increases after the 2nd HU, presumably explained by extended benefits of exercise. The hypothesis that percent changes would be similar for mechanical and densitometric properties was also not always accurate. At the femoral neck, the change from pre-to post-recovery for total BMC was +28%, while axial maximum force change was +71% . Mechanical properties showed greater benefits than mineral properties. At the femur diaphysis, the percent change for cortical vBMD was similar to maximum force change after recovery but opposite in magnitude. Similar to the femoral neck, at the distal femur metaphysis, the change in mechanical properties

after recovery was much higher than densitometric. Ultimate stress showed an increase of 216% while cancellous BMC showed an increase of 20%. The hypothesis that the three sites would show similar patterns was correct mostly for the distal femur metaphysis and the femoral neck while the femur diaphysis was less affected by exercise recovery.

Despite the data in ultimate strength at the femur diaphysis, it is important to keep in mind that osteoporotic fractures do not usually occur at the midshaft, and these data are of little relevance to human risk of fracture. Fractures at the hip, involving cortical and cancellous bone, are the most common consequence of osteoporosis. The data presented in this thesis indicate clear benefits of exercise at the femoral neck and the distal femur metaphysis, both mixed bone regions. Exercise following a single bout of unloading showed benefits for mechanical and densitometric properties after recovery, which benefits also extended into the response of the 2nd HU.

REFERENCES

[1] T.F. Lang, A. LeBlanc, H. Evans, Y. Lu, H. Genant, A. Yu, Cortical and trabecular bone mineral loss from the spine and hip in long-duration spaceflight, Journal of Bone and Mineral Research, 19 (2004) 1006-1012.

[2] J.A. Cauley, L. Lui, K.L. Stone, T.A. Hillier, J.M. Zmuda, M. Hochberg, T.J. Beck, K.E. Ensrud, Longitudinal study of changes in hip bone mineral density in Caucasian and African American women, Journal of the American Geriatrics Society, 53 (2005) 183-189.

[3] T.F. Lang, A. LeBlanc, H. Evans, Y. Lu, Adaptation of the proximal femur to skeletal reloading after long-duration spaceflight, Journal of Bone and Mineral Research, 21 (2006) 1224-1230.

[4] R.D. Carpenter, A.D. LeBlanc, H. Evans, J.D. Sibonga, T.F. Lang, Long-term changes in the density and structure of the human hip and spine after long-duration spaceflight, Acta Astronautica, 67 (2010) 71-81.

[5] B.L. Riggs, L.J. Melton, R.A. Robb, J.J. Camp, E.J. Atkinson, J.M. Peterson, P.A. Rouleau, C.H. McCollough, M.L. Bouxsein, S. Khosla, Population-based study of age and sex differences in bone volumetric density, size, geometry, and structure, at different skeletal sites, Journal of Bone and Mineral Research, 19 (2004) 1945-1954.

[6] P.R. Cavanagh, A.J. Rice, Bone Loss During Spaceflight: Etiology, Countermeasures, and Implications for Bone Health on Earth, The Cleveland Clinic Foundation, Cleveland, 2007.

[7] J. Rittweger, G. Beller, G. Armbrecht, E. Mulder, B. Buehring, U. Gast, F. Dimeo, H. Schubert, A.d. Haan, D.F. Stegeman, H. Schiessl, D. Felsenberg, Prevention of bone loss during 56 days of strict bed rest by side-alternating resistive vibration exercise, Bone, 46 (2010) 137-147.

[8] J.D. Fluckey, E.E. Dupont-Versteegden, D.C. Montague, M. Knox, P. Tesch, C.A. Peterson, D. Gaddy-Kurten, A rat resistance exercise regimen attenuates losses of musculoskeletal mass during hindlimb suspension, Acta Physiol Scand, 176 (2002) 293-900.

[9] R.B. Martin, D.B. Burr, N.A. Sharkey, Skeletal Tissue Mechanics, Springer-Verlag, New York, 1998.

[10] L. Onslow, Prevention and Management of Hip Fractures, Whurr Publishers Ltd, West Sussex, 2005.

[11] E.R. Morey-Holton, R.K. Globus, Hindlimb unloading of growing rats: a model for predicting skeletal changes during space flight, Bone, 22 (1998) 83S-88S.

[12] E.R. Morey-Holton, R. Globus, Hindlimb unloading rodent model: technical aspects, Journal of Applied Physiology, 92 (2001) 1367-1377.

[13] J.M. Davis, Characterization of the bone loss and recovery response at the distal femur metaphysis of the adult male hindlimb unloaded rat, in: Mechanical Engineering, Texas A&M University, College Station, TX, 2011.

[14] D.S. Morgan, The effects of multiple unloading exposures on bone properties in the femur of adult male rats, in: Mechanical Engineering, Texas A&M University, College Station, TX, 2012.

[15] J.S. Kupke, Characterization of the femoral neck regions response to the rat hindlimb unloading model through tomographic scanning, mechanical testing and estimated strengths, in: Biomedical Engineering, Texas A&M University, College Station, TX, 2010.

[16] K.C. Westerlind, J.D. Fluckey, S.E. Gordon, W.J. Kraemer, P.A. Farrell, R.T. Turner, Effect of resistance exercise training on cortical and cancellous bone in mature male rats, Journal of Applied Physiology, 84 (1998) 459-464.

[17] J.S. Khurana, Bone Pathology, in: J.S. Khurana (Ed.), Humana Press, New York, 2009.

[18] R.A. Bergman, A.K. Afifi, P.M. Heidger, Histology, W.B. Suanders Company, Philadelphia, 1996.

[19] S.C. Cowin, Bone Mechanics Handbook, 2nd ed., CRC Press, Boca Raton, 2001.

[20] F. Bronner, M.C. Farach-Carson, J. Rubin, Bone Resorption, in: F. Bronner, M.C. Farach-Carson, J. Rubin (Eds.) Topics in Bone Biology, Springer, London, 2005.

[21] L. Weiss, Histology, Cell and Tissue Biology, 5th ed., Elsevier Biomedical, New York, 1983.

[22] S.A. Bloomfield, M.R. Allen, H.A. Hogan, M.D. Delp, Site- and compartment-specific changes in bone with hindlimb unloading in mature adult rats, Bone, 31 (2002) 149-157.

[23] H.W. Deng, Y.Z. Lui, C.Y. Guo, D. Chen, Current Topics in Bone Biology, World Scientific, Hackensack, 2005.

[24] E.H. Burger, J. Klein-Nulend, Microgravity and bone cell mechanosensitivity, Bone, 22 (1998) 127S-130S.

[25] G. Zhang, L. Qin, Y. Shi, K. Leung, A comparative study between axial compression and lateral fall configuration tested in a rat proximal femur model, Clinical Biomechanics, 20 (2005) 729-735.

[26] R.K. Globus, D.D. Bikle, E.R. Morey-Holton, The temporal response of bone to unloading, Endocrinology, 118 (1986) 733-742.

[27] C.H. Turner, D.B. Burr, Basic biomechanical measurements of bone: a tutorial, Bone, 14 (1993) 595-608.

[28] H.Z. Ke, V.W. Shen, H.Qi, D.T. Crawford, D.D. Wu, X.G. Liang, K.L. Chidsey-Frink, C.M. Pirie, H.A. Simmons, D.D. Thompson, Prostoglandin E2 increases bone strength in intact rats and in ovariectomized rats with established osteopenia, Bone, 23 (1998) 249-255.

[29] L. Mosekilde, J.S. Thomsen, P.B. Orhii, D.N. Kalu, Growth hormone increases vertebral and femoral bone strength in osteopenic, ovariectomized, aged rats in a dose-dependent and site-specific manner, Bone, 23 (1998) 343-352.

[30] J.A. Grisso, J.L. Kelsey, B.L. Strom, G.Y. Chiu, G. Maislin, L.A. O'Brien, S. Hoffman, F. Kaplan, Risk factors for falls as a cause of hip fracture in women. The Notheast hip fracture study group, New England Journal of Medicine, 324 (1991) 1326-1331.

[31] A. Odgaard, F. Linde, The underestimation of Young's modulus in compressive testing of cancellous bone specimens, Journal of Biomechanics, 24 (1991) 691-698.

[32] X.W. Meng, X.G. Liang, R. Birchman, D.D. Wu, D.W. Dempster, Temporal expression of the anabolic action of PTH in cancellous bone of ovariectomized rats, Journal of Bone and Mineral Research, 11 (1996) 421-429.

[33] V. Shen, R. Birchman, R. Xu, M. Otter, D. Wu, R. Lindsay, D.W. Dempster, Effects of reciprocal treatment with estrogen and estrogen plus parathyroid hormone on bone structure and strength in ovariectomized rats, Journal of Clinical Investigation, 96 (1995) 2331-2338.

[34] L.C. Shackelford, A.D. LeBlanc, T.B. Driscoll, H.J. Evans, N.J. Rianon, S.M. Smith, E. Spector, D.L. Feeback, D. Lai, Resistance exercise as a countermeasure to disuse-induced bone loss, Journal of Applied Physiology, 97 (2004) 119-129.

[35] S. Bouse, Investigation of transfer function analysis as a means to predict strain on rat tibiae from ankle torque waveforms, in: Mechanical Engineering, Texas A&M Univeristy, College Station, 2008.

[36] N. Basso, Y. Jia, C.G. Bellows, J.N.M. Heersche, The effect of reloading on bone volume, osteoblast number, and osteoprogenitor characteristics: studies in hind limb unloaded rats, Bone, 37 (2005) 370-378.

[37] L. Vico, S. Bourrin, J.M. Very, M. Radziszowska, P. Collet, C. Alexandre, Bone changes in 6-mo-old rats after head-down suspension and a reambulation period, Journal of Applied Physiology, 79 (1995) 1426-1433.

[38] Y.-I. Ju, T. Stone, K. Ohnaru, H.-J. Choi, M. Fukunaga, Differential effects of jump versus running exercise on trabecular architecture during remobilization after suspension-induced osteopenia in growing rats, Journal of Applied Physiology, 112 (2012) 766-772.

[39] Y.-I. Ju, T. Okamoto, M. Fukunaga, Jump exercise during remobiliation restores integrity of the trabecular architecture after tail suspension in young rats, Journal of Applied Physiology, 104 (2008) 1594-1600.

[40] Y.-I. Ju, T. Stone, M. Fulkanage, S.G. Lim, S. Onodera, Effects of endurace exercise on three-dimensional trabecular bone microarchitecture in young growing rats, Bone, 33 (2003) 485-493.

[41] A. Honda, N. Sogo, S. Nagasawa, T. Kato, Y. Umemura, Bones benefits gained by jump training are preserved after detraining in young and adult rats, Journal of Applied Physiology, 105 (2008) 849-853.

[42] J.M. Swift, H.G. Gasier, S.N. Swift, M.P. Wiggs, H.A.Hogan, J.D. Fluckey, S.A. Bloomfield, Increased training loads do not magnify cancellous bone gains with rodent jump exercise, Journal of Applied Physiology, 109 (2010) 1600-1607.

[43] M.M. Shimano, J.B. Volpon, Biomechanics and structural adaptations of the rat femur after hindlimb suspension and treadmill running, Brazilian Journal of Medical and Biological Research, 42 (2009) 330-338.

[44] S. Judex, R.F. Zernicke, High-impact exercise and growing bone: relation between high strain rates and enhanced bone formation, Journal of Applied Physiology, 88 (2000) 1283-2191.

[45] S.L. Bass, L. Saxon, R.M. Daly, C.H. Turner, A.G. Robling, E. Seeman, S. Stuckey, The effect of mechanical loading on the size and shape of bone in pre-, peri-, and postpubertal girls: a study in tennis players, Journal of Bone and Mineral Research, 17 (2002) 2274-2280.

APPENDIX

Nomenclature

FN	Femoral Neck
FD	Femur Diaphysis
DFM	Distal Femur Metaphysis
BMC	Bone Mineral Content
vBMD	Volumetric Bone Mineral Density
SSI	Structural Strength Index
CSI	Compressive Strength Index
BSI	Bending Strength Index
AP	Anteroposterior
HU	Hindlimb Unloaded
BL	Baseline
AC	Aging Cage Control
DXA	Dual-energy X-ray Absorptiometry
pQCT	Peripheral Quantitative Computed Tomography

Number of Animals per group

Number of animals per group at the FN, FD, and DFM							
	R FN Densitometric Properties	R FN Mechanical Properties	L FN Mechanical Properties	FD Densitometric properties	FD Mechanical Properties	DFM Densitometric properties	DFM Mechanical Properties
6 Months Old							
BL6	34	34	33	35	34	35	33
7 Months Old							
AC7	15	15	15	15	15	19	19
1HU7	16	15	19	19	19	19	19
8 Months Old							
AC8	15	15	14	15	14	15	14
1HU7+R1	14	14	14	14	14	14	13
9 Months Old							
AC9	14	14	14	14	14	15	15
1HU7+R2	15	15	15	15	14	15	15
1HU7+Ex	15	15	14	15	15	15	15
10 Months Old							
AC10	29	29	28	29	29	29	29
1HU7+R3	14	14	14	14	13	14	14
1HU10	18	18	18	18	16	18	18
2HU10	16	15	16	16	16	16	16
2HU10+Ex	18	18	18	18	18	18	18
12 Months Old							
AC12	13	12	13	14	13	14	14
1HU10+R2	17	17	17	17	17	17	17
2HU10+R2	16	16	16	16	16	16	16

Matlab P-Values

Femur Diaphysis p values

	FD_ElasticModulus.csv	FD_EnergytoFracture.csv	FD_EnergytoYield.csv
bl,cc28	0.41594 Mann-Whitney	0.2461 t-test	0.0056772 Mann-Whitney
bl,cc56	0.99095 Mann-Whitney	0.038243 t-test	0.044708 Mann-Whitney
bl,cc84	0.33504 Mann-Whitney	0.050731 t-test	0.11493 Mann-Whitney
bl,cc112	0.022476 Mann-Whitney	0.338 t-test	0.00061074 Mann-Whitney
bl,control	0.69475 Mann-Whitney	0.068855 Mann-Whitney	0.62587 Mann-Whitney
bl,hu	0.10864 Mann-Whitney	0.11573 t-test	0.51027 Mann-Whitney
bl,rec28	0.10008 Mann-Whitney	0.85078 t-test	0.79421 Mann-Whitney
bl,rec56	0.64194 Mann-Whitney	0.38214 t-test	0.23372 Mann-Whitney
bl,rec84	0.78447 Mann-Whitney	0.15658 t-test	0.084665 Mann-Whitney
bl,1hu	0.35472 Mann-Whitney	0.40489 t-test	0.5082 Mann-Whitney
bl,1hu+rec	0.0032061 Mann-Whitney	0.34876 t-test	0.71164 Mann-Whitney
bl,2hu	0.23998 Mann-Whitney	0.69484 t-test	0.63983 Mann-Whitney
bl,2hu+rec	0.010845 Mann-Whitney	0.10354 t-test	0.28414 Mann-Whitney
bl,1hu+ex	0.00027951 Mann-Whitney	0.18258 t-test	0.13164 Mann-Whitney
bl,2hu+ex	5.3922e-006 Mann-Whitney	0.39759 t-test	0.014968 Mann-Whitney
1hu+ex,2hu+ex	0.061273 t-test	0.57258 t-test	0.5508 Mann-Whitney
rec56,2hu	0.43551 t-test	0.23193 t-test	0.37145 Mann-Whitney
cc84,1hu	0.46693 Mann-Whitney	0.039288 t-test	0.49874 Mann-Whitney
hu,cc28	0.034366 Mann-Whitney	0.72958 t-test	0.018824 t-test
rec28,cc56	0.20639 Mann-Whitney	0.052835 t-test	0.046062 t-test
1hu+ex,cc84	7.1774e-005 t-test	0.0098328 t-test	0.8443 Mann-Whitney
rec56,cc84	0.85954 t-test	0.04086 Mann-Whitney	0.90861 t-test
rec56,1hu+ex	0.0018053 Mann-Whitney	0.61321 t-test	0.61574 Mann-Whitney

2hu+ex,cc112	0.0011547 Mann-Whitney	0.97548 t-test	0.57681 Mann-Whitney
1hu,cc112	0.069693 Mann-Whitney	0.94282 t-test	0.070695 Mann-Whitney
2hu,cc112	0.099368 Mann-Whitney	0.24379 t-test	0.023549 Mann-Whitney
rec84,cc112	0.072545 Mann-Whitney	0.44145 t-test	0.15713 Mann-Whitney
1hu+rec,control	0.094117 Mann-Whitney	0.33575 Mann-Whitney	0.47679 Mann-Whitney
2hu+rec,control	0.10946 Mann-Whitney	0.9127 Mann-Whitney	0.19578 Mann-Whitney

	FD_Force.csv	FD_PreyieldToughness.csv	FD_UltimateStress.csv
bl,cc28	1.4514e-008 t-test	0.0050693 Mann-Whitney	0.019011 t-test
bl,cc56	3.0057e-009 t-test	0.083091 Mann-Whitney	0.14242 t-test
bl,cc84	1.721e-005 Mann-Whitney	0.1128 Mann-Whitney	0.34945 t-test
bl,cc112	1.1831e-008 Mann-Whitney	0.0033413 Mann-Whitney	0.19013 t-test
bl,control	1.4649e-006 Mann-Whitney	0.69629 Mann-Whitney	0.20972 t-test
bl,hu	9.9081e-005 t-test	0.40308 Mann-Whitney	0.02043 t-test
bl,rec28	2.6993e-006 t-test	0.66694 Mann-Whitney	0.013002 Mann-Whitney
bl,rec56	5.8816e-009 t-test	0.35817 Mann-Whitney	0.13437 t-test
bl,rec84	5.8822e-006 Mann-Whitney	0.36672 Mann-Whitney	0.21525 t-test
bl,1hu	1.2603e-006 t-test	0.77348 Mann-Whitney	0.44779 Mann-Whitney
bl,1hu+rec	2.2561e-012 t-test	0.12741 Mann-Whitney	0.074509 t-test
bl,2hu	4.753e-009 t-test	0.50185 Mann-Whitney	0.033401 t-test
bl,2hu+rec	1.0894e-005 Mann-Whitney	0.082284 Mann-Whitney	0.019507 t-test
bl,1hu+ex	0.001343 t-test	0.26608 Mann-Whitney	0.12652 t-test
bl,2hu+ex	0.00014541 Mann-Whitney	0.099801 Mann-Whitney	0.030475 Mann-Whitney
1hu+ex,2hu+ex	0.52692 Mann-Whitney	0.5508 Mann-Whitney	0.45858 Mann-Whitney
rec56,2hu	0.80389 t-test	0.39411 Mann-Whitney	0.67373 t-test

cc84,1hu	0.47225 t-test	0.26346 Mann-Whitney	0.88432 Mann-Whitney
hu,cc28	0.1049 t-test	0.034075 t-test	0.94551 t-test
rec28,cc56	0.20639 Mann-Whitney	0.16471 t-test	0.18252 t-test
1hu+ex,cc84	0.035045 t-test	0.85381 Mann-Whitney	0.030169 t-test
rec56,cc84	0.87224 Mann-Whitney	0.45196 Mann-Whitney	0.63035 t-test
rec56,1hu+ex	0.012746 t-test	0.77665 Mann-Whitney	0.0078303 t-test
2hu+ex,cc112	0.0060236 Mann-Whitney	0.4906 Mann-Whitney	0.0018176 Mann-Whitney
1hu,cc112	0.19158 t-test	0.038012 Mann-Whitney	0.64382 Mann-Whitney
2hu,cc112	0.55048 t-test	0.035867 Mann-Whitney	0.37511 t-test
rec84,cc112	0.30759 t-test	0.21765 t-test	0.88398 t-test
1hu+rec,control	0.72453 t-test	0.46933 Mann-Whitney	0.82869 t-test
2hu+rec,control	0.87802 Mann-Whitney	0.24519 Mann-Whitney	0.43497 t-test

	FD_YieldStress.csv	FD_pQCT_BSI.csv	FD_pQCT_CSI.csv
bl,cc28	0.088586 Mann-Whitney	0.018779 Mann-Whitney	8.8001e-005 t-test
bl,cc56	0.2813 Mann-Whitney	0.000706 Mann-Whitney	2.0917e-006 t-test
bl,cc84	0.1809 t-test	0.0017387 Mann-Whitney	4.4244e-007 t-test
bl,cc112	0.072223 t-test	2.5786e-005 Mann-Whitney	2.7215e-009 Mann-Whitney
bl,control	0.37248 Mann-Whitney	1.5138e-005 Mann-Whitney	1.0536e-013 t-test
bl,hu	0.21059 Mann-Whitney	0.057184 Mann-Whitney	0.098791 t-test
bl,rec28	0.16854 t-test	0.06147 Mann-Whitney	0.0058629 Mann-Whitney
bl,rec56	0.21377 t-test	0.010419 Mann-Whitney	3.2014e-006 Mann-Whitney
bl,rec84	0.41596 t-test	0.00073808 Mann-Whitney	1.5682e-009 t-test
bl,1hu	0.20132 t-test	0.00060901 Mann-Whitney	4.3996e-008 t-test
bl,1hu+rec	0.9555 t-test	1.5965e-006 Mann-Whitney	1.0703e-010 t-test

bl,2hu	0.28414 Mann-Whitney	0.00057991 Mann-Whitney	2.4122e-005 t-test
bl,2hu+rec	0.46033 Mann-Whitney	0.00012996 Mann-Whitney	2.3615e-006 Mann-Whitney
bl,1hu+ex	0.4808 Mann-Whitney	0.00019457 Mann-Whitney	8.0116e-009 t-test
bl,2hu+ex	0.092374 Mann-Whitney	2.7966e-007 Mann-Whitney	7.6297e-014 t-test
1hu+ex,2hu+ex	0.52692 Mann-Whitney	0.010182 t-test	0.063349 t-test
rec56,2hu	0.91914 t-test	0.38351 t-test	0.52528 t-test
cc84,1hu	0.90973 t-test	0.73784 t-test	0.75346 t-test
hu,cc28	0.27485 t-test	0.12698 Mann-Whitney	0.027954 t-test
rec28,cc56	0.71302 t-test	0.12937 t-test	0.063617 Mann-Whitney
1hu+ex,cc84	0.057631 Mann-Whitney	0.82702 t-test	0.58837 t-test
rec56,cc84	0.96496 t-test	0.26281 t-test	0.30507 Mann-Whitney
rec56,1hu+ex	0.10171 Mann-Whitney	0.24868 t-test	0.06197 Mann-Whitney
2hu+ex,cc112	0.00027288 t-test	0.035186 t-test	0.88688 Mann-Whitney
1hu,cc112	0.90115 t-test	0.73108 t-test	0.010787 Mann-Whitney
2hu,cc112	0.85285 t-test	0.72986 t-test	0.001113 Mann-Whitney
rec84,cc112	0.55015 t-test	0.76313 t-test	0.94834 Mann-Whitney
1hu+rec,control	0.64525 Mann-Whitney	0.76593 Mann-Whitney	0.076801 t-test
2hu+rec,control	0.79958 t-test	0.38675 t-test	0.28472 t-test

	FD_pQCT_CorticalArea.csv	FD_pQCT_CorticalBMC.csv	FD_pQCT_CorticalThickness.csv
bl,cc28	5.5934e-005 t-test	6.3904e-005 t-test	6.3778e-006 t-test
bl,cc56	1.0506e-005 t-test	4.2485e-006 t-test	0.00015318 t-test
bl,cc84	3.093e-006 t-test	1.0444e-006 t-test	6.149e-006 t-test
bl,cc112	6.1634e-010 t-test	1.0719e-011 t-test	2.2327e-007 Mann-Whitney
bl,control	4.894e-011 t-test	1.7164e-012 t-test	1.052e-009 t-test
bl,hu	0.084471 t-test	0.090474 t-test	0.47431 Mann-Whitney
bl,rec28	0.03849 Mann-Whitney	0.013593 Mann-Whitney	0.028059 t-test
bl,rec56	1.6417e-005 Mann-Whitney	5.8772e-006 Mann-Whitney	1.8792e-005 t-test
bl,rec84	1.2352e-005 Mann-	3.9404e-006 Mann-	3.6674e-005 Mann-

	Whitney	Whitney	Whitney
bl,1hu	9.5054e-006 t-test	5.5864e-007 t-test	0.0001235 t-test
bl,1hu+rec	5.8923e-009 t-test	6.608e-010 t-test	4.7688e-006 t-test
bl,2hu	0.0010466 t-test	0.00014334 t-test	0.063702 t-test
bl,2hu+rec	5.1132e-005 Mann-Whitney	1.2152e-005 Mann-Whitney	0.00041201 Mann-Whitney
bl,1hu+ex	2.3525e-006 t-test	1.1351e-007 t-test	3.565e-005 t-test
bl,2hu+ex	1.1474e-009 t-test	6.3105e-012 t-test	9.8961e-006 t-test
1hu+ex,2hu+ex	0.19789 t-test	0.11071 t-test	0.72663 t-test
rec56,2hu	0.26219 t-test	0.38193 t-test	0.020342 t-test
cc84,1hu	0.35873 t-test	0.53551 t-test	0.21174 t-test
hu,cc28	0.026877 t-test	0.026268 t-test	0.016615 t-test
rec28,cc56	0.063487 Mann-Whitney	0.063585 Mann-Whitney	0.16274 t-test
1hu+ex,cc84	0.69248 t-test	0.9363 t-test	0.6706 t-test
rec56,cc84	0.29483 Mann-Whitney	0.28483 Mann-Whitney	0.65018 t-test
rec56,1hu+ex	0.3775 t-test	0.11499 Mann-Whitney	0.99807 t-test
2hu+ex,cc112	0.84114 t-test	0.85979 t-test	0.011483 Mann-Whitney
1hu,cc112	0.05948 t-test	0.039413 t-test	0.0042902 Mann-Whitney
2hu,cc112	0.006016 t-test	0.0029316 t-test	0.00051336 Mann-Whitney
rec84,cc112	0.67615 t-test	0.74601 t-test	0.92772 Mann-Whitney
1hu+rec,control	0.23897 t-test	0.13695 t-test	0.088548 t-test
2hu+rec,control	0.42928 t-test	0.35375 t-test	0.45862 t-test

	FD_pQCT_CorticalvBMD.csv	FD_pQCT_Imax.csv	FD_pQCT_Imin.csv
bl,cc28	0.3763 t-test	0.0026555 t-test	0.00040711 Mann-Whitney
bl,cc56	0.00048867 t-test	0.00014606 t-test	9.663e-006 Mann-Whitney
bl,cc84	4.2288e-005 Mann-Whitney	0.00014113 t-test	2.7421e-005 Mann-Whitney
bl,cc112	3.3075e-017 t-test	5.1531e-006 Mann-Whitney	1.1567e-007 Mann-Whitney
bl,control	3.4515e-016 t-test	2.5522e-009 t-test	3.9426e-006 Mann-

			Whitney
bl,hu	0.65544 t-test	0.20343 t-test	0.0055826 Mann-Whitney
bl,rec28	0.00020687 t-test	0.079994 t-test	0.0016121 Mann-Whitney
bl,rec56	7.7271e-006 t-test	0.00099507 t-test	2.7686e-005 Mann-Whitney
bl,rec84	5.7615e-011 t-test	7.1156e-006 t-test	7.4087e-006 Mann-Whitney
bl,1hu	1.8542e-008 Mann-Whitney	0.00052997 Mann-Whitney	0.00022381 Mann-Whitney
bl,1hu+rec	4.7016e-008 Mann-Whitney	2.8088e-008 t-test	1.5424e-007 Mann-Whitney
bl,2hu	1.5405e-007 Mann-Whitney	0.0011386 t-test	0.00046223 Mann-Whitney
bl,2hu+rec	1.3943e-008 Mann-Whitney	0.00011965 Mann-Whitney	2.3107e-005 Mann-Whitney
bl,1hu+ex	1.2506e-013 t-test	1.537e-005 t-test	3.0388e-005 Mann-Whitney
bl,2hu+ex	1.2784e-019 t-test	1.0844e-009 t-test	1.5264e-007 Mann-Whitney
1hu+ex,2hu+ex	0.0014452 t-test	0.040569 t-test	0.053494 t-test
rec56,2hu	0.04354 t-test	0.96128 t-test	0.29487 Mann-Whitney
cc84,1hu	1.5698e-005 t-test	0.86427 Mann-Whitney	0.32261 t-test
hu,cc28	0.62859 t-test	0.093586 t-test	0.024166 Mann-Whitney
rec28,cc56	0.62457 t-test	0.093448 t-test	0.093347 t-test
1hu+ex,cc84	7.3035e-007 t-test	0.91158 t-test	0.46689 t-test
rec56,cc84	0.72329 t-test	0.37098 t-test	0.1213 Mann-Whitney
rec56,1hu+ex	1.7684e-005 t-test	0.30095 t-test	0.26275 Mann-Whitney
2hu+ex,cc112	0.00067212 t-test	0.16519 t-test	0.62861 t-test
1hu,cc112	0.052767 Mann-Whitney	0.51854 Mann-Whitney	0.10066 t-test
2hu,cc112	0.0022212 Mann-Whitney	0.16512 t-test	0.05 t-test
rec84,cc112	0.25538 t-test	0.67261 t-test	0.76036 t-test
1hu+rec,control	9.2192e-005 Mann-Whitney	0.66643 t-test	0.38602 t-test
2hu+rec,control	0.011034 t-test	0.35501 t-test	0.51599 t-test
	FD_pQCT_Ip.csv	FD_pQCT_SSI.csv	FD_stiffness.csv
bl,cc28	0.0012073 t-test	0.00082313 Mann-	0.5082 Mann-Whitney

		Whitney	
bl,cc56	3.2483e-005 t-test	2.5214e-005 Mann-Whitney	0.14346 Mann-Whitney
bl,cc84	1.9006e-005 t-test	9.3767e-005 Mann-Whitney	0.0094005 Mann-Whitney
bl,cc112	6.4732e-007 Mann-Whitney	6.8668e-008 Mann-Whitney	0.47759 Mann-Whitney
bl,control	3.8934e-010 t-test	1.4826e-006 Mann-Whitney	0.00053944 Mann-Whitney
bl,hu	0.054856 Mann-Whitney	0.013762 Mann-Whitney	0.013991 Mann-Whitney
bl,rec28	0.024368 t-test	0.012782 Mann-Whitney	0.033938 Mann-Whitney
bl,rec56	0.00027091 t-test	3.0388e-005 Mann-Whitney	0.047177 Mann-Whitney
bl,rec84	5.2821e-007 t-test	1.8488e-005 Mann-Whitney	0.0013802 Mann-Whitney
bl,1hu	1.9234e-005 t-test	7.7034e-005 Mann-Whitney	0.036607 Mann-Whitney
bl,1hu+rec	3.3796e-009 t-test	1.7143e-007 Mann-Whitney	3.6889e-005 Mann-Whitney
bl,2hu	0.00035418 t-test	0.00015313 Mann-Whitney	0.057047 Mann-Whitney
bl,2hu+rec	3.6113e-005 Mann-Whitney	6.9101e-006 Mann-Whitney	5.6815e-007 Mann-Whitney
bl,1hu+ex	6.9648e-006 t-test	5.8863e-006 Mann-Whitney	0.11084 Mann-Whitney
bl,2hu+ex	2.5817e-010 t-test	5.4137e-008 Mann-Whitney	0.0012741 Mann-Whitney
1hu+ex,2hu+ex	0.037982 t-test	0.011801 t-test	0.14623 t-test
rec56,2hu	0.88834 t-test	0.79799 t-test	0.66248 Mann-Whitney
cc84,1hu	0.49252 t-test	0.78917 t-test	0.79036 t-test
hu,cc28	0.024166 Mann-Whitney	0.13306 t-test	0.089218 Mann-Whitney
rec28,cc56	0.087088 t-test	0.057631 Mann-Whitney	0.39531 Mann-Whitney
1hu+ex,cc84	0.69315 t-test	0.9775 t-test	0.0009839 Mann-Whitney
rec56,cc84	0.24745 Mann-Whitney	0.32611 Mann-Whitney	0.59722 Mann-Whitney
rec56,1hu+ex	0.22492 t-test	0.13857 t-test	0.0042544 Mann-Whitney
2hu+ex,cc112	0.30543 t-test	0.22077 t-test	0.00091483 Mann-Whitney

1hu,cc112	0.22681 t-test	0.11303 t-test	0.10949 Mann-Whitney
2hu,cc112	0.096337 t-test	0.024692 t-test	0.16541 Mann-Whitney
rec84,cc112	0.70434 t-test	0.93392 t-test	0.013291 Mann-Whitney
1hu+rec,control	0.51822 t-test	0.23262 t-test	0.086176 Mann-Whitney
2hu+rec,control	0.41162 t-test	0.37872 t-test	0.18106 Mann-Whitney

Left Femoral Neck p values

	L_FN_Force.csv	L_FN_Stiffness.csv
bl,cc28	0.45777 t-test	0.1421 Mann-Whitney
bl,cc56	0.84326 Mann-Whitney	0.060487 t-test
bl,cc84	0.92912 t-test	0.013495 t-test
bl,cc112	0.58639 t-test	0.051278 t-test
bl,control	0.74176 t-test	0.0067067 t-test
bl,hu	0.00054315 Mann-Whitney	0.85841 t-test
bl,rec28	0.022135 t-test	0.48323 t-test
bl,rec56	0.14565 t-test	0.051181 t-test
bl,rec84	0.11637 Mann-Whitney	0.0011414 t-test
bl,1hu	0.0037796 t-test	0.82537 t-test
bl,1hu+rec	0.037959 t-test	0.85497 t-test
bl,2hu	0.0005312 Mann-Whitney	0.33371 t-test
bl,2hu+rec	0.81213 t-test	0.014641 Mann-Whitney
bl,1hu+ex	6.8969e-006 t-test	0.0059458 t-test
bl,2hu+ex	1.8109e-005 Mann-Whitney	6.3894e-005 t-test
1hu+ex,2hu+ex	0.556 Mann-Whitney	0.39443 t-test
rec56,2hu	0.013491 Mann-Whitney	0.038562 t-test
cc84,1hu	0.036067 t-test	0.033568 t-test
hu,cc28	6.8112e-005 t-test	0.066022 Mann-Whitney
rec28,cc56	0.032633 Mann-Whitney	0.31005 t-test
1hu+ex,cc84	0.00052744 t-test	0.63009 t-test
rec56,cc84	0.39474 Mann-Whitney	0.63444 t-test
rec56,1hu+ex	2.8059e-007 t-test	0.38237 t-test
2hu+ex,cc112	1.3295e-005 Mann-Whitney	0.015286 t-test
1hu,cc112	0.00026831 t-test	0.087021 t-test
2hu,cc112	5.3958e-005 Mann-Whitney	0.027514 t-test
rec84,cc112	0.16941 Mann-Whitney	0.09012 t-test
1hu+rec,control	0.19898 t-test	0.028277 t-test
2hu+rec,control	0.95906 t-test	0.9015 t-test

Right Femoral Neck p values

	RFN_Force.csv	RFN_pQCT_BSI.csv	RFN_pQCT_CSI.csv
bl,cc28	0.40362 Mann-Whitney	0.70241 t-test	0.034424 Mann-Whitney
bl,cc56	0.088586 Mann-Whitney	0.24045 t-test	0.010151 Mann-Whitney
bl,cc84	0.38251 Mann-Whitney	0.6315 t-test	0.061304 Mann-Whitney
bl,cc112	6.1762e-005 Mann-Whitney	0.0030153 t-test	5.4939e-005 Mann-Whitney
bl,control	0.44548 Mann-Whitney	0.16105 t-test	0.00037727 Mann-Whitney
bl,hu	2.0199e-005 Mann-Whitney	0.2936 Mann-Whitney	4.0004e-005 Mann-Whitney
bl,rec28	0.56299 Mann-Whitney	0.30576 t-test	0.0018157 Mann-Whitney
bl,rec56	0.036315 Mann-Whitney	0.83865 t-test	0.030892 Mann-Whitney
bl,rec84	3.48e-005 Mann-Whitney	0.0067172 Mann-Whitney	0.00058953 Mann-Whitney
bl,1hu	0.00051699 Mann-Whitney	0.55177 t-test	0.14118 Mann-Whitney
bl,1hu+rec	0.0076415 Mann-Whitney	0.42343 t-test	0.0076415 Mann-Whitney
bl,2hu	0.04253 Mann-Whitney	0.33229 t-test	0.2484 Mann-Whitney
bl,2hu+rec	0.10256 Mann-Whitney	0.98503 t-test	0.00064765 Mann-Whitney
bl,1hu+ex	4.5677e-007 Mann-Whitney	2.1242e-005 t-test	1.5474e-006 Mann-Whitney
bl,2hu+ex	6.1473e-008 Mann-Whitney	1.353e-006 t-test	3.2047e-008 Mann-Whitney
1hu+ex,2hu+ex	0.79021 t-test	0.75193 t-test	0.38107 t-test
rec56,2hu	0.0028226 Mann-Whitney	0.23388 t-test	0.01618 t-test
cc84,1hu	0.0052378 Mann-Whitney	0.95195 t-test	0.0065494 t-test
hu,cc28	1.2549e-005 t-test	0.1094 Mann-Whitney	2.825e-006 t-test
rec28,cc56	0.36962 t-test	0.032255 t-test	3.9876e-005 t-test
1hu+ex,cc84	5.8189e-007 t-test	0.0011759 t-test	0.00021521 t-test
rec56,cc84	0.32611 Mann-Whitney	0.75572 t-test	0.87357 t-test
rec56,1hu+ex	5.7371e-005 Mann-Whitney	6.3149e-005 t-test	0.00015863 t-test
2hu+ex,cc112	0.00024672 Mann-Whitney	0.03531 t-test	3.8552e-006 t-test
1hu,cc112	1.1449e-005 Mann-	0.047247 t-test	4.5371e-006 t-test

	Whitney		
2hu,cc112	0.00015175 Mann-Whitney	0.0017524 t-test	6.714e-005 t-test
rec84,cc112	0.20875 Mann-Whitney	0.80551 Mann-Whitney	0.88665 Mann-Whitney
1hu+rec,control	0.29122 t-test	0.54579 t-test	0.007395 Mann-Whitney
2hu+rec,control	0.85357 t-test	0.17365 t-test	0.67697 Mann-Whitney

	RFN_pQCT_CortThick.csv	RFN_pQCT_Imax.csv	RFN_pQCT_Imin.csv
bl,cc28	0.020871 Mann-Whitney	0.76624 t-test	0.62548 Mann-Whitney
bl,cc56	0.4808 Mann-Whitney	0.38368 t-test	0.049621 Mann-Whitney
bl,cc84	0.037946 Mann-Whitney	0.53278 Mann-Whitney	0.14346 Mann-Whitney
bl,cc112	1.0203e-005 Mann-Whitney	0.011392 Mann-Whitney	0.029862 Mann-Whitney
bl,control	7.3596e-006 Mann-Whitney	0.67455 t-test	0.089046 Mann-Whitney
bl,hu	0.013326 Mann-Whitney	0.19366 Mann-Whitney	0.68508 Mann-Whitney
bl,rec28	0.071349 Mann-Whitney	0.43911 t-test	0.48905 Mann-Whitney
bl,rec56	0.00027951 Mann-Whitney	0.55262 t-test	0.99135 Mann-Whitney
bl,rec84	3.1517e-005 Mann-Whitney	0.028608 Mann-Whitney	0.044708 Mann-Whitney
bl,1hu	0.044433 Mann-Whitney	0.90196 t-test	0.20087 Mann-Whitney
bl,1hu+rec	5.6653e-005 Mann-Whitney	0.99327 t-test	0.19061 Mann-Whitney
bl,2hu	0.00072603 Mann-Whitney	0.11832 t-test	0.35472 Mann-Whitney
bl,2hu+rec	2.735e-006 Mann-Whitney	0.30974 t-test	0.70042 Mann-Whitney
bl,1hu+ex	0.003911 Mann-Whitney	2.5073e-005 t-test	0.00063396 Mann-Whitney
bl,2hu+ex	0.00038709 Mann-Whitney	3.8201e-006 t-test	6.0627e-005 Mann-Whitney
1hu+ex,2hu+	0.17089 t-test	0.89126 t-test	0.7586 Mann-Whitney

ex			
rec56,2hu	0.25306 t-test	0.30812 t-test	0.44082 Mann-Whitney
cc84,1hu	0.95509 t-test	0.66222 Mann-Whitney	0.67853 t-test
hu,cc28	0.00038306 t-test	0.19891 Mann-Whitney	0.95272 Mann-Whitney
rec28,cc56	0.042415 Mann-Whitney	0.13887 t-test	0.032751 t-test
1hu+ex,cc84	0.14662 t-test	0.0018053 Mann-Whitney	0.037222 t-test
rec56,cc84	0.040459 t-test	0.74342 Mann-Whitney	0.21356 Mann-Whitney
rec56,1hu+ex	0.72354 t-test	9.6615e-005 Mann-Whitney	0.0042099 Mann-Whitney
2hu+ex,cc112	0.051443 Mann-Whitney	0.052146 t-test	0.058107 t-test
1hu,cc112	0.049647 t-test	0.072628 t-test	0.43722 Mann-Whitney
2hu,cc112	0.49717 t-test	0.0032333 t-test	0.014921 t-test
rec84,cc112	0.23282 t-test	0.84587 Mann-Whitney	0.64997 t-test
1hu+rec,control	0.086386 t-test	0.73365 t-test	0.73675 t-test
2hu+rec,control	0.37044 t-test	0.18246 t-test	0.19578 Mann-Whitney

	RFN_pQCT_Ip.csv	RFN_pQCT_SSI.csv	RFN_pQCT_cortArea.csv
bl,cc28	0.58015 Mann-Whitney	0.84907 t-test	0.10142 Mann-Whitney
bl,cc56	0.11084 Mann-Whitney	0.21085 t-test	0.018576 Mann-Whitney
bl,cc84	0.84712 Mann-Whitney	0.82939 Mann-Whitney	0.035859 Mann-Whitney
bl,cc112	0.0079411 Mann-Whitney	0.14349 t-test	5.9678e-007 Mann-Whitney
bl,control	0.22974 Mann-Whitney	0.38701 t-test	7.4941e-005 Mann-Whitney
bl,hu	0.47306 Mann-Whitney	0.88882 t-test	0.029741 Mann-Whitney
bl,rec28	0.67476 Mann-Whitney	0.83394 t-test	0.22059 Mann-Whitney
bl,rec56	0.99135 Mann-Whitney	0.2371 Mann-Whitney	0.00058433 Mann-Whitney
bl,rec84	0.026999 Mann-Whitney	0.20441 t-test	1.0244e-005 Mann-Whitney
bl,1hu	0.63061 Mann-Whitney	0.95206 t-test	0.017511 Mann-Whitney
bl,1hu+rec	0.65301 Mann-Whitney	0.5942 t-test	0.00015254 Mann-Whitney

bl,2hu	0.15427 Mann-Whitney	0.086987 t-test	0.18658 Mann-Whitney
bl,2hu+rec	0.94197 Mann-Whitney	0.12129 Mann-Whitney	8.8307e-005 Mann-Whitney
bl,1hu+ex	7.527e-005 Mann-Whitney	0.00070716 t-test	1.9158e-006 Mann-Whitney
bl,2hu+ex	1.4422e-005 Mann-Whitney	0.00059319 t-test	2.1733e-007 Mann-Whitney
1hu+ex,2hu+ex	0.97946 t-test	0.5642 t-test	0.21435 t-test
rec56,2hu	0.30058 t-test	0.54008 Mann-Whitney	0.043462 t-test
cc84,1hu	0.74678 Mann-Whitney	0.89423 Mann-Whitney	0.94338 t-test
hu,cc28	0.27702 Mann-Whitney	0.7344 t-test	0.0023148 t-test
rec28,cc56	0.067095 t-test	0.40814 t-test	0.0037044 Mann-Whitney
1hu+ex,cc84	0.0037044 Mann-Whitney	0.0082799 Mann-Whitney	7.0227e-005 t-test
rec56,cc84	0.98259 Mann-Whitney	0.13214 Mann-Whitney	0.25006 t-test
rec56,1hu+ex	0.00018919 Mann-Whitney	0.00049369 Mann-Whitney	0.00027903 t-test
2hu+ex,cc112	0.039598 t-test	0.061686 t-test	0.0020301 Mann-Whitney
1hu,cc112	0.084052 t-test	0.18942 t-test	0.0049187 Mann-Whitney
2hu,cc112	0.0030815 t-test	0.010363 t-test	0.00029897 Mann-Whitney
rec84,cc112	0.80551 Mann-Whitney	0.94744 t-test	0.46008 Mann-Whitney
1hu+rec,control	0.71862 t-test	0.67738 t-test	0.1144 t-test
2hu+rec,control	0.17675 t-test	0.34576 Mann-Whitney	0.6075 t-test

	RFN_pQCT_cortBMC.csv	RFN_pQCT_cortBMD.csv	RFN_pQCT_totArea.csv
bl,cc28	0.07523 Mann-Whitney	0.24845 t-test	0.79274 t-test
bl,cc56	0.0089434 Mann-Whitney	0.081553 t-test	0.33419 t-test
bl,cc84	0.0047378 Mann-Whitney	0.0022462 t-test	0.72516 Mann-Whitney
bl,cc112	1.7893e-007 Mann-Whitney	8.6954e-006 Mann-Whitney	0.2576 t-test
bl,control	8.2155e-006 Mann-	1.0713e-010 t-test	0.28499 t-test

	Whitney		
bl,hu	0.044726 Mann-Whitney	0.33931 t-test	0.98014 t-test
bl,rec28	0.26634 Mann-Whitney	0.69197 t-test	0.92471 t-test
bl,rec56	8.2339e-005 Mann-Whitney	2.0458e-005 t-test	0.19253 t-test
bl,rec84	7.4637e-006 Mann-Whitney	0.0010999 t-test	0.31566 t-test
bl,1hu	0.0046886 Mann-Whitney	0.00053027 t-test	0.82578 t-test
bl,1hu+rec	4.5197e-006 Mann-Whitney	2.561e-009 t-test	0.30634 t-test
bl,2hu	0.021534 Mann-Whitney	2.1814e-007 t-test	0.029289 t-test
bl,2hu+rec	4.0889e-006 Mann-Whitney	1.6306e-013 t-test	0.019373 t-test
bl,1hu+ex	1.2431e-006 Mann-Whitney	0.053989 t-test	0.0019074 t-test
bl,2hu+ex	2.8081e-007 Mann-Whitney	0.0002275 t-test	0.0015461 t-test
1hu+ex,2hu+ex	0.14477 t-test	0.13873 t-test	0.64308 t-test
rec56,2hu	0.042435 t-test	0.50754 t-test	0.38014 t-test
cc84,1hu	0.91035 t-test	0.79582 t-test	0.71819 Mann-Whitney
hu,cc28	0.0019646 t-test	0.86307 t-test	0.8077 t-test
rec28,cc56	0.0012807 t-test	0.27022 t-test	0.35432 t-test
1hu+ex,cc84	0.00011836 t-test	0.23998 t-test	0.01209 Mann-Whitney
rec56,cc84	0.15522 t-test	0.48417 t-test	0.71066 Mann-Whitney
rec56,1hu+ex	0.00105 Mann-Whitney	0.029857 t-test	0.00042247 Mann-Whitney
2hu+ex,cc112	0.0023493 Mann-Whitney	0.38734 Mann-Whitney	0.047157 t-test
1hu,cc112	0.0027138 Mann-Whitney	0.22451 Mann-Whitney	0.24357 t-test
2hu,cc112	0.00061119 Mann-Whitney	0.26003 Mann-Whitney	0.0052386 t-test
rec84,cc112	0.31207 Mann-Whitney	0.96898 Mann-Whitney	0.94191 t-test
1hu+rec,control	0.043726 t-test	0.063593 t-test	0.89508 t-test
2hu+rec,contr	0.63361 t-test	0.7047 t-test	0.22225 t-test

ol			

	RFN_pQCT_totBMC.csv	RFN_pQCT_totBMD.csv	RFN_pQCT_trabArea.csv
bl,cc28	0.42844 Mann-Whitney	0.11066 t-test	0.5222 Mann-Whitney
bl,cc56	0.044775 Mann-Whitney	0.63117 t-test	0.29274 Mann-Whitney
bl,cc84	0.60186 Mann-Whitney	0.15827 t-test	0.1845 Mann-Whitney
bl,cc112	0.0079381 Mann-Whitney	0.057802 t-test	0.49484 Mann-Whitney
bl,control	0.095937 Mann-Whitney	2.239e-005 t-test	0.0029491 Mann-Whitney
bl,hu	0.027477 Mann-Whitney	0.00014292 t-test	0.23991 Mann-Whitney
bl,rec28	0.26149 Mann-Whitney	0.018735 t-test	0.54777 Mann-Whitney
bl,rec56	0.93948 Mann-Whitney	0.0033994 t-test	0.014666 Mann-Whitney
bl,rec84	0.017229 Mann-Whitney	0.062454 t-test	0.31279 Mann-Whitney
bl,1hu	0.5008 Mann-Whitney	0.40903 t-test	0.40817 Mann-Whitney
bl,1hu+rec	0.66022 Mann-Whitney	0.0098626 t-test	0.0085987 Mann-Whitney
bl,2hu	0.034775 Mann-Whitney	0.094095 Mann-Whitney	0.0062373 Mann-Whitney
bl,2hu+rec	0.39961 Mann-Whitney	1.0062e-007 t-test	8.5498e-006 Mann-Whitney
bl,1hu+ex	6.2685e-005 Mann-Whitney	0.15757 t-test	0.2829 Mann-Whitney
bl,2hu+ex	1.5941e-006 Mann-Whitney	0.0050261 t-test	0.855 Mann-Whitney
1hu+ex,2hu+ex	0.95421 t-test	0.26585 t-test	0.60011 Mann-Whitney
rec56,2hu	0.098406 t-test	0.29487 Mann-Whitney	0.77887 t-test
cc84,1hu	0.20706 t-test	0.089472 t-test	0.8345 Mann-Whitney
hu,cc28	0.018664 Mann-Whitney	2.0421e-005 t-test	0.093801 t-test
rec28,cc56	0.010659 t-test	0.021441 t-test	0.95996 t-test
1hu+ex,cc84	0.0010904 t-test	0.99606 t-test	0.070109 Mann-Whitney
rec56,cc84	0.53807 t-test	0.20591 t-test	0.32611 Mann-Whitney
rec56,1hu+ex	0.00036093 Mann-Whitney	0.22065 t-test	0.0054521 Mann-Whitney
2hu+ex,cc112	0.00055902 t-test	0.20682 t-test	0.51409 t-test
1hu,cc112	0.0033605 Mann-Whitney	0.029037 t-test	0.79969 t-test
2hu,cc112	0.00040388 t-test	0.82178 Mann-Whitney	0.032799 t-test

rec84,cc112	0.7927 t-test	0.75912 t-test	0.7425 t-test
1hu+rec,control	0.30225 t-test	0.058141 t-test	0.44547 t-test
2hu+rec,control	0.45591 Mann-Whitney	0.27101 t-test	0.20969 t-test

	RFN_pQCT_trabBMC.csv	RFN_pQCT_trabBMD.csv	RFN_stiffness.csv
bl,cc28	0.5829 t-test	0.22219 t-test	0.4944 Mann-Whitney
bl,cc56	0.62479 t-test	0.63397 t-test	0.71023 t-test
bl,cc84	0.097723 Mann-Whitney	0.30452 t-test	0.010718 Mann-Whitney
bl,cc112	0.22722 t-test	0.1616 Mann-Whitney	0.00037554 t-test
bl,control	0.0031759 t-test	0.032124 t-test	0.0071628 Mann-Whitney
bl,hu	0.2358 Mann-Whitney	4.6023e-010 t-test	0.52287 t-test
bl,rec28	0.58453 t-test	0.00010221 t-test	0.073236 t-test
bl,rec56	0.012363 t-test	0.030888 Mann-Whitney	0.0033101 t-test
bl,rec84	0.18895 t-test	0.23371 Mann-Whitney	0.15101 t-test
bl,1hu	0.011843 t-test	2.9845e-008 t-test	0.29315 t-test
bl,1hu+rec	0.001507 t-test	3.4247e-005 t-test	0.078571 t-test
bl,2hu	0.00055505 Mann-Whitney	6.1295e-006 t-test	0.12211 t-test
bl,2hu+rec	5.278e-005 t-test	0.25701 Mann-Whitney	0.0010545 Mann-Whitney
bl,1hu+ex	0.13947 t-test	0.18215 Mann-Whitney	0.0013756 Mann-Whitney
bl,2hu+ex	0.73734 t-test	0.4296 t-test	0.0035683 Mann-Whitney
1hu+ex,2hu+ex	0.37828 t-test	0.87644 t-test	0.7586 Mann-Whitney
rec56,2hu	0.54004 Mann-Whitney	0.072091 Mann-Whitney	0.18034 t-test
cc84,1hu	0.40327 Mann-Whitney	0.00051505 t-test	0.48221 Mann-Whitney
hu,cc28	0.48207 t-test	9.4435e-008 t-test	0.93389 Mann-Whitney
rec28,cc56	0.2939 t-test	0.0014098 t-test	0.23218 t-test
1hu+ex,cc84	0.04703 Mann-Whitney	0.20484 t-test	0.13214 Mann-Whitney
rec56,cc84	0.2474 Mann-Whitney	0.47145 Mann-Whitney	0.37943 t-test
rec56,1hu+ex	0.0041797 t-test	0.051239 Mann-	0.4553 Mann-Whitney

		Whitney	
2hu+ex,cc112	0.21443 t-test	0.048338 t-test	0.41184 Mann-Whitney
1hu,cc112	0.1271 t-test	0.00094347 t-test	0.044115 t-test
2hu,cc112	0.008194 Mann-Whitney	0.03702 t-test	0.1279 t-test
rec84,cc112	0.70227 t-test	0.75361 t-test	0.16738 t-test
1hu+rec,control	0.83188 t-test	0.1973 t-test	0.16306 Mann-Whitney
2hu+rec,control	0.29874 t-test	0.93428 t-test	0.79847 Mann-Whitney

Distal Femur Metaphysis p values

	DFM_Elastic_modulus.csv	DFM_Energy_to_Yield.csv	DFM_Energy_to_ultimate.csv
bl,cc28	0.060444 Mann-Whitney	0.21526 Mann-Whitney	0.33215 Mann-Whitney
bl,cc56	0.050841 Mann-Whitney	0.81582 Mann-Whitney	0.82564 Mann-Whitney
bl,cc84	0.78187 Mann-Whitney	0.74286 Mann-Whitney	0.84299 Mann-Whitney
bl,cc112	0.51843 Mann-Whitney	0.066607 Mann-Whitney	0.099263 Mann-Whitney
bl,control	0.88978 Mann-Whitney	0.8541 Mann-Whitney	1 Mann-Whitney
bl,hu	0.148 Mann-Whitney	0.27162 Mann-Whitney	0.19118 Mann-Whitney
bl,rec28	0.70139 Mann-Whitney	0.4104 Mann-Whitney	0.74406 Mann-Whitney
bl,rec56	0.952 Mann-Whitney	0.76065 Mann-Whitney	0.67382 Mann-Whitney
bl,rec84	0.45728 Mann-Whitney	0.58119 Mann-Whitney	0.78552 Mann-Whitney
bl,1hu	0.0010796 Mann-Whitney	0.000513 Mann-Whitney	0.0016866 Mann-Whitney
bl,1hu+rec	0.21096 Mann-Whitney	0.063747 Mann-Whitney	0.034309 Mann-Whitney
bl,2hu	0.54108 Mann-Whitney	0.26642 Mann-Whitney	0.094585 Mann-Whitney
bl,2hu+rec	0.294 Mann-Whitney	0.76182 Mann-Whitney	0.74889 Mann-Whitney
bl,1hu+ex	0.64595 Mann-Whitney	0.0063952 Mann-Whitney	0.0056913 Mann-Whitney
bl,2hu+ex	0.002408 Mann-Whitney	0.0015627 Mann-Whitney	0.00027143 Mann-Whitney
1hu+ex,2hu+ex	0.021045 Mann-Whitney	0.82573 Mann-Whitney	0.62632 t-test
rec56,2hu	0.73688 Mann-Whitney	0.1094 Mann-Whitney	0.078545 Mann-Whitney
cc84,1hu	0.010805 Mann-Whitney	0.00063396 Mann-Whitney	0.00032101 Mann-Whitney
hu,cc28	0.0011927 Mann-Whitney	0.0093639 Mann-Whitney	0.028553 Mann-Whitney
rec28,cc56	0.034062 t-test	0.39577 Mann-Whitney	0.5124 Mann-Whitney
1hu+ex,cc84	0.71439 Mann-Whitney	0.0023633 Mann-Whitney	0.0090401 Mann-Whitney
rec56,cc84	1 Mann-Whitney	0.70892 Mann-Whitney	0.6783 Mann-Whitney

rec56,1hu+ex	0.90291 Mann-Whitney	0.0023633 Mann-Whitney	0.0067665 Mann-Whitney
2hu+ex,cc112	0.00016325 Mann-Whitney	0.061329 Mann-Whitney	0.013119 Mann-Whitney
1hu,cc112	0.0033117 Mann-Whitney	5.5984e-006 Mann-Whitney	1.9749e-005 Mann-Whitney
2hu,cc112	0.96871 t-test	0.0018207 Mann-Whitney	0.0013137 Mann-Whitney
rec84,cc112	0.2351 Mann-Whitney	0.30595 Mann-Whitney	0.41426 Mann-Whitney
1hu+rec,control	0.43891 Mann-Whitney	0.07733 Mann-Whitney	0.027593 Mann-Whitney
2hu+rec,control	0.32861 Mann-Whitney	0.55152 t-test	0.98342 Mann-Whitney

	DFM_Ultimate_strain.csv	DFM_Ultimate_stress.csv	DFM_Yield_strain.csv
bl,cc28	0.2906 Mann-Whitney	0.045429 Mann-Whitney	0.71898 Mann-Whitney
bl,cc56	0.12117 Mann-Whitney	0.16967 Mann-Whitney	0.21565 Mann-Whitney
bl,cc84	0.94241 Mann-Whitney	0.727 Mann-Whitney	0.62262 Mann-Whitney
bl,cc112	0.027409 Mann-Whitney	0.78633 Mann-Whitney	0.0074164 Mann-Whitney
bl,control	0.33196 Mann-Whitney	0.90972 Mann-Whitney	0.42554 Mann-Whitney
bl,hu	0.71184 Mann-Whitney	0.12133 Mann-Whitney	0.64571 Mann-Whitney
bl,rec28	0.16904 Mann-Whitney	0.76104 Mann-Whitney	0.20747 Mann-Whitney
bl,rec56	0.53127 Mann-Whitney	0.952 Mann-Whitney	0.52688 Mann-Whitney
bl,rec84	0.6868 Mann-Whitney	0.38467 Mann-Whitney	0.72217 Mann-Whitney
bl,1hu	0.14457 Mann-Whitney	0.00022003 Mann-Whitney	0.11982 Mann-Whitney
bl,1hu+rec	0.10843 Mann-Whitney	0.11855 Mann-Whitney	0.51083 Mann-Whitney
bl,2hu	0.4129 Mann-Whitney	0.25361 Mann-Whitney	0.88397 Mann-Whitney
bl,2hu+rec	0.33847 Mann-Whitney	0.48179 Mann-Whitney	0.50776 Mann-Whitney
bl,1hu+ex	0.012448 Mann-	0.081834 Mann-Whitney	0.017946 Mann-

	Whitney		Whitney
bl,2hu+ex	0.086166 Mann-Whitney	0.00027043 Mann-Whitney	0.090967 Mann-Whitney
1hu+ex,2hu+ex	0.20928 Mann-Whitney	0.065858 t-test	0.30734 Mann-Whitney
rec56,2hu	0.81827 t-test	0.24358 Mann-Whitney	0.40671 t-test
cc84,1hu	0.34495 t-test	0.00042329 Mann-Whitney	0.40561 Mann-Whitney
hu,cc28	0.73227 t-test	0.0019705 Mann-Whitney	0.99786 t-test
rec28,cc56	0.91903 t-test	0.11587 t-test	0.84607 Mann-Whitney
1hu+ex,cc84	0.014628 Mann-Whitney	0.097442 t-test	0.0065707 Mann-Whitney
rec56,cc84	0.22614 t-test	0.79036 t-test	0.98345 Mann-Whitney
rec56,1hu+ex	0.0029623 Mann-Whitney	0.20178 t-test	0.0075448 Mann-Whitney
2hu+ex,cc112	0.3597 Mann-Whitney	4.8789e-005 Mann-Whitney	0.29857 Mann-Whitney
1hu,cc112	0.001228 Mann-Whitney	0.00011569 Mann-Whitney	0.0004259 Mann-Whitney
2hu,cc112	0.0031542 Mann-Whitney	0.13984 Mann-Whitney	0.0094214 Mann-Whitney
rec84,cc112	0.0093748 Mann-Whitney	0.31411 Mann-Whitney	0.0073049 Mann-Whitney
1hu+rec,control	0.028781 t-test	0.15879 Mann-Whitney	0.14276 t-test
2hu+rec,control	0.021154 t-test	0.51935 Mann-Whitney	0.053232 Mann-Whitney

	DFM_Yield_stress.csv	DFM_pQCT_CanCSI.csv	DFM_pQCT_CortThickness.csv
bl,cc28	0.035849 Mann-Whitney	0.10306 Mann-Whitney	0.58685 Mann-Whitney
bl,cc56	0.20672 Mann-Whitney	0.37122 t-test	0.040018 Mann-Whitney
bl,cc84	0.96262 Mann-Whitney	0.2766 t-test	0.25295 Mann-Whitney
bl,cc112	0.32525 Mann-Whitney	0.13443 t-test	0.56651 Mann-Whitney
bl,control	0.95113 Mann-Whitney	0.1408 t-test	0.12398 Mann-Whitney
bl,hu	0.22277 Mann-Whitney	0.012099 t-test	2.077e-006 Mann-Whitney
bl,rec28	0.83696 Mann-Whitney	0.01397 t-test	5.3623e-007 Mann-Whitney
bl,rec56	0.90673 Mann-Whitney	0.075149 t-test	7.5286e-005 Mann-Whitney
bl,rec84	0.38411 Mann-Whitney	0.66693 t-test	0.0646 Mann-Whitney
bl,1hu	0.00011453 Mann-Whitney	0.00164 t-test	0.00024085 Mann-Whitney
bl,1hu+rec	0.17787 Mann-Whitney	0.092046 t-test	0.00051578 Mann-Whitney
bl,2hu	0.29649 Mann-Whitney	0.035745 t-test	5.6138e-007 Mann-Whitney
bl,2hu+rec	0.39984 Mann-Whitney	0.036075 t-test	1.6045e-005 Mann-Whitney
bl,1hu+ex	0.050584 Mann-Whitney	0.041227 t-test	0.02921 Mann-Whitney
bl,2hu+ex	0.00051317 Mann-Whitney	0.0082083 t-test	0.00080082 Mann-Whitney
1hu+ex,2hu+ex	0.1333 Mann-Whitney	0.60618 t-test	0.84649 t-test
rec56,2hu	0.12526 t-test	0.90915 t-test	0.015057 Mann-Whitney
cc84,1hu	0.0013756 Mann-Whitney	0.041678 t-test	0.0076453 t-test
hu,cc28	0.0014615 Mann-Whitney	0.0060639 Mann-Whitney	6.0435e-007 t-test
rec28,cc56	0.16667 Mann-Whitney	0.023381 t-test	2.9058e-005 t-test
1hu+ex,cc84	0.047613 Mann-Whitney	0.0047281 t-test	0.020178 Mann-Whitney
rec56,cc84	0.70866 t-test	0.4738 t-test	0.0043127 t-test
rec56,1hu+ex	0.1069 Mann-Whitney	0.0018859 t-test	0.00026175 Mann-Whitney
2hu+ex,cc112	0.00072186 Mann-Whitney	0.00012318 t-test	0.00064256 t-test
1hu,cc112	3.3672e-005 Mann-	0.034547 t-test	0.00083184 t-test

	Whitney		
2hu,cc112	0.030034 Mann-Whitney	0.33972 t-test	5.6071e-006 Mann-Whitney
rec84,cc112	0.65014 Mann-Whitney	0.43336 t-test	0.12727 t-test
1hu+rec,control	0.3308 Mann-Whitney	0.95453 t-test	0.020838 t-test
2hu+rec,control	0.49277 Mann-Whitney	0.66699 t-test	0.0028915 t-test

	DFM_pQCT_Imax.csv	DFM_pQCT_Imin.csv	DFM_pQCT_Ip.csv
bl,cc28	0.15599 t-test	0.2934 t-test	0.18297 t-test
bl,cc56	0.20459 t-test	0.26239 t-test	0.20952 t-test
bl,cc84	0.19481 t-test	0.25732 t-test	0.20452 t-test
bl,cc112	0.016654 t-test	0.00058371 Mann-Whitney	0.0073834 t-test
bl,control	0.0028339 t-test	0.0319 t-test	0.0060351 t-test
bl,hu	0.019581 t-test	0.28521 Mann-Whitney	0.10694 Mann-Whitney
bl,rec28	0.027655 t-test	0.84965 t-test	0.17791 t-test
bl,rec56	0.47788 t-test	0.99481 t-test	0.64723 t-test
bl,rec84	0.34919 t-test	0.14743 t-test	0.24499 t-test
bl,1hu	0.067076 Mann-Whitney	0.0047049 Mann-Whitney	0.019374 Mann-Whitney
bl,1hu+rec	0.0041172 t-test	0.0015487 t-test	0.0022032 t-test
bl,2hu	0.57993 t-test	0.29194 t-test	0.94804 t-test
bl,2hu+rec	0.10656 Mann-Whitney	0.040587 t-test	0.15482 t-test
bl,1hu+ex	0.0011822 t-test	9.2431e-005 t-test	0.00031351 t-test
bl,2hu+ex	2.8248e-005 t-test	2.3562e-010 t-test	2.0653e-007 t-test
1hu+ex,2hu+ex	0.44563 t-test	0.013944 t-test	0.14305 t-test
rec56,2hu	0.85121 t-test	0.26541 t-test	0.5803 t-test
cc84,1hu	0.88761 t-test	0.34002 t-test	0.77592 t-test
hu,cc28	0.00045023 t-test	0.39331 t-test	0.0047279 t-test
rec28,cc56	0.001296 t-test	0.34029 t-test	0.010722 t-test
1hu+ex,cc84	0.029557 t-test	0.0029629 t-test	0.0098418 t-test
rec56,cc84	0.035946 t-test	0.18887 t-test	0.060389 t-test
rec56,1hu+ex	0.00041207 t-test	0.00018921 t-test	0.00019441 t-test
2hu+ex,cc112	0.017222 t-test	1.3988e-005 Mann-Whitney	0.00062646 t-test
1hu,cc112	0.35233 Mann-	0.47693 Mann-Whitney	0.39948 Mann-

	Whitney		Whitney
2hu,cc112	0.008092 t-test	0.2046 Mann-Whitney	0.020022 t-test
rec84,cc112	0.27752 t-test	0.35753 Mann-Whitney	0.2594 t-test
1hu+rec,control	0.92213 t-test	0.30082 t-test	0.75501 t-test
2hu+rec,control	0.053232 Mann-Whitney	0.8524 t-test	0.14827 t-test

	DFM_pQCT_SSI.csv	DFM_pQCT_TotalCSI.csv	DFM_pQCT_cortArea.csv
bl,cc28	0.048342 Mann-Whitney	0.32252 t-test	0.16267 t-test
bl,cc56	0.071944 Mann-Whitney	0.60219 t-test	0.79446 t-test
bl,cc84	0.040023 Mann-Whitney	0.2061 t-test	0.7479 t-test
bl,cc112	0.001837 Mann-Whitney	0.047147 t-test	0.027736 t-test
bl,control	0.00053309 Mann-Whitney	0.20365 t-test	0.33397 t-test
bl,hu	0.052603 Mann-Whitney	5.5367e-008 t-test	0.00017696 Mann-Whitney
bl,rec28	0.082333 Mann-Whitney	9.3699e-009 t-test	0.00021389 t-test
bl,rec56	0.52536 Mann-Whitney	0.00017476 t-test	0.015679 t-test
bl,rec84	0.094738 Mann-Whitney	0.22092 t-test	0.95619 t-test
bl,1hu	0.041574 Mann-Whitney	8.3568e-006 t-test	0.59895 Mann-Whitney
bl,1hu+rec	0.0036542 Mann-Whitney	0.00074271 t-test	0.89684 t-test
bl,2hu	0.73766 Mann-Whitney	7.3169e-008 t-test	0.0014929 t-test
bl,2hu+rec	0.035637 Mann-Whitney	8.8707e-005 t-test	0.23802 t-test
bl,1hu+ex	8.2278e-005 Mann-Whitney	0.0030894 t-test	0.0001217 Mann-Whitney
bl,2hu+ex	8.2202e-007 Mann-Whitney	0.00019156 t-test	5.3844e-009 t-test
1hu+ex,2hu+ex	0.053077 Mann-Whitney	0.83587 t-test	0.25475 Mann-Whitney
rec56,2hu	0.91432 t-test	0.073231 t-test	0.36973 t-test
cc84,1hu	0.73319 t-test	0.0039443 t-test	0.33789 Mann-Whitney

hu,cc28	0.0017832 t-test	2.85e-006 t-test	5.8617e-006 t-test
rec28,cc56	0.010486 t-test	0.00031749 Mann-Whitney	0.00083373 t-test
1hu+ex,cc84	0.020191 Mann-Whitney	0.0014112 t-test	0.0047854 Mann-Whitney
rec56,cc84	0.042243 t-test	0.022999 t-test	0.003107 t-test
rec56,1hu+ex	0.00013564 Mann-Whitney	3.4467e-006 t-test	1.9352e-005 Mann-Whitney
2hu+ex,cc112	0.00016533 t-test	1.8761e-007 t-test	4.2493e-005 t-test
1hu,cc112	0.21628 Mann-Whitney	0.001621 t-test	0.0068677 Mann-Whitney
2hu,cc112	0.0049777 t-test	1.2743e-005 t-test	1.0177e-005 t-test
rec84,cc112	0.37312 t-test	0.82986 t-test	0.082227 t-test
1hu+rec,control	0.78948 t-test	0.051582 t-test	0.37041 t-test
2hu+rec,control	0.27063 Mann-Whitney	0.010576 t-test	0.022279 t-test

	DFM_pQCT_cortBMC.csv	DFM_pQCT_cortBMD.csv	DFM_pQCT_totArea.csv
bl,cc28	0.36555 t-test	0.1333 t-test	0.13736 t-test
bl,cc56	0.56157 t-test	0.29939 t-test	0.058537 t-test
bl,cc84	0.79181 t-test	0.88544 t-test	0.054776 t-test
bl,cc112	0.36786 t-test	0.017614 Mann-Whitney	0.00020273 Mann-Whitney
bl,control	0.16171 t-test	0.13373 t-test	0.0017497 t-test
bl,hu	2.0638e-005 t-test	0.00013172 t-test	0.13273 Mann-Whitney
bl,rec28	1.3736e-005 t-test	0.00020741 t-test	0.20146 t-test
bl,rec56	0.008256 t-test	0.15396 t-test	0.29177 t-test
bl,rec84	0.83694 t-test	0.54278 Mann-Whitney	0.032132 t-test
bl,1hu	0.19196 t-test	0.10156 t-test	0.00035967 t-test
bl,1hu+rec	0.65938 t-test	0.05837 t-test	1.2807e-005 t-test
bl,2hu	0.00024817 Mann-Whitney	4.0695e-005 t-test	0.0044274 t-test
bl,2hu+rec	0.12479 t-test	0.1503 t-test	0.002025 t-test
bl,1hu+ex	0.00052547 t-test	0.015693 t-test	0.00039074 t-test
bl,2hu+ex	4.1681e-006 t-test	0.0059333 Mann-Whitney	6.94e-008 t-test
1hu+ex,2hu+ex	0.69454 t-test	0.50529 t-test	0.052719 t-test

rec56,2hu	0.078575 Mann-Whitney	0.013485 t-test	0.075552 t-test
cc84,1hu	0.10611 t-test	0.10764 Mann-Whitney	0.082614 t-test
hu,cc28	1.2837e-006 t-test	0.0065725 t-test	0.48346 Mann-Whitney
rec28,cc56	0.0001674 t-test	0.0085414 t-test	0.53351 t-test
1hu+ex,cc84	0.008972 Mann-Whitney	0.11499 Mann-Whitney	0.060401 t-test
rec56,cc84	0.0027509 t-test	0.18815 t-test	0.37548 t-test
rec56,1hu+ex	4.8063e-005 Mann-Whitney	0.31996 t-test	0.011302 t-test
2hu+ex,cc112	8.9784e-006 t-test	0.51854 Mann-Whitney	0.0016866 Mann-Whitney
1hu,cc112	0.019382 t-test	0.51147 Mann-Whitney	0.37545 Mann-Whitney
2hu,cc112	3.0022e-005 Mann-Whitney	0.22204 Mann-Whitney	0.85885 Mann-Whitney
rec84,cc112	0.3199 t-test	0.15031 Mann-Whitney	0.50038 Mann-Whitney
1hu+rec,control	0.073346 t-test	0.0033936 t-test	0.18009 t-test
2hu+rec,control	0.0038138 t-test	0.010358 t-test	0.91249 t-test

	DFM_pQCT_totBMC.csv	DFM_pQCT_totBMD.csv	DFM_pQCT_trabArea.csv
bl,cc28	0.193 t-test	0.77034 t-test	0.21644 t-test
bl,cc56	0.61872 t-test	0.024235 t-test	0.0139 t-test
bl,cc84	0.98793 t-test	0.0070138 t-test	0.024646 t-test
bl,cc112	0.63918 t-test	1.8487e-006 t-test	0.00029756 t-test
bl,control	0.47034 t-test	9.0674e-005 t-test	0.0005273 t-test
bl,hu	0.00018267 t-test	9.4383e-010 t-test	0.0022496 t-test
bl,rec28	6.4719e-005 Mann-Whitney	3.2613e-011 t-test	0.0010497 t-test
bl,rec56	0.017108 t-test	6.5782e-006 t-test	0.021814 t-test
bl,rec84	0.96807 t-test	0.0024762 t-test	0.007208 t-test
bl,1hu	0.025411 Mann-Whitney	3.4303e-010 t-test	2.4825e-005 Mann-Whitney
bl,1hu+rec	0.86 t-test	4.8375e-011 t-test	2.2234e-007 t-test
bl,2hu	0.0023372 t-test	1.1428e-012 t-test	6.4644e-006 t-test
bl,2hu+rec	0.20451 Mann-Whitney	2.1399e-007 Mann-Whitney	3.0032e-005 t-test
bl,1hu+ex	0.00013264 Mann-	0.92702 t-test	0.03719 t-test

	Whitney		
bl,2hu+ex	5.1342e-007 t-test	0.14864 t-test	6.6286e-005 t-test
1hu+ex,2hu+ex	0.17516 Mann-Whitney	0.2744 t-test	0.088368 t-test
rec56,2hu	0.48212 t-test	0.0054854 t-test	0.02234 t-test
cc84,1hu	0.042764 t-test	0.0016058 t-test	0.037625 Mann-Whitney
hu,cc28	2.9833e-005 t-test	6.5882e-006 t-test	0.045539 t-test
rec28,cc56	0.00061249 Mann-Whitney	1.9515e-005 t-test	0.36401 t-test
1hu+ex,cc84	0.00090465 Mann-Whitney	0.04447 t-test	0.94539 t-test
rec56,cc84	0.012208 t-test	0.11014 t-test	0.90693 t-test
rec56,1hu+ex	1.0992e-005 Mann-Whitney	0.00062302 t-test	0.86459 t-test
2hu+ex,cc112	1.1904e-007 t-test	0.0014908 t-test	0.40918 t-test
1hu,cc112	0.0092841 t-test	0.0069215 t-test	0.071002 Mann-Whitney
2hu,cc112	0.00012324 t-test	7.6967e-005 t-test	0.072926 t-test
rec84,cc112	0.72556 t-test	0.41289 t-test	0.66387 t-test
1hu+rec,control	0.37273 t-test	0.00080809 t-test	0.053573 t-test
2hu+rec,control	0.050697 Mann-Whitney	0.0012742 Mann-Whitney	0.45008 t-test

	DFM_pQCT_trabBMC.csv	DFM_pQCT_trabBMD.csv
bl,cc28	0.25158 t-test	0.062087 Mann-Whitney
bl,cc56	0.21597 t-test	0.64862 t-test
bl,cc84	0.7952 t-test	0.030986 t-test
bl,cc112	0.84043 t-test	0.00021961 Mann-Whitney
bl,control	0.78215 t-test	0.00059644 t-test
bl,hu	0.1703 t-test	3.8405e-005 t-test
bl,rec28	0.18737 t-test	2.4313e-005 t-test
bl,rec56	0.34217 t-test	0.0014033 t-test
bl,rec84	0.7698 t-test	0.060447 t-test
bl,1hu	0.18954 t-test	3.6203e-008 t-test
bl,1hu+rec	0.85571 t-test	1.8873e-006 t-test
bl,2hu	0.76128 t-test	2.3615e-006 Mann-Whitney
bl,2hu+rec	0.49356 t-test	1.6583e-006 t-test
bl,1hu+ex	0.061399 t-test	0.47353 t-test

bl,2hu+ex	0.002824 Mann-Whitney	0.75664 Mann-Whitney
1hu+ex,2hu+ex	0.17512 Mann-Whitney	0.84238 Mann-Whitney
rec56,2hu	0.50837 t-test	0.14908 Mann-Whitney
cc84,1hu	0.24173 t-test	0.0030458 t-test
hu,cc28	0.039957 t-test	0.0019705 Mann-Whitney
rec28,cc56	0.043926 t-test	0.0063017 t-test
1hu+ex,cc84	0.024048 t-test	0.014053 t-test
rec56,cc84	0.46313 t-test	0.34426 t-test
rec56,1hu+ex	0.012409 t-test	0.001277 t-test
2hu+ex,cc112	0.00037623 Mann-Whitney	0.0028153 Mann-Whitney
1hu,cc112	0.16369 t-test	0.0052665 Mann-Whitney
2hu,cc112	0.86121 t-test	0.090009 Mann-Whitney
rec84,cc112	0.57999 t-test	0.42924 Mann-Whitney
1hu+rec,control	0.69417 t-test	0.41116 t-test
2hu+rec,control	0.75212 t-test	0.3468 t-test

VITA

Name:	Estela Gonzalez
Address:	Department of Mechanical Engineering 3123 TAMU College Station, TX 77843, C/O Dr. Harry Hogan
Email Address:	estela.2010@gmail.com
Education:	B.S., Mechanical Engineering, Columbia University, 2010 M.S., Mechanical Engineering, Texas A&M University, 2012